Environmental Chemistry Letters (2023) 21:2583–2617
https://doi.org/10.1007/s10311-023-01616-z

REVIEW ARTICLE

# Optimizing hydrogen production by alkaline water decomposition with transition metal-based electrocatalysts

**Jingjing Li[1] · Zhengyin Jing[2] · Haotian Bai[1] · Zhonghao Chen[1] · Ahmed I. Osman[3] · Mohamed Farghali[4,5] · David W. Rooney[3] · Pow-Seng Yap[1]**

Received: 19 April 2023 / Accepted: 21 May 2023 / Published online: 3 June 2023


## Abstract

Burning fossil fuels account for over 75% of global greenhouse gas emissions and over 90% of carbon dioxide emissions, calling for alternative fuels such as hydrogen. Since the hydrogen demand could reach 120 million tons in 2024, efficient and large-scale production methods are required. Here we review electrocatalytic water splitting with a focus on reaction mechanisms, transition metal catalysts, and optimization strategies. We discuss mechanisms of water decomposition and hydrogen evolution. Transition metal catalysts include alloys, sulfides, carbides, nitrides, phosphides, selenides, oxides, hydroxides, and metal-organic frameworks. The reaction can be optimized by modifying the nanostructure or the electronic structure. We observe that transition metal-based electrocatalysts are excellent catalysts due to their abundant sources, low cost, and controllable electronic structures. Concerning optimization, fluorine anion doping at 1 mol/L potassium hydroxide yields an overpotential of 38 mV at a current density of 10 mA/cm$^2$. The electrocatalytic efficiency can also be enhanced by adding metal atoms to the nickel sulfide framework.

**Keywords** Electrocatalysts · Transition metal · Alkaline water hydrolysis · Hydrogen production · Optimization

## Introduction

Adopting renewable energy sources is essential for achieving sustainable development, as using non-renewable energy sources has resulted in environmental problems and depletion of resources. Hydrogen is a promising alternative to traditional fossil fuels due to its high energy density, clean combustion products, and renewable nature (Osman et al. 2023). Various hydrogen energy sources exist, including reforming traditional fossil fuels, biotechnology, and water electrolysis (Osman et al. 2022; Theerthagiri et al. 2022; Yang et al. 2023a). Water electrolysis for hydrogen production is environmentally friendly and has emerged as the most commonly used method, with alkaline water electrolysis and proton exchange membrane water electrolysis representing the two established technical routes for hydrogen production (Suen et al. 2017). Proton exchange membrane water electrolysis offers favorable conditions for industrialization and large-scale development. However, most catalysts perform poorly under harsh acidic conditions, substantially hindering their widespread adoption (Seh et al. 2017). Compared with proton exchange membrane, alkaline water electrolysis technology uses non-noble metal catalysts that can be used stably under alkaline conditions, effectively reducing the cost of catalytic materials (Rossmeisl et al. 2005; Ursua et al. 2012). However, the current water decomposition technology still faces low energy efficiency and high-cost problems (Roger et al. 2017), despite over 230 years of research.

✉ Ahmed I. Osman
aosmanahmed01@qub.ac.uk

✉ Pow-Seng Yap
PowSeng.Yap@xjtlu.edu.cn

[1] Department of Civil Engineering, Xi'an Jiaotong-Liverpool University, Suzhou 215123, China

[2] School of Chemistry and Chemical Engineering, Southeast University, Nanjing 211189, China

[3] School of Chemistry and Chemical Engineering, Queen's University Belfast, Belfast BT9 5AG, Northern Ireland, UK

[4] Department of Agricultural Engineering and Socio-Economics, Kobe University, Kobe 657-8501, Japan

[5] Department of Animal and Poultry Hygiene and Environmental Sanitation, Faculty of Veterinary Medicine, Assiut University, Assiut 71526, Egypt

This article offers an overview of the fundamental principle of catalytic hydrogen production through alkaline water electrolysis, summarizes the progress in transition metals as electrocatalytic hydrogen evolution materials, and proposes effective approaches for optimizing electrocatalytic performance to achieve large-scale hydrogen production, as shown in Fig. 1. The findings suggest that optimizing the electrocatalytic performance of these materials is critical for achieving large-scale hydrogen production, and various strategies for achieving this goal have been proposed and studied.

Most electrocatalytic hydrogen evolution reactions still rely on precious metals, and research on transition metal-based hydrogen evolution reactions is in its early stages. However, there is significant potential for developing transition metal-based alkaline hydrogen evolution reactions. This review explores and optimizes transition metal-based electrocatalysts for alkaline hydrogen evolution reactions. It provides an in-depth summary of the characteristics of different transition metal catalysts and their optimization strategies, highlighting the effects of nanostructures and electronic structures on the physical, chemical, and structural properties of transition metal electrocatalysts. From the perspective of rational material design, this review offers simple and low-cost preparation methods for synthesizing electrocatalysts with high activity and catalytic stability, providing new insights for optimizing electrocatalyst design to achieve optimal catalytic reaction performance. This facilitates the development of new high-efficiency transition metal electrocatalysts, addresses the blind spots in electrocatalyst optimization strategies, and identifies research directions for optimizing transition metal electrocatalysts to achieve green and sustainable large-scale industrial hydrogen production.

## Reaction mechanism

There is a high amount of hydrogen on the earth, most of which exists in water. Among many hydrogen production methods, electrocatalytic water decomposition provides an effective method for preparing high-purity hydrogen and has been widely used in industry. It converts electrical energy into chemical energy through two processes: hydrogen evolution reaction on the cathode and oxygen evolution reaction on the anode (Wang et al. 2022).

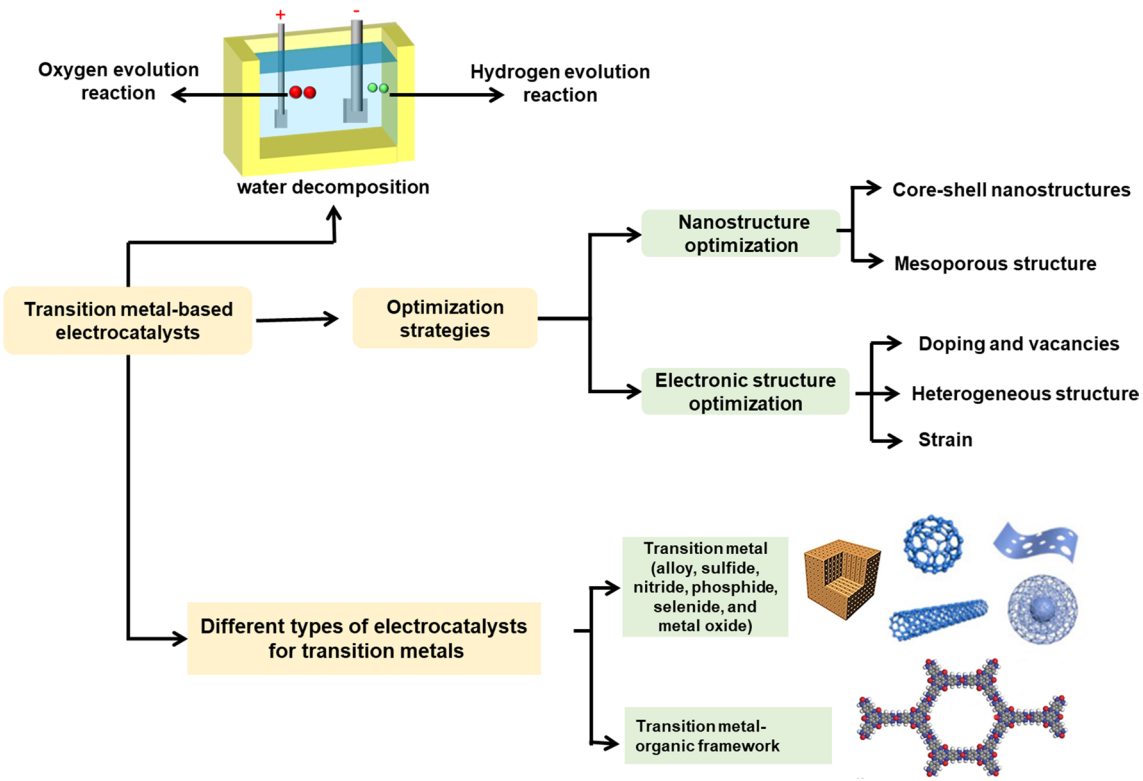


**Fig. 1** Applications of transition metals as electrocatalysts in hydrolysis reactions and methods for catalyst performance improvement. Transition metal electrocatalysts can catalyze both the hydrogen evolution and oxygen reduction reactions, with some even possessing bifunctional activities. These catalysts can be classified according to the specific transition metal combined with different elements. The properties of each type of catalyst can vary greatly, and the appropriate catalyst can be selected based on the reaction conditions. Moreover, modifying the nanostructure and electronic structure of the catalyst can significantly enhance the catalytic performance

Electrocatalytic water decomposition is crucial for advancing the field of sustainable energy. This section focuses on one of its most important semi-reactions—the hydrogen evolution reaction. Our review specifically looks at the behavior of this reaction under alkaline conditions, which is a key factor in optimizing its efficiency (Wei et al. 2018b).

## Electrocatalytic water decomposition

The basic principle of electrocatalytic water decomposition is that water is used as raw material to apply voltage from outside to form a complete electrified circuit. Because the injection breaks the internal balance of water molecules of electric energy, it is cracked, and at the same time, the hydrogen atoms and oxygen atoms are reconstructed, and finally, hydrogen and oxygen are precipitated (Dittmeyer et al. 2015).

As shown in Fig. 2, the water decomposition electrolyzer usually comprises a cathode, anode, electrolyte, and power supply. An external circuit connects the cathode and anode to form a complete conductive loop (Roger et al. 2017). Electrons are transmitted to the cathode by the external circuit, and hydrogen protons on the cathode surface get electrons to generate hydrogen; at the same time, water molecules oxidize on the anode surface to form oxygen (David et al. 2019). In the electrocatalytic water decomposition process, pure water's low ionization degree results in poor electrolyte conductivity and low electric energy utilization efficiency. To address this, acidic or alkaline electrolytes like sodium hydroxide, potassium hydroxide, or sulfuric acid are typically added to pure water to enhance conductivity. The reaction steps of the cathode and anode in different electrolyte systems are also different (Zhang et al. 2019a).

To increase the conductivity of the solution, acidic or alkaline electrolytes, such as sodium hydroxide, potassium hydroxide, or sulfuric acid, are often added to pure water during electrocatalytic water decomposition. Furthermore, the reaction steps of the cathode and anode vary depending on the type of electrolyte utilized, according to research conducted by Zhang et al. (2019b).

Thermodynamic factors determine the theoretical decomposition voltage $E_d$ of electrolyzed water when the applied reaction conditions are constant. It is generally considered that the thermodynamic decomposition voltage $E_d$ of water is 1.23 V at normal temperature and pressure, which is usually called the reversible equilibrium potential of the electrocatalytic water decomposition process (Roger et al. 2017; Ursua et al. 2012; Zeng and Zhang 2011). The reversible equilibrium potential of 1.23 V is mainly composed of 0 V for the hydrogen evolution reaction and 1.23 V for the oxygen evolution reaction.

Theoretically, the minimum voltage for water cracking at room temperature (25 °C) and 1 standard atmosphere is 1.23 V. However, water electrolysis always needs a voltage higher than 1.23 V because various resistance must be overcome in the reaction process. The part of the voltage exceeding the theoretical value by 1.23 V is overpotential $\eta$.

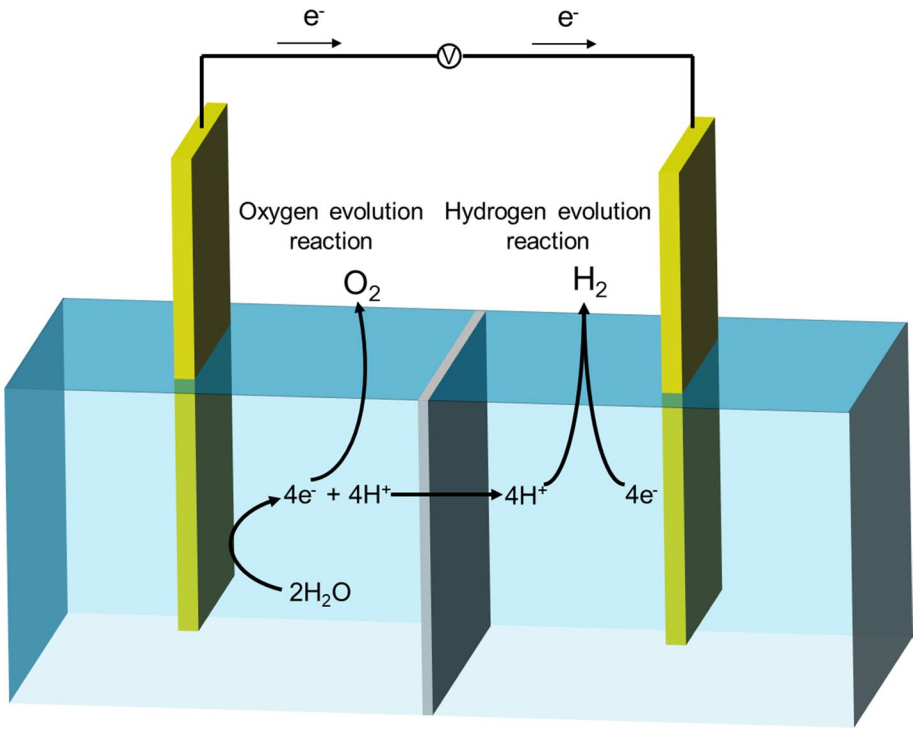


**Fig. 2** Water decomposition electrolyzer setup. As illustrated, the water decomposition electrolyzer consists of a cathode, anode, electrolyte, and power supply. A fully conductive circuit connects the cathode and anode to an external circuit, which transfers electrons ($e^-$) to the cathode. Hydrogen protons ($H^+$) on the cathode surface obtain these electrons ($e^-$) to produce hydrogen ($H_2$), while water molecules ($H_2O$) oxidize on the anode surface to generate oxygen ($O_2$). $H_2$, $O_2$, $e^-$, and $H^+$ refer to hydrogen, oxygen, electron, and hydrogen ion, respectively. Modified from Ursua et al. (2012)

Overpotential is the main cause of energy loss in electrolytic water. Finding a suitable catalyst to reduce overpotential $\eta$ is the most fundamental way to reduce energy consumption (Hou et al. 2019).

The major challenge in electrocatalytic water decomposition to produce hydrogen is to design and synthesize efficient and stable catalysts. In electrocatalytic water decomposition, the main functions of catalysts are (Sultan et al. 2019): to achieve stable charge transfer, provide adsorption sites for reaction intermediate species, and reduce the activation energy of oxidation and reduction of water molecules. The electrocatalyst for hydrogen evolution reaction with excellent activity is a noble metal platinum-based catalyst (Liang et al. 2020). However, this kind of catalyst's high cost and low stability restrict its large-scale industrial application. To obtain an efficient and low-cost electrocatalyst, it is necessary to fully understand the basic principle of hydrogen reaction.

In summary, electrocatalytic water decomposition is a promising approach for hydrogen production. The process involves the application of an external voltage to water, which results in the decomposition of water molecules into hydrogen and oxygen. However, using acidic or alkaline electrolytes is necessary to improve the conductivity of the solution. The major challenge in electrocatalytic water decomposition is the design and synthesis of efficient and stable catalysts to reduce overpotential and lower energy consumption.

## Electrocatalytic hydrogen evolution

Hydrogen evolution reaction in different electrolyte environments (acidic, neutral, or alkaline) involves three elementary reactions, which are generally accepted by researchers at present (Safizadeh et al. 2015). According to the elementary reaction expressions in different electrolyte environments, it can be seen that the elementary reaction process of it is basically the same regardless of the pH conditions, as shown in Fig. 3.

The Volmer reaction is also known as the electrochemical hydrogen adsorption step; in this process, the surface of the catalytic electrode ($M_{cat}$) as the cathode adsorbs hydrogen protons in the electrolyte and combines with a single electron $e^-$ to form the adsorption intermediate state ($M_{cat}H_{ads}$) (Krstajić et al. 2001). The Heyrovsky reaction is also known as the electrochemical hydrogen desorption step; in this process, the number of adsorption intermediate state ($M_{cat}H_{ads}$) on the surface of the cathode is small, and with the participation of electron ($e^-$), adsorption intermediate state ($M_{cat}H_{ads}$) is easy to combine with hydronium ion ($H_3O^+$) or water to generate hydrogen. Tafel reaction is also known as the composite desorption process; in this process, there are more adsorption intermediate states ($M_{cat}H_{ads}$) on the cathode surface, and two adjacent adsorption intermediate states ($M_{cat}H_{ads}$) are easy to recombine to generate hydrogen (de Chialvo and Chialvo 1999). The only difference is that during the Volmer reaction, in an acidic environment, the hydrogen protons in hydronium ion ($H_3O^+$) are directly adsorbed on the electrode surface; while in an alkaline environment, hydrogen protons are provided by water (Lasia 2019).

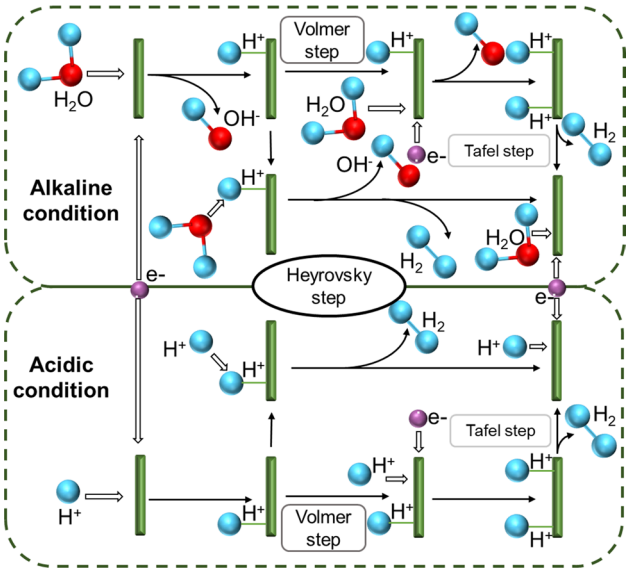


**Fig. 3** Hydrogen evolution mechanism under acidic (bottom) and alkaline (top) conditions. Three different reactions occur during electrochemical hydrogen adsorption and desorption. These are the Volmer reaction, the Heyrovsky reaction, and the Tafel reaction. In the Volmer reaction, the catalytic electrode ($M_{cat}$) acts as the cathode and adsorbs hydrogen ions ($H^+$) from the electrolyte. It combines with a single electron ($e^-$) to produce the adsorption intermediate state ($M_{cat}H_{ads}$). The Heyrovsky reaction, on the other hand, involves the electrochemical hydrogen desorption step. The adsorption intermediate state ($M_{cat}H_{ads}$) on the surface of the cathode combines with hydronium ion ($H_3O^+$) or water to generate hydrogen, with the participation of $e^-$. During the Tafel reaction, also known as the composite desorption process, there are more adsorption intermediate states ($M_{cat}H_{ads}$) on the cathode surface, and two adjacent adsorption intermediate states ($M_{cat}H_{ads}$) can easily recombine to generate hydrogen. One notable difference between the Volmer reaction in acidic and alkaline environments is that in the former, hydrogen ion ($H^+$) in hydronium ion ($H_3O^+$) are directly adsorbed on the electrode surface. In contrast, in the latter, hydrogen ions ($H^+$) are provided by water. Modified from Wei et al. (2018b)

Different reaction paths have different reaction energy barriers in the reaction process. In practice, the activity of electrocatalysts in a basic system is usually 2–3 orders of magnitude lower than that in an acidic system (Wang et al. 2017a); this is mainly due to the Volmer reaction in the alkaline reaction process, which requires the initial water dissociation process. The breakage of the hydrogen–oxygen–hydrogen bond in water molecules needs to overcome the high reaction energy barrier, which severely restricts the rate of the whole alkaline catalytic reaction process

(Liu et al. 2021c). In the electrocatalysis process, all three reaction steps above may become the reaction rate-determining steps. Usually, the reaction rate and mechanism can be judged by analyzing the Tafel slope of the polarization curve obtained by the electrochemical test. The smaller the value of the Tafel slope obtained by linear fitting means that the smaller the overpotential is needed to provide the same current density, which reflects that the electrocatalyst has better reaction kinetics performance (Guo et al. 2019; Lv et al. 2019).

It is generally considered that the chemisorption and desorption of hydrogen atoms on the catalyst surface are a pair of competitive reactions. If the degree of chemisorption is too strong, it is easy to form hydrogen, but it is not conducive to hydrogen escape. If the chemisorption degree is too weak, it is not conducive to the formation of hydrogen. Generally speaking, the binding ability between hydrogen atoms and active sites in catalysts can be characterized by hydrogen adsorption-free energy $\Delta GH^*$ (Roldan Cuenya and Behafarid 2015). In the chemisorption process, it is necessary that the active catalytic site can form a strong enough combination with a hydrogen atom to promote the transfer of proton-coupled electrons. In the subsequent chemical desorption process, it is necessary to have a weak bond between the active catalytic site and the hydrogen atom to ensure that the formed hydrogen is easily released from the catalyst surface (He et al. 2017; Lin et al. 2017; Sun et al. 2017). It is generally believed that an ideal electrocatalyst needs a value of $\Delta GH^*$ approaching 0 electron volt.

In summary, the hydrogen evolution reaction in different electrolyte environments involves three elementary reactions that are essentially the same regardless of the pH conditions. However, the activity of electrocatalysts in a basic system is usually much lower than in an acidic system due to the high energy barrier required for the initial water dissociation process. In addition, the binding ability between hydrogen atoms and active sites in catalysts can be characterized by hydrogen adsorption-free energy. An ideal electrocatalyst needs a value of hydrogen adsorption-free energy $\Delta GH^*$ approaching 0 eV.

## Transition metal-based electrocatalysts for alkaline hydrolysis

The anodic oxygen evolution and cathodic hydrogen evolution reactions, regarded as efficient and environmentally responsible methods to produce hydrogen without polluting the environment, can be improved by creating efficient electrocatalysts (Jian et al. 2018; Liu et al. 2018b). The high cost (Chen et al. 2016), slow kinetics, and scarcity of conventional precious metal-based hydrolysis catalysts are the main barriers to their widespread application (Chen et al. 2021a) because of the high potential difference in the hydrogen precipitation reaction, which results in high energy consumption in the electrolysis of water. Based on this, we will demonstrate in this chapter how these transition metal-based electrocatalysts have advanced recently. This paper reviews the hydrogen precipitation efficiency of different types of electrocatalysts for metals, as shown in Table 1.

### Transition metal alloy

By altering the electronic abundance of states at its Fermi energy level, alloying can increase catalytic activity (Rosalbino et al. 2014). Conversely, transition metal alloying can modify the catalyst's electrical structure through doping, strain, and heterostructure, modulating the active metal's d-band electrical structure to alter the electrocatalytic activity (Xiong et al. 2022). Shi et al. (2020) effectively isolated the intermetallic copper from the nanoporous compound tricobalt molybdate as a multipurpose electrocatalyst to obtain a low Tafel slope (40 mV $decade^{-1}$) and a current density of $-$ 400 $mA^{-2}$ cm at overpotentials as low as 96 mV in 1 mol/L potassium hydroxide. Copper, cobalt, and a zeolitic imidazolate framework (ZIF-67) were inserted in a nitrogen-rich mesoporous carbon framework (CuCo@NC) and pre-grown on copper hydroxide nanowires by Kuang et al. (2017). Below 450 °C, copper ions were uniformly contained within ZIF-67 pores. At higher pyrolysis temperatures, the presence of copper-nitrogen bonds further increased the nitrogen content of the ZIF-67 framework, which significantly enhanced the electrocatalytic performance of the hydrogen evolution reaction and oxygen reduction reaction. Su et al. (2017) described an electrocatalyst made of ruthenium and cobalt bimetallic nanoalloys enclosed in a sheet of nitrogen-doped graphene that is both efficient and stable. In addition to being reasonably priced, the ruthenium atom in the platinum group added to the cobalt shell enhances the efficiency of electron transfer from the alloy core to the graphene shell layer, which is helpful for enhancing the carbon-hydrogen bonding and lowering the $\Delta GH^*$ of hydrogen evolution reaction. Similar efforts have been undertaken to optimize the catalyst arrangement to improve the performance of transition metal catalysts in catalyzing hydrogen precipitation. Nickel-molybdenum alloys (Csernica et al. 2017; Wang et al. 2016a; Zhang et al. 2017), nickel–coper alloys, and iron-cobalt are a few earth-abundant metal alloys that have been designed and claimed to have good hydrogen precipitation yields and stability under alkaline conditions.

In summary, changes in the Fermi energy level resulting from alloying and modifications to the alloy nanostructure and electronic structure achieved through methods such as doping, strain, and heterostructures allow transition metal alloys to function as effective electrocatalysts.

**Table 1** Transition-metal-based electrocatalysts for the alkaline hydrogen evolution reaction

| Category | Electrocatalyst | Modification strategies | Electrolyte | Tafel slope (mV decade$^{-1}$) | Overpotential $\eta_{10}$ (mA cm$^{-2}$) (mV) | References |
|---|---|---|---|---|---|---|
| Transition-metal alloys | $Co_3Mo$ | Hybridization | 1 mol/L potassium hydroxide | 40 | 96 ($\eta_{400}$) | |
| | CuCo@NC | Hybridization | | 79 | 115 | Kuang et al. (2017) |
| | RuCo@NC | Doping | | 31 | 28 | Su et al. (2017) |
| Transition metal sulfides | F–$Ni_3S_2$/NF | Doping | 1 mol/L potassium hydroxide | 78 | 38 | He et al. (2019) |
| | Mo–$Co_9S_8$@C | Doping | | 34.6 | 98 | Wang et al. (2019b) |
| | Sn–$Ni_3S_2$/NF | Doping | | 33.8 | 170 ($\eta_{100}$) | Jian et al. (2018) |
| | NiS–CoS | Hybridization | | 92 | 102 | Ma et al. (2018 |
| | $CoS_2$ | Doping | | 60.1 | 112 | Zhu et al. (2020) |
| Transition metal carbides | $Mo_2C$/CC | Hybridization | 1 mol/L potassium hydroxide | 124 | 140 | Fan et al. (2015) |
| | Mo/$Mo_2C$–HNS–750 | Hybridization | | 62.86 | 79 | Xiong et al. (2018) |
| | $Mo_2C$/G3–NCS750 | Doping Porous structure | | 37 | 66 | Wei et al. (2018a) |
| | $Mo_2C$@2D–NPC | Doping, interface | | 46 | 45 | Lu et al. (2017a) |
| | MoC–$Mo_2C$–790 | Heterojunction three-dimensional porous structure | | 59 | 292 ($\eta_{500}$) | Liu et al. (2021c) |
| Transition metal nitrides | $Ni_3N_{1-x}$/NF | Vacancies | 1 mol/L potassium hydroxide | 54 | 55 | Liu et al. (2018a) |
| | $Mo_5N_6$ | Component optimization | | 66 | 94 | Wang et al. (2016b) |
| | $Co_3FeN_x$ | Porous structure | | 94 | 23 | Wang et al. (2016b) |
| | Ni–MoN | Vacancies | | 35.5 | 61 ($\eta_{100}$) | Wu et al. (2022a) |
| | dr-MoN | Vacancies | | 67.82 | 139 | Xiong et al. (2017) |
| | $Ni_3N$-$Mo_2$ N/NF | Heterojunction | | 67.4 | 118 | Dai et al. (2022) |
| | $Mo_{0.7}W_{0.3}N_{1.2}$ | Nano-architecture | | 47 | 122 | Jin et al. (2020) |
| | Ni-Mo–O/$Ni_4Mo$@NC | Vacancies | | 135 | 61 | Jin et al. (2021b) |
| Transition metal phosphides | V–CoP/CC | Doping | 1 mol/L potassium hydroxide | 67.6 | 71 | Xiao et al. (2018) |
| | Co–WP | Vacancies | | 55 | 119 | Guo et al. (2019) |
| | MoP/MWCNT | Doping | | 56.5 | 109 | Xiao et al. (2021) |
| Transition metal selenides | NiWSe | Nano-architecture | 1 mol/L potassium hydroxide | 137 | 162 | Zhao et al. (2018) |
| | $MoSe_2$–$NiSe_2$–$CoSe_2$/PNCF | Doping | | 38 | 38 | He et al. (2017) |
| | $PdSe_2$ | Nano-architecture | | 100 | 138 | |
| Transition metal oxide | α-$MoO_{3-x}$($x$ = 0.045) | Vacancies | 1 mol/L potassium hydroxide | 58 | 142 | Datta et al. (2017) |
| | S–$NiFe_2O_4$ | Vacancies | | 80 | 61 | Jin et al. (2021a) |
| | $Co_3O_4$/$MoS_2$ | Heterojunction | | 98 | 205 | Muthurasu et al. (2019) |
| | $MoO_2$ | Doping | | 57 | 176 | Geng et al. (2019) |
| Transition metal hydroxide | NiCo2–B–P HNPs | Doping | 1 mol/L potassium hydroxide | 73 | 78 | Liu et al. (2021b) |
| | NiCo-LDH/NiCo2S4/CC | Heterojunction | | 48 | 219 ($\eta_{50}$) | Liu et al. (2021e) |
| | 2D-$MoS_2$/$Ni(OH)_2$ | Heterojunction | | 73 | 128 | Dong et al. (2021) |
| Transition metal-based-metal organic framework | Ru-HPC | Doping | 1 mol/L potassium hydroxide | 33.9 | 22.7 ($\eta_{25}$) | Qiu et al. (2019) |
| | $Ni_3(Ni_3$·HAHATN$)_2$ | Nano-architecture | | 45.6 | 115 | Dai et al. (2022) |
| | Co–MOF–74 | Heterojunction | | 68 | 147 | Do et al. (2021) |

Different types of transition metal catalysts exhibit significant variations in their catalytic performance. In general, transition metal nitrides tend to exhibit superior catalytic performance. Various strategies can be utilized to enhance the catalytic performance of catalysts, such as doping, heterojunction, mesoporous structure regulation, vacancy, and microstructure adjustment. Several optimization techniques can also be employed to improve the catalyst's performance. Researchers often use carbon cloth and foam nickel substrates to enhance the catalyst's conductivity. Since the catalytic intrinsic characteristics of sulfide and selenide are similar, the optimization strategies for both are interchangeable

## Transition metal sulfide

Recent developments have led to earth-abundant transition metal-based nanoscale metal sulfides becoming cost-competitive alternatives to precious metal-based hydrolytic electrocatalysts (Yu and David Lou 2018). Studies have shown that the transition metal sulfide sequences $Co_xS_y$, $Ni_xS_y$, $Fe_xS_y$, $Mo_xS_y$, and $W_xS_y$ have excellent hydrolytic catalytic activity in alkaline media (Wu et al. 2017). However, many studies have shown that metal sulfides in energy conversion applications have low electronic conductivity and durability (Santhosh Kumar et al. 2022). The performance of these materials can be improved by doping, mixing, strain, phase engineering, heterostructure engineering (Fu et al. 2018; Zhong et al. 2017), and interface engineering (Huang et al. 2016; Li and Zeng 2017). The electronic conductivity can be altered, and the electrocatalytic hydrogen production efficiency can be significantly enhanced (Shen et al. 2015). Therefore, most studies have focused on tuning species and stoichiometry of these materials. The majority have therefore focused on tuning the type and stoichiometry of these materials to obtain the greatest possible hydrogen production efficiency by water electrolysis. Several papers have extensively reviewed the preparation and catalysis of molybdenum(IV) sulfide (Wei et al. 2018b). Therefore, this section focuses on the hydrogen precipitation efficiency of mixed metal sulfide basic hydrogen evolution reaction with other hybrids, transition metal anion doping, and other modification strategies.

Building on the work of Chen et al. (2017), Kou et al. (2018) and He et al. (2019) colleagues recently reported anionic engineering to modulate the electronic structure of transition metal catalysts by substituting sulfur, which is more electronegative than nitrogen. However, the desired catalytic hydrogen precipitation yields were not achieved. Subsequently, by reasonable speculation and experiment, nickel hydroxide nanosheet arrays were synthesized on nickel foam by simple hydrothermal synthesis. Then F–$Ni_3S_2$/NF was obtained by hydrothermal sulfidation after doping with fluorine using a gas-phase fluorination reaction on $Ni(OH)_2$/NF, and the synthesis process is shown in Fig. 4a. Technical tests demonstrated that fluorine anion doping at 1 mol/L potassium hydroxide yielding an overpotential of 38 mV at a current density of 10 mA $cm^{-2}$, even better than Pt/C/NF (50 mV at 10 mA $cm^{-2}$), a Tafel slope of mV $decate^{-1}$ and a current exchange density of 3.05 mA $cm^{-2}$, all of which significantly improved the hydrogen precipitation activity and long-term durability up to 30 h. In addition to anion doping, adding metal atoms to the nickel sulfide framework enhances electrocatalytic efficiency. For instance, Ye et al. (2020) developed 320 mV overpotential, 500 mA $cm^{-2}$ current density NiFeLa hydroxide modified tungsten-doped nickel sulfide nanoparticles on three-dimensional nickel foam. Tin-doped nickel sulfide nanosheets were also created on nickel (Sn–$Ni_3S_2$/NF) using the hydrothermal technique on nickel foam. The voltage needed for the total water splitting was only 1.46 V at a current density of 10 mA $cm^{-2}$, which was significantly greater than the voltage needed for the nitrogen-doped tri-nickel disulfide framework. To enhance the catalytic efficacy of electrocatalysts, solid elements iron (Zhang et al. 2018a) and manganese can also be used as dopants in addition to tin (Jian et al. 2018).

Other transition metal sulfide compounds (cobalt, nickel) have recently been considered promising alternatives to precious metal-based compounds for water splitting. For example, transition metal cobalt sulfides have important applications in electrocatalysis, including electronic devices, ion storage, supercapacitors, redox reactions, oxygen precipitation reactions, and hydrogen precipitation reactions. For the hydrogen precipitation reaction of cobalt-based transition metal sulfide, on the one hand, the sulfur atoms are doped into the metal lattice to form a cleavage compound, the distance between metal atoms increases, the d-band gap narrows, and the density of states near the Fermi energy level is enhanced (Wang et al. 2021a). On the other hand, since sulfur and oxygen atoms are in the same main group and have similar physical and chemical properties, cobalt sulfide has good hydrophilicity in an aqueous solution, density of 10 mA $cm^{-2}$, 1.0-mol potassium hydroxide. Zhu et al. (2020) prepared nitrogen-doped cobalt sulfide nanosheets with a Tafel slope of 60.1 mV $decade^{-1}$ and an overpotential as low as 112 mV (Fig. 4c). Wang et al. (2019b) used molybdenum atomically dispersed on metal $Co_9S_8$ nanosheets as an advanced noble metal-free bifunctional water cracking catalyst Mo–$Co_9S_8$@C (Fig. 4d), which also exhibited excellent hydrogen evolution reaction performance in a wide pH range, obtaining an overpotential of 98 mV and a Tafel slope of 34.6 mV $decade^{-1}$. As shown in Fig. 4b, comparing overpotential and Tafel slope histograms of different cobalt-based electrocatalysts at 1 mol/L potassium hydroxide, current density 10 mA $cm^{-2}$ in recent years. However, previously reported studies have shown that they still suffer from the defects of active sites and insufficient conductivity.

Along with the doping mentioned above and mixing, interfacial constructs can alter the electrocatalyst by altering the electronic structure, increasing intrinsic activity, and improving electrical conductivity. This alters the catalyst's intrinsic activity and increases the efficiency of hydrogen precipitation (Zhang and Lv 2018). Given these factors, creating hollow/porous nano-rectangles, a regular hollow structure that doubles as a deity by providing an abundance of active surface sites and enabling ion diffusion, is a viable course of action (Guo et al. 2018a, b; Zheng et al. 2020). More importantly, the hollow structure can accommodate large expansion and improve the catalyst's lifetime. However, the design steps of previous hollow structures are tedious

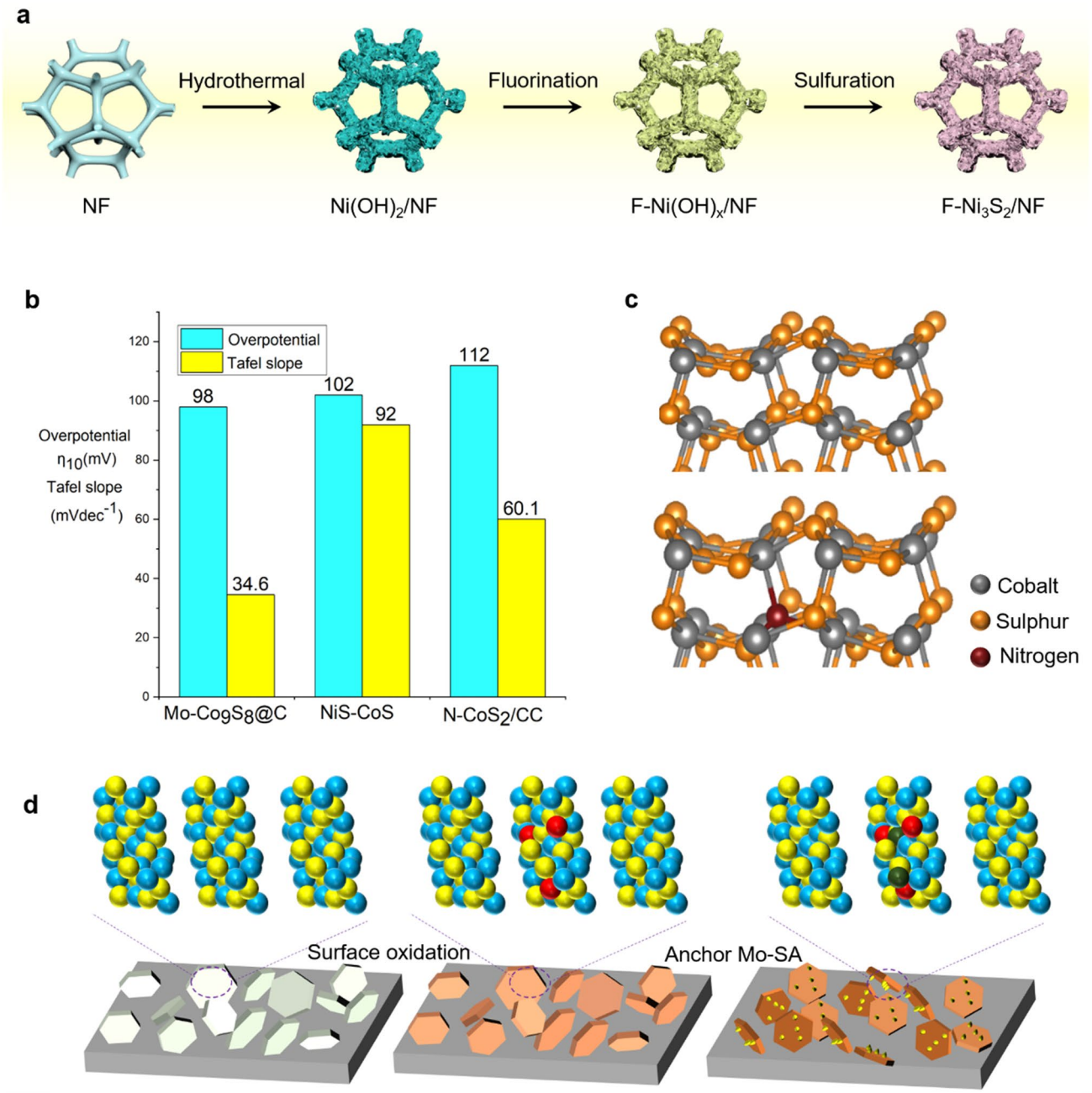


**Fig. 4** **a** The fluorine-doped nickel sulfide nanosheet array synthesis on nickel foam (NF). Nickel hydroxide ($Ni(OH)_2$) is grown on foam nickel by hydrothermal synthesis. Then the required product is obtained by fluorination and sulfuration. **b** Histograms depicting overpotential and Tafel slope of various electrocatalysts based on cobalt at a current density of 10 mA $cm^{-2}$ in a potassium hydroxide solution with a concentration of 1 mol/L. N-$CoS_2$/CC refers to nitrogen-doped cobalt disulfide deposited on carbon cloth, NiS–CoS refers to nickel sulfide-cobalt sulfide. Mo–$Co_9S_8$@C refers to single-atom molybdenum loaded on $Co_9S_8$@C-supported. **c** Optimized (0 0 1) slabs of cobalt sulfide (top) and nitrogen-cobalt sulfide (bottom). The cobalt atoms in nitrogen-cobalt sulfide are affected by the electronegativity of nitrogen, which weakens the cobalt-hydrogen bond and allows cobalt-hydrogen cleavage and thus accelerates hydrogen precipitation. Co refers to cobalt, S refers to sulfur, and N refers to nitrogen. **d** Synthetic process for Mo–$Co_9S_8$@C. Electron microscope analysis of the Mo–$Co_9S_8$@C sample. Mo–SA refers to molybdenum single atom. Figure 4a is modified from He et al. (2019), Fig. 4b is modified from Ma et al. (2018), Wang et al. (2019b), Zhu et al. (2020) and Fig. 4c is modified from Zhu et al. (2020)

and expensive, which are not available for large-scale applications (Ma et al. 2020a). Therefore, a simple method to prepare morphology-controlled hollow structures is urgently needed. Recently, hollow porous squares of cobalt sulfide ($CoS_2$·HNs) were produced with a greater specific surface area using a novel chemical etching-phosphatization/

sulfuration technique. The equivalent electrocatalytic activity of selenide hydrolysis and transition metal sulfides has also been documented (Abdel Maksoud et al. 2021; Wang et al. 2021a).

In summary, it is found that sulfur possesses greater electronegativity, but its transition metal compounds possess low electron conduction rates and durability. Based on this, the electronic structure of the catalyst is adjusted to increase the electrical conductivity and the number of catalytic sites of the material, which in turn leads to high-performance catalysis.

## Transition metal carbide

Transition metal carbides, also called "quasi-platinum catalysts," exhibit that it can have a large enough surface area to contact the electrolyte, thus greatly improving the efficiency of hydrogen precipitation. For example, Ma et al. (2018) developed a three-dimensional hybrid/dense NiS–CoS nanorod array with an overpotential of 102 mV at a current exceptional electrocatalytic properties for aqueous decomposition as they possess a d-band electronic structure similar to the noble metal's platinum. Additionally, they possess high electrical conductivity, high hydrophilicity, good mechanical strength, and good topology, making them highly desirable. On this basis, transition metal carbides have given rise to alternative electrocatalysts for the aqueous decomposition of precious metals. Although these catalysts have demonstrated excellent performance, they do not satisfy the needs of real uses, and it is still difficult to overcome the complicated preparation process and subpar stability. However, modifying the catalysts' structure and shape can increase surface area and reveal more active sites, increasing electrocatalytic activity. Developing heterostructures, doping, and defect engineering can improve electrocatalytic performance (Chen et al. 2021b). Among them, molybdenum carbide is a promising candidate for electrocatalysis due to its high thermal and chemical stability and surface activity. The electronic structure in the d-band is most similar to that of platinum, the best noble metal electrocatalyst for hydrogen evolution reactions. Researchers have investigated cobalt carbide as an electrocatalyst for hydrogen precipitation reactions (Mir et al. 2023). This section will discuss the alkaline electrocatalytic hydrolysis of transition metal molybdenum carbide.

Despite these benefits, transition metal carbides' generally low conductivity necessitates a highly conductive base. In Vrubel and Hu (2012), first reported the existence of molybdenum carbide as a noble metal-free catalyst active. However, its catalytic activity is low due to the conductivity problem, which requires a reduced catalyst particle size as well as good dispersion and exposure to more active sites to improve the electrocatalytic activity. Fan et al. (2015) suggested that a straightforward thermal treatment of flexible carbon fabric filled with Mo–CTA supramolecular hybrids would develop well-dispersed molybdenum carbide microislands. Tight junctions, high electrical conductivity, and the plentiful catalytic active sites of molybdenum carbide itself were said to be the causes of the molybdenum carbide/carbon fabric composites' outstanding electrocatalytic characteristics. In addition, molybdenum carbide nanoparticles were constructed as nanowires (nanoparticles), which were used as the catalysts for the catalytic activity. In addition, molybdenum carbide nanoparticles have been constructed as nanowires, nanosheets (Xing et al. 2019), nanotubes (Xu et al. 2017), quantum dots (Zhang et al. 2018c), nano-octahedra (Wu et al. 2015), and nanofibers (Liu et al. 2018c). The introduction of molybdenum groups into these various nanostructured carbon materials can increase electrocatalytic activity.

An example is the synthesis of large-size atomically thin heterogeneous nanosheets of molybdenum/molybdenum carbide with abundant nanoscale heterogeneous interfaces through the salt-template method. This involves reducing molybdenum oxide precursors grown on sodium chloride crystals while forming molybdenum/molybdenum carbide-heterogeneous nanosheets in a methane/hydrogen mixture. At the nanoscale, the metal molybdenum and molybdenum carbide are interconnected, resulting in an abundance of molybdenum/molybdenum carbide-heterogeneous interfaces, as illustrated in Fig. 5a. This dual-phase interface achieves high dispersion of nanoparticles and enhanced electrical conductivity. The atomic ratios of three Mo/$Mo_2C$-hetero-nanosheets electrocatalysts were also tested in this research (the atomic ratios of cobalt to cobalt carbide for molybdenum/molybdenum carbide- hetero-nanosheets-650, molybdenum/molybdenum carbide-hetero-nanosheets-700, molybdenum/molybdenum carbide—hetero-nanosheets-750, and 72:28, 61:39, and 89:11, 72:28, and 61:39, respectively, were verified), where the best-performing molybdenum/molybdenum carbide-heterogeneous nanosheets-750 obtained a Tafel slope of 62.86 mV $decade^{-1}$, a low 10 mA $cm^{-2}$ of 79 mV, and basic hydrogen evolution reaction activity comparable to 20% platinum/carbon catalyst at high overpotentials, indicating that molybdenum/molybdenum carbide-heterogeneous nanosheets-750 has a lower activation energy and faster reaction kinetics (Xiong et al. 2018).

Besides developing various new nanostructured molybdenum carbides, there are sophisticated methods to enhance the intrinsic activity of molybdenum carbides, including heteroatomic doping. Lin et al. (2016) have successfully introduced cobalt elements into molybdenum carbide. His colleagues introduced nickel into molybdenum carbide (Chen et al. 2018b), while non-metallic elements doped into molybdenum carbide have been widely reported, phosphorus, nitrogen (Lu et al. 2017a; Wei et al. 2018a), sulfur,

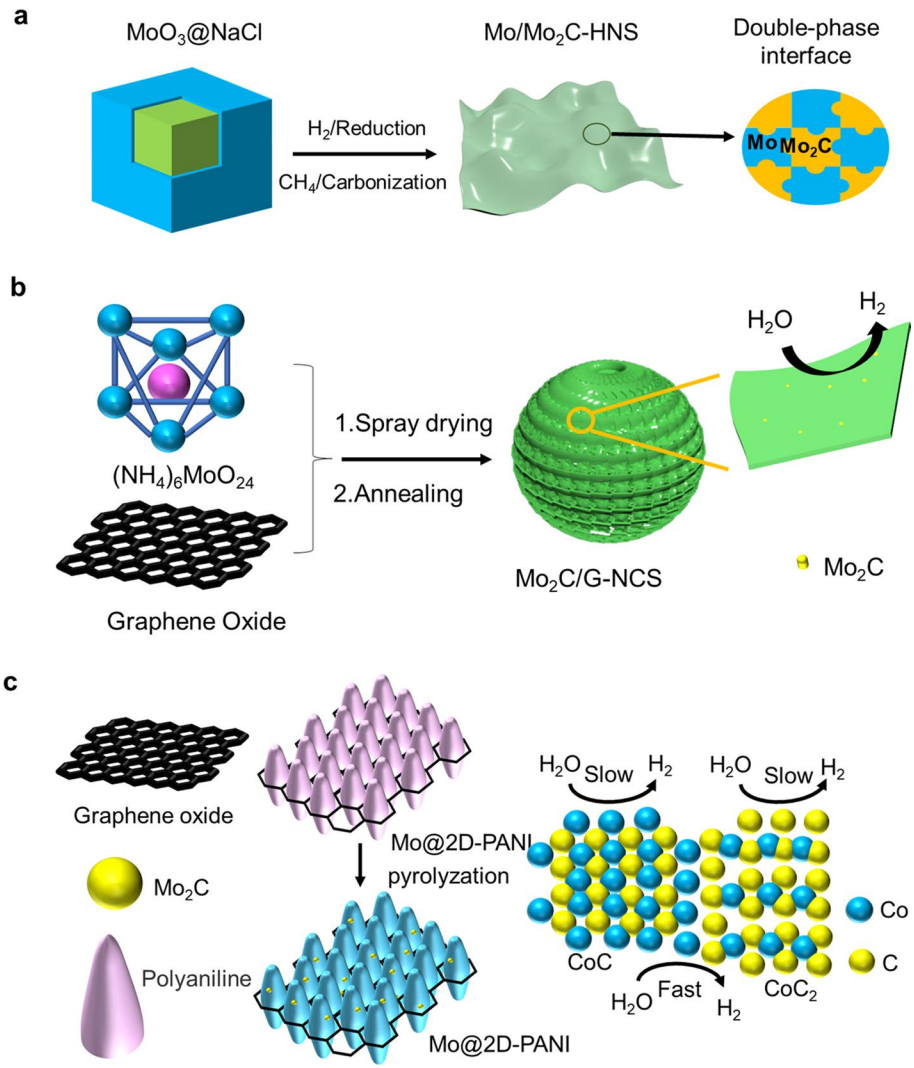


**Fig. 5** **a** Salt-template synthesis of molybdenum/molybdenum carbide atomically thin heterojunction nanosheets. The molybdenum and molybdenum carbide nanoscale interconnections produce a rich molybdenum/molybdenum carbide-heterogeneous interface that provides a biphasic interface consisting of catalytic sites and electron transfer channels. $MoO_3$@NaCl refers to molybdenum trioxide@sodium chloride, $H_2$ refers to hydrogen, $CH_4$ refers to methane, Mo refers to molybdenum, $Mo_2C$ refers to molybdenum carbide, Mo/$Mo_2C$ refers to molybdenum/molybdenum carbide-hetero-nanosheets. Modified from Xiong et al. (2018); **b** cobalt carbide nanoparticle is uniformly embedded in nitrogen-doped chitosan porous carbon microsphere coated with graphene, forming a coating structure as shown in the figure. $Mo_2C$/G–NCS refers to nitrogen-doped porous carbon microspheres, $H_2$ refers to hydrogen, and $H_2O$ refers to water. Modified from Wei et al. (2021); **c** cobalt carbide nitrogen-doped porous carbon nanotubes ($Mo_2C$@2D–NPCs) synthesis steps, Mo@2D–PANI refers to molybdenum/two dimension-polyaniline. Modified from Lu et al. (2017a); **d** cobalt carbide-schematic diagram of molybdenum carbide dissociation on molybdenum carbide boundary. CoC refers to molybdenum(IV) carbide, $Co_2C$ refers to molybdenum carbide, Co refers to cobalt, C refers to Carbon, $H_2$ refers to hydrogen, and $H_2O$ refers to water. Modified from Liu et al. (2021c)

and others. However, the molybdenum carbide nanoparticles were homogeneously embedded in graphene-wrapped nitrogen-doped chitosan porous carbon microspheres, forming an encapsulated structure as shown below. Wei et al. (2018a) reported the use of chitosan and ammonium molybdate tetrahydrate as carbon and molybdenum sources, respectively (Fig. 5b). In contrast, Lu et al. (2017a) reported the borrowing of an interfacial strategy to synthesize polyaniline nanosheets with controlled components to achieve $Mo_2C$-embedded nitrogen-doped porous carbon nanosheets ($Mo_2C$@2D–NPCs). The synthesis process is shown in Fig. 5c, with aniline as the monomer, graphene oxide as the two-dimensional template, and $Mo_4O_{13}^{2-}$ as the molybdenum source, in the toluene to $Mo_4O_{13}^{2-}$ anchored. Polyaniline(PANI) nanosheets (Mo@2D–PANI) were prepared by in situ polymerization at the interface between toluene and water at room temperature, and in the second stage, Mo@2D-NPCs were obtained by pyrolysis of

Mo@2D–PANI at 900 °C under argon (5%) atmosphere for 2 h (Wei et al. 2018a). Both teams used nitrogen doping of the ultra-small size of molybdenum carbide. More vital interaction between the carbon matrix provided a larger exposed active site, and both used graphene structures, significantly improving molybdenum carbide's conductivity problem. Wei et al. (2018a)'s team primarily used doping through porous microsphere structures to increase the contact point between electrolyte and electrode and decrease charge transfer resistance. In contrast, Lu et al. (2017a)'s team reduced the energy barrier for hydrogen precipitation by using a practical interfacial strategy and strong interaction between molybdenum carbide and nitrogen-doped porous carbon nanosheets to improve the hydrogen precipitation yield. However, there are slight differences in the modification strategies both teams use.

According to research by Ang et al. (2015), partial nitrogen doping as an electron-rich dopant lowers the density of the hollow d-band in molybdenum carbide, which diminishes the molybdenum-hydrogen intensity and raises hydrogen evolution reaction activity. The intrinsic activity of electrocatalysts can be successfully increased through reasonably modified element doping.

In addition, nitrogen-doped graphene was added to lessen the contact between transition metal carbide ($M$ = tungsten, vanadium, titanium, and molybdenum) and $H^*$ (Wei et al. 2018a). The heterogeneous interfaces of heterostructured catalysts, which can offer multiple functional sites for the complete reaction process, have fascinating synergistic effects. Then Liu et al. (2021c)'s team reported the potential of a hydrogen-universal self-standing molybdenum carbide-molybdenum carbide(II) heterojunction electrode with a multilayer structure that outperformed the noble metal catalyst (platinum) in terms of alkali resistance, achieving an overpotential of 256 mV at a current density of 500 mA $cm^{-2}$ and a Tafel slope of 59 mV·$decade^{-1}$. Then comparing each electrode's turnover frequency values, the molybdenum carbide-molybdenum carbide(II)-790 electrode was significantly larger than the other electrodes, indicating that the electrode has excellent activity. In addition, its performance was also tested under acidic conditions, and the molybdenum carbide-molybdenum carbide(II) heterojunction H* adsorption Gibbs free energy was the best ($\Delta GH^* = -0.13$ eV). The water dissociation energy barrier at the molybdenum carbide-molybdenum carbide(II) interface (1.15 eV) was lower than that at the molybdenum carbide (3.33 eV) or molybdenum carbide (1.90 eV) interfaces, further hydrogen evolution reaction indicating that the molybdenum carbide-molybdenum carbide(II) heterojunction has excellent hydrogen evolution reaction activity. Its mechanism is shown in Fig. 5d. The corresponding free energy diagrams were plotted to explain the performance of hydrogen evolution reactions in alkaline solutions.

In summary, transition metal carbides have a d-band electronic structure similar to the noble metal platinum. They are, therefore, ideal electrocatalysts for hydrolysis, but the conductivity and the number of catalytic sites are still lacking.

## Transition metal nitride

Transition metal nitrides are interstitial compounds with face-centered cubic, hexagonal dense, and simple cubic arrangements that exhibit the properties of covalent compounds, ionic compounds, and transition metals simultaneously. Nitrogen atoms are embedded into the interstitial positions of metal atoms in these interstitial compounds (Chen et al. 2021b). In addition to their distinctive electronic structure, high stability, high catalytic activity, higher mechanical robustness for corrosion resistance, and improved surface morphology, transition metal nitrides also have numerous other benefits. The behavioral characteristics of noble metals, which are currently promising catalysts across a wide potential hydrogen range, are produced via metal- nitrogen bonding, which induces lattice expansion and band contraction of the metal (Wang et al. 2021c). The catalytic performance of transition metal nitride depends on the catalyst's shape, structure, and size distribution. By nitriding metal precursors such as metals, metal oxides, metal halides, and organometallic precursors in ammonia gas or nitrogen/hydrogen gas mixtures prepared by controlled temperature rise and fall under high-temperature conditions, it is possible to achieve the controlled synthesis of catalyst morphology (Tareen et al. 2019). The controlled temperature increase reaction is the name of this synthesis method. The main factors affecting the performance index of electrocatalysts include the quantity of active catalytic sites, intrinsic activity, conductivity, and the ability to adsorb and desorb reaction intermediates; this is also the direction in which transition metal nitride catalysts are being developed.

$Co_2N/CoN/Co_2Mo_3O_8$ heterostructured catalysts were created on cobalt foam using hydrothermal and nitridation treatment in two stages (Hu et al. 2021). The catalysts' numerous active sites showed extraordinarily high activity and stability in the alkaline hydrogen evolution process. They were equal to the noble metal platinum's catalytic performance at a current density of 100 mA·$cm^{-2}$ and were made feasible by their nanoporous and multilayer structure. A combination of nickel and molybdenum nitride was used to create homogeneous nickel–molybdenum nitride catalysts on amorphous molybdenum nitride nanorods (Wu et al. 2022a). The layered nanorod-nanoparticle structure, with its wide surface area and multidimensional interfaces/defects, allowed the existence of active sites at current densities of 100 and 1000 mA $cm^{-2}$, respectively, in 1 mol/L potassium hydroxide. This combination also successfully modulated

the boundary electron distribution. In contrast to intact molybdenum nitride nanosheets, which have more active sites on these defects and have better catalytic performance, molybdenum nitride (dr-molybdenum nitride) nanosheets rich in defects have extra edge defects (Xiong et al. 2017).

Using urea as the source of nitrogen, Dai et al. (2022) prepared self-supported $Ni_3N$–$Mo_2N$/NF heterostructures using a hydrothermal method that produced controlled nanowire arrays, attributed to the faster charge transfer rate of the catalyst, exhibiting a more favorable intrinsic electrocatalytic performance, exhibiting an overpotential of only 66 mV under alkaline conditions. Cobalt nitride-vanadium oxynitride (VN1-*x*O*x*) nanohybrids were synthesized on carbon cloth using a polyaniline-mediated method. This approach can form a layer of nitrogen-doped carbon, which serves as an electron transfer mediator between the active catalyst and the conducting carrier (Dutta et al. 2019). This results in accelerated processes and increased hydrolysis activity. The nanohybrids showed an overpotential of only 118 mV at a current density of 10 mA $cm^{-2}$ and maintained long-term stability for up to 100 h. Using the molten salt technique, a series of two-dimensional layered transition metal nitrides ($MoN_{1.2}$, $WN_{1.5}$, and $Mo_{0.7}W_{0.3}N_{1.2}$). As a result of their outstanding electron conductivity and metal-like electronic structure, they showed good electrocatalytic activity (Jin et al. 2021b). These materials have a lower overpotential need than other two-dimensional layered electrocatalysts, just 122 mV at a current density of 10 mA $cm^{-2}$. On nitrogen-doped carbon carriers, Ni–Mo–O/$Ni_4Mo$@NC nanointerfaces were used using an electrodeposition-calcination-electrodeposition method (Fig. 6b) (Jin et al. 2020). Due to nitrogen's electronegativity, it interacts with the transition metal after being added to carbon carriers and improves the catalyst's electrical conductivity, showing a low overpotential of 61 mV (10 mA $cm^{-2}$) under alkaline conditions at 1 mol/L potassium hydroxide.

Transition metal nitride possesses superior metallicity, but the unfavorable d-band energy level hinders the catalytic performance of hydrogen precipitation reactions, which can be solved by optimizing the metal abundance. The in situ hybridization of $Ni_2Fe_2N$ nanoparticles with another metal tri-nickel ferrite electrocatalyst (Hu et al. 2020). Due to the catalyst's improved metallicity, enhanced hydrolytic kinetics, and decreased hydrogen adsorption-free energy, $Ni_2Fe_2N$/$Ni_3Fe$ nanoparticles demonstrated excellent hydrogen evolution reaction catalytic activity with an overpotential of 74 mV and a low Tafel slope of 53 mV $decade^{-1}$ at a current density of 10 mA $cm^{-2}$. The one-pot method (Park et al. 2021) was used to grow $Ni_2Mo_3N$ with nanostructures on nickel foam. According to density function theory calculations, the nitrogen sites in the four-coordination number $Ni_2Mo_3N$ have favorable hydrogen adsorption energy (near platinum), and this catalyst has a low overpotential (21.3 mV @ 10 mA $cm^{-2}$ and 123.8 mV @ 100 mA $cm^{-2}$) and excellent durability for 24 h. When the electrical mechanism for cobalt nitride is tweaked to get strong hydrogen binding ability (Fig. 6a), the chromium-doped cobalt nitride nanorod arrays on carbon cloth demonstrate a low overpotential of 21 mV (10 mA $cm^{-2}$ under alkaline conditions at 1 mol/L potassium hydroxide), outperforming platinum/carbon catalysts in terms of performance (Huang et al. 2018; Yao et al. 2019).

In summary, transition metal nitride is a catalyst with a wide range of acid–base applications and possesses the characteristics of good metallicity, but the d-band energy level is not conducive to the catalytic effect, which is the direction to improve the catalytic properties of transition metal nitride.

## Transition metal phosphide

Phosphorus has an electronic structure similar to that of metals, and when combined with transition metals in phosphides, it forms metal–metal-like bonds with covalent characteristics. These bonds prevent the achievement of close stacking, resulting in an often asymmetrical structure (Pu et al. 2020). Transition metal phosphides typically form a trigonal prism shape, with phosphorus atoms at the center and metal atoms surrounding them. The metal–metal bonds are spread throughout the catalyst, resulting in good electrical conductivity, which is crucial for high-performing electric catalysts (Carenco et al. 2013). The entry of phosphorus also improves the stability of transition metal carbide and can reduce the degradation of the sample, e.g., molybdenum nitride < molybdenum carbide < molybdenum phosphide for comparison with molybdenum catalysts (Oyama et al. 2009).

As the phosphorus atom enters the catalyst, the transition metal's d-band center and Fermi energy level change, which affects the metal's *d*-orbit width and the electron density in the active site. The catalytic process is supported by adding phosphorus, which also expedites the adsorption and desorption of reactants and reaction intermediates during the reaction (Han et al. 2019a). Combined with Sabatier's principle, these two elements enable the reaction intermediate to have the best binding energy and catalytic activity. Due to phosphorus's high electronegativity, a tiny electron is transferred from metal to phosphorus. The hydrogen evolution reaction process predominantly uses phosphorus as the active site; hence, adding more phosphorus to the catalyst helps it work better (Zhou and He 2021). To create even more active sites, phosphorus can also induce the emergence of vacancies. Positively charged metal can be a hydride acceptor, and negatively charged phosphorus can be a proton acceptor. Electrons in transition metal phosphide are highly delocalized, in the conductivity of phosphide is weaker than that of metal. However, phosphorus atoms can also accelerate the charge transfer, so transition metal phosphide with a suitable

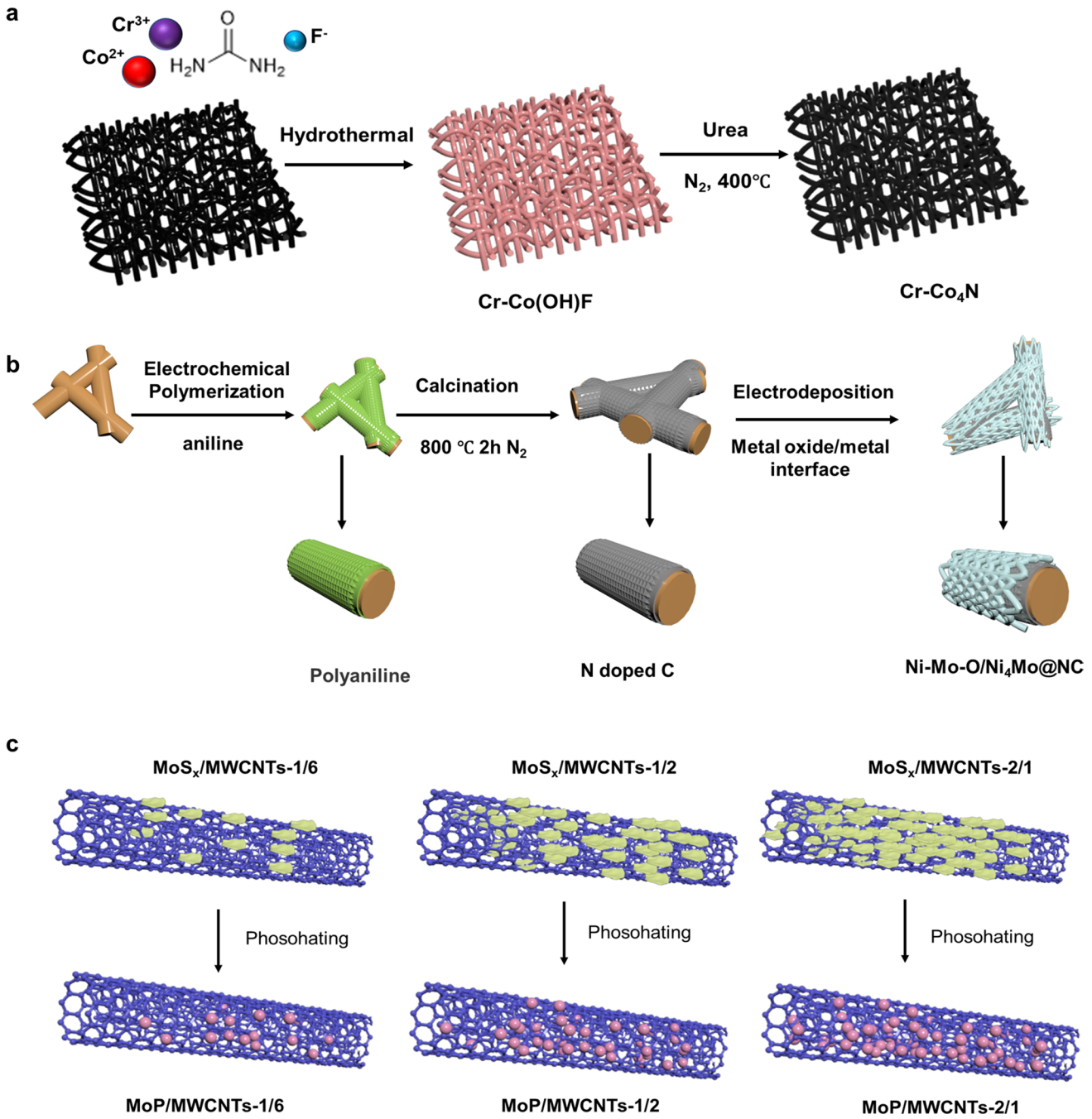


**Fig. 6** **a** Fabrication of Cr–$Co_4N$. Cr–$Co_4N$/CC nanorods were synthesized by hydrothermal deposition of Cr–Co(OH)F precursors and annealed at 400 °C under a nitrogen gas atmosphere to obtain the desired products. $Cr^{3+}$ refers to chromium ions, $Co^{2+}$ refers to cobalt ions, $F^-$ refers to fluoride ions, $N_2$ refers to nitrogen, and Cr-$Co_4N$ refers to chromium-tetra cobalt nitride. Modified from Yao et al. (2019); **b** schematic illustration of the fabrication of Ni–Mo–O/$Ni_4Mo$@NC. The polyaniline was first deposited on carbon cloth and calcined at 800 °C under a nitrogen atmosphere to obtain nitrogen-doped carbon. An electrodeposition step introduced the Ni–Mo–O/$Ni_4Mo$ nano-interface. $N_2$ refers to nitrogen, and C refers to carbon. Modified from Jin et al. (2020); **c** molybdenum phosphide nanoparticles grown in situ on multi-walled carbon nanotubes are used to enhance the hydrogen evolution reaction through a simple path. MWCNTs refer to multi-walled carbon nanotubes, and MoP refers to molybdenum phosphide. Modified from Xiao et al. (2021)

ratio of phosphorus to metal atoms still has good conductivity, especially for compounds with high phosphorus content, and thus exhibits good catalytic properties (Pan et al. 2015). Furthermore, it was discovered that catalysts with a high proportion of unoccupied three-dimensional orbitals had enhanced water-activated oxygenophilic sites and could

also modulate the electronic structure for the best hydrogen adsorption. These findings were made using discrete Fourier transform calculations using cobalt phosphide as a model (Men et al. 2020).

Xiao et al. (2018) utilized hydrothermal phosphorylation to synthesize dibasic cobalt phosphide nanowire arrays with bound transition metal vanadium. This catalyst was deposited on a three-dimensional conductive and pliable carbon fabric with a large surface area. The incorporation of vanadium into the cobalt-phosphorus lattice increased the lattice constant, resulting in a stronger electronic interaction between vanadium and cobalt-phosphorus. This interaction also increased the electron density in the cobalt phosphide, leading to an improvement in its conductivity. The catalyst exhibited an ultra-low overpotential of 123 mV at a current density of 10 mA $cm^{-2}$ in 1 mol/L potassium hydroxide. Using precipitation reaction and in situ phosphorylation, cobalt phosphide nanosheet arrays were made on $Ti_3C_2$MXene by Yan et al. (2020). These arrays had a heterogeneous structure with cobalt phosphide nanosheets distributed vertically on the material. This structure created a hierarchical porous structure with a significant surface area and high conductivity. In order to produce a current density of 10 mA $cm^{-2}$, there must be enough active sites for catalytic processes, and the charge transfer rate must be increased at 1.0 mol/L potassium hydroxide with an overpotential of 102 mV.

A porous nanostructure with a larger surface area was made by introducing transition metals (molybdenum and cobalt) to the original tungsten phosphide, exposing more active sites. More notably, after cobalt doping, the water dissociation and hydrogen production steps were adjusted, greatly increasing the catalyst's reaction (Guo et al. 2019). Since they have a larger area of exposed active sites and a high surface porosity, hollow nanoparticles are an effective technique to boost the catalytic capacity of hydrogen evolution reactions. Due to their structural characteristics, metal–organic frameworks are suitable precursors for producing hollow nanoparticles. Luo et al. (2022) used metal–organic frameworks as models to make hollow cobalt–ferrum–phosphorus/cerium oxide hexagonal rods. Due to the synergistic effect and the influence of the oxygen vacancies at the interface on the electrical structure, a current density of 10 mA $cm^{-2}$ in alkaline media may be reached at an overpotential of just 69.7 mV, allowing the catalyst hydrogen adsorption-free energy to be tuned.

Often seen on multi-walled carbon nanotubes, the smaller pore-like defects are effective locations for forming active materials (Fig. 6c) (Xiao et al. 2021). At a distance of 10 mA $cm^{-2}$, overpotentials of 109 mV and 155 mV were observed in acidic and basic solutions, respectively, with mild Tafel slopes of 56.5 mV $decade^{-1}$ and 56.8 mV $decade^{-1}$.

In conclusion, the catalytic performance of the transition metal catalysts is significantly enhanced by the addition of phosphorus, which can be attributed to the introduction of phosphorus to create more vacancies and enhance the conductivity of the catalysts. The modification of the nanostructure and electronic structure further enhances the catalytic performance.

## Transition metal selenide

Transition metals can react with elements in the sulfur group, resulting in the formation of compounds. Similarly, transition metal selenides have structures comparable to the corresponding sulfides, but they exhibit better electrical conductivity due to the stronger metallic properties of selenium (Zeng and Li 2015). IVB–VIIB group transition metals interact with cesium to form a lamellar structure. The VIII group is a non-lamellar structure; the lamellar structure has very strong chemical, thermodynamic and mechanical properties, and others (Peng et al. 2020). Diverse anisotropy, metal selenide is a typical layered structure, similar to sulfide, with three common phases: 1T (triangular), 2H (hexagonal), and 3R (rhombic). Among these phases, 1T has good metallicity, and all the basal sites can be used as active catalytic sites, making it an effective catalyst for the hydrogen evolution reaction. As the non-layered structure makes it easier for active oxygen sites to generate via surface oxidation, non-layered transition metal selenide are employed more frequently for catalytic oxygen evolution reaction procedures (Lu et al. 2017b; Peng et al. 2020; Wilson et al. 2001).

Transition metal selenides are gradually filled with non-bonded d-bands from IVB–VIIB and group VIII elements, and the electronic structure is changed. Catalysts with monolayer structures are direct band gap semiconductors with better conductivity. Developing layered transition metal selenide with single or multiple layers can enhance the hydrogen evolution reaction process. Two-dimensional NiWSe nanosheets were synthesized (Zhao et al. 2018). The introduction of tungsten promoted the formation of two-dimensional nanosheets, which exhibited an overpotential of 162 mV in alkaline media, relying on the layered structure and the synergistic electronic effect between layers. After being plasma-treated, Mo–Ni–Co trimetallic selenide nanorod arrangements were constructed on top of nickel–cobalt foams (Wang et al. 2020b), the molybdenum–nickel–cobalt trimetallic selenide nanorod arrays showed a low overpotential of 38 mV and were catalytically stable for more than 100 h as a result of the cumulative effects of the different metals and the interconversion between the mixed phases of molybdenum selenide 1T–2H.

The amount of electrochemically active sites and the surface shape of the catalysts are key components in the

catalytic process. Uncovering more transition metal selenide edge planes is crucial because they have more favorable catalytic activity. When exfoliated into lamellar nanosheets, palladium and selenium in palladium diselenide reveal more active sites and have high catalytic characteristics for the hydrogen evolution reaction process. Exfoliated palladium diselenide nanosheets also have a low overpotential of 138 mV at 10 mA $cm^{-2}$ and a Tafel slope of 100 mV $decade^{-1}$. Planar coordination of palladium diselenide was developed as a basic catalytic hydrogen evolution reaction (Lin et al. 2021). An in situ-induced growth technique was developed by altering nanocrystalline ferrous selenide on two-dimensional ultrathin $Ti_3C_2$TxMXene sheets to create zero-dimensional to two-dimensional heterostructures (Hao et al. 2022) (Fig. 7a), which led to the high exposed surface area, strong electronic coupling properties, and high conductivity, resulting in a competitive onset potential of 89 mV, a favorable Tc, and improved selenium nanocrystal characteristics. On a conductive substrate, transition metal selenides can be produced to lower contact impedance and

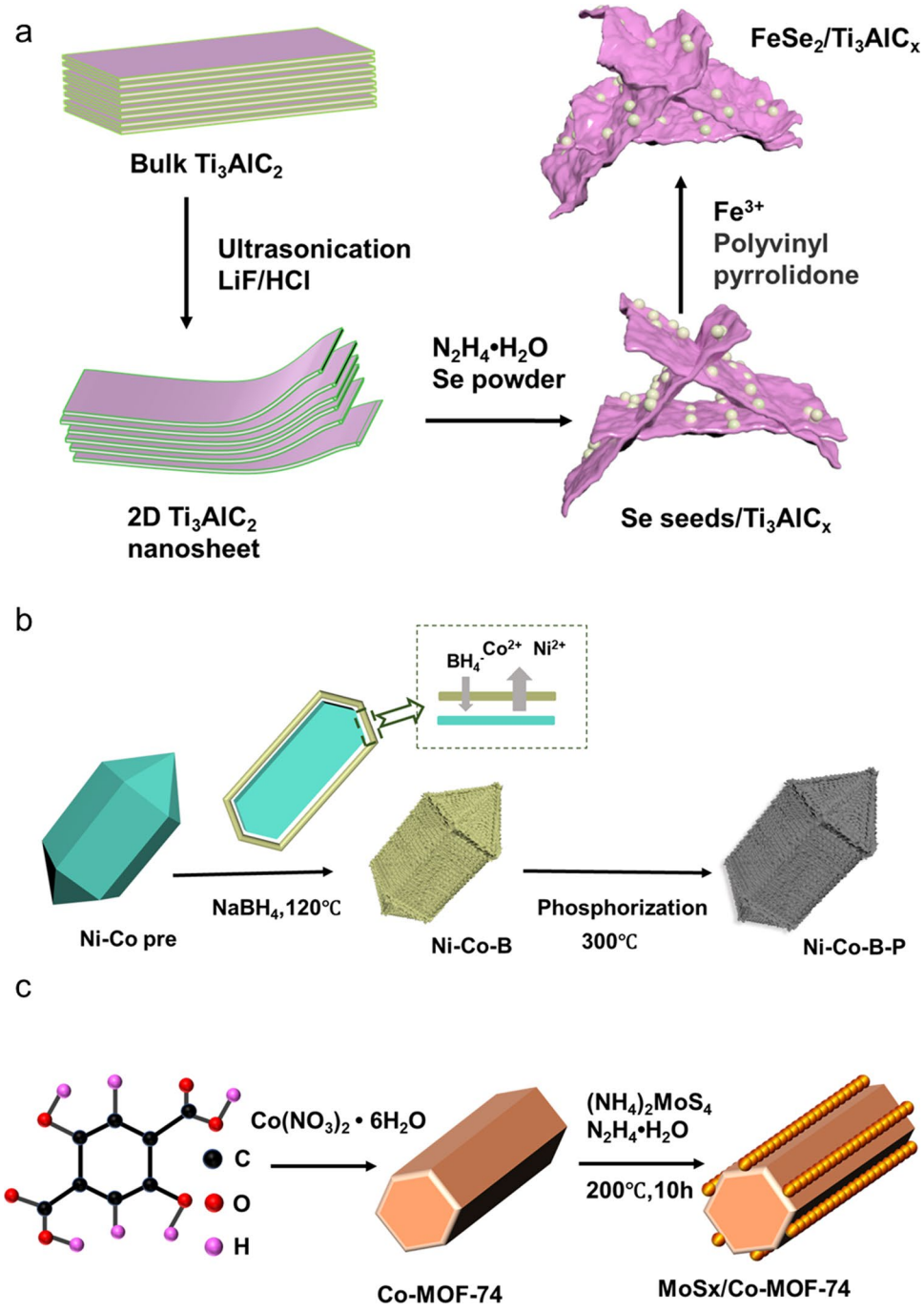


**Fig. 7** **a** Synthetic steps of the $FeSe_2/Ti_3C_2$Txhybrid. $Ti_3C_2T_x$ nanospheres were obtained by etching, then by attaching nanoscale selenium seeds to the two-dimensional surface using hydrazine hydrate. Finally, ferrous selenide nanoparticles were attached to $Ti_3C_2T_x$ by a solvothermal procedure with the help of polyvinyl pyrrolidone. $Fe^{3+}$ refers to iron ions, $N_2H_4{\cdot}H_2O$ refers to hydrazine hydrate, and Se refers to selenium. Modified from Hao et al. ( 2022); **b** schematic illustration for synthesizing boron-doped Ni–Co–P hollow nanoprisms. Ni–Co refers to nickel–cobalt, Ni–Co–B refers to nickel–cobalt–boron, and Ni–Co–B–P refers to nickel–cobalt–boron–phosphorus. Modified from Liu et al. (2021b); **c** graphical diagram of the preparation of Co–MOF–74 and $MoS_x$/Co–MOF–74 composites. C refers to carbon, O refers to oxygen, H refers to hydrogen, $Co(NO_3)_2{\cdot}6H_2O$ refers to cobalt nitrate hexahydrate, and $N_2H_4{\cdot}H_2O$ refers to hydrazine hydrate. Modified from Do et al. (2021)

boost the catalyst's ability to react with hydrogen (Yang et al. 2020b). Molybdenum selenide nanosheets and nickel selenide microislands were produced on nickel foam in a single hydrothermal stage. This method produced 10 mA $cm^{-2}$ and a very low Tafel slope of 85.7 mV $decade^{-1}$ while significantly lowering the resistance at the electrocatalyst/substrate interface, speeding up the charge and mass transfer rate of hydrolysis, and exposing more active sites. In their research, Song et al. (2020b) successfully created a ternary phase based on nickel–iron selenide on a stainless steel pad. This phase includes selenium, which is capable of forming strong covalent bonds with the metal surface, leading to increased resistivity and improved charge transfer stability. The researchers found that a low potential of just 260 mV at 75 °C was sufficient to drive a high current density of 1000 mA $cm^{-2}$.

In summary, selenium and sulfur are in the same leading group; thus, the corresponding transition metal compounds are similar to transition metal sulfides and often exist in a sheet-like structure, which also facilitates the preparation of nanosheets, increasing the specific surface area, exposing more catalytic sites and enhancing the performance of catalysts.

## Transition metal oxide

Metal oxides are helpful in various contexts due to their cheap cost and diverse chemical makeup (Abdel Maksoud et al. 2020). The most notable properties of metal oxides are their composition and structure variety and capacity to dynamically rearrange the crystal structure and quantity of electrons. Metal oxides, however, have a limited role in hydrogen evolution reaction processes because of their weak electrical conductivity, inadequate hydrogen adsorption, and low activity.

The existence of gaps modifies the electrocatalysts' electrical structure properties, which can be used to boost the catalyst's efficiency. Molybdenum oxides are typically found as α-$MoO_3$ flakes, and by exfoliating the flakes, Datta et al. (2017) created two-dimensional nanosheets. The two-dimensional structure makes it easier for exposed atoms to spill from the surface and create vacancy defects. The development of vacancies results in less surface atomic coordination, increasing the number of surface vacancies. The creation of vacancies causes a drop in the number of surface atomic coordination sites and an increase in the number of active sites, which causes the two-dimensional-$MoO_{3-x}$ nanosheets to exhibit an overpotential 142 mV value at a typical current density of 10 mA $cm^{-2}$. Existing oxygen gaps might be filled with sulfur rather than being created to generate active sites with better electron transport capacities. The catalyst has a low overpotential of 61 mV at a current density of 10 mA $cm^{-2}$. It can maintain long-term stability of up to 60 h at 1000 mA $cm^{-2}$ in a 1.0 mol/L potassium hydroxide medium. This is because sulfur adsorbs hydrogen to form SH*, which enhances the hydrogen evolution process and improves the catalytic activity (Jin et al. 2021a).

It was discovered that metal and oxide synergy enhanced hydrogen evolution reaction efficacy. A heterogeneous nickel/ nickel oxide structure was created using in situ Raman spectroscopy. It was shown that the surface β-$Ni(OH)_2$ correlated with the hydrogen evolution reaction activity of nickel/nickel oxide nanosheets. However, after maintaining a high cathodic electric potential for 2000s, the species β-$Ni(OH)_2$ disappeared (Faid et al. 2020). In order to achieve high hydrogen evolution reaction catalysis efficacy, the hydroxide species must be maintained. Developing many nickel oxide worm-like structures on nickel nanosheets increased the efficiency of oxide/metal heterojunctions (Jin et al. 2021a), resulting in heterostructures with oxygen-rich gaps and hydroxyl compounds. Nickel/nickel oxide-cp considerably reduced the 10 mA $cm^{-2}$ overpotential by 124 mV. Cobalt–MOF was calcined and grown on nickel foam, and molybdenum disulfide nanosheets were hydrothermally produced on the surface to produce $Co_3O_4/MoS_2$ heterostructures. Tafel slope driving potential at 10 mA $cm^{-2}$ is 98 mV $decade^{-1}$ (Faid et al. 2020; Muthurasu et al. 2019).

A photosensitive $WS_2$/ZnO (WZO) nano-heterojunction is constructed to improve frontal catalyst stability (Pataniya et al. 2021). The material can maintain hydrogen evolution reaction activity constant for 25 h of chronoamperometry and 2000 cycles of cyclic voltammetry. Copper impurities were doped into cobalt(III) oxide nanowire precursors to obtain $Co_3O_4$–CuO nanocomposites. This resulted in reduced hydrogen adsorption, improved conductivity, and hydrogen evolution reaction catalysts exhibiting a low Tafel slope of 65 mV $decade^{-1}$ (Tahira et al. 2019). In order to modify the material's electrical structure and fill it with oxygen gaps, sulfur was infused into cobalt oxide nanosheets (Geng et al. 2019). As a consequence, the material's hydrogen evolution reaction performance was enhanced. A controlled microporous CoMo network was used to build a $MoO_2$@CoMo heterostructure, and the catalyst's optimum overpotential for hydrogen precipitation at – 50 mA $cm^{-2}$ was just 76 mV (Han et al. 2020).

In conclusion, oxides have compositional diversity, and the presence of oxygen facilitates the construction of oxygen vacancies and enhances catalytic performance. In contrast, the preparation of oxides is relatively simple, and it becomes easy to construct heterojunctions of oxide composition as well as specific structures, which is beneficial to hydrogen production.

## Transition metal hydroxide

Nickel, cobalt, and ferrum-based hydroxides are commonly used to catalyze hydrogen evolution reaction processes, and these pristine hydroxides possess different crystalline forms, including layered mono-hydroxides and dihydroxides having the structure of bruckite-type hydroxide magnesium hydroxide, which are compounds consisting of octahedral metal ions surrounded by hydroxide ions (Evans and Slade 2006). The nickel and cobalt hydroxides are typical hydromagnesite-type hydroxides that exhibit good hydrogen evolution reaction properties in alkali, and nickel hydroxide exhibits a higher overpotential margin than cobalt hydroxide. Nickel hydroxide comprises many $Ni(OH)_{2-x}$ layers, between which anions and water molecules can be inserted. Inserting water molecules increases the interlayer spacing and decreases the interaction between neighboring layers. Nickel can also be substituted to form $Ni(OH)_2$-type hydroxides, such as NiFe-layered double hydroxide and NiCo-layered double hydroxide (Hall et al. 2015; Xu et al. 2018; Yu et al. 2018).

The pristine $TM(OH)_2$ does not exhibit weak adsorption to hydrogen. Therefore, a poor hydrogen evolution reaction in active materials shows good hydrogen evolution reaction ability when $TM(OH)_2$ modifies other metallic materials. Yuan et al. (2022) connected metal hydroxides and organic backbones using aromatic carboxylates to construct mutually cross-linked two-dimensional sheet structures, and adjacent stacks can be linked by $\pi$–$\pi$ interaction determining stability. NiCo–B–P was produced using in situ phosphorylation, taking advantage of the structural and doping properties (Liu et al. 2021b), the material possesses more active sites and high activity, and $NiCo_2$–B–PHNPs exhibited excellent hydrogen evolution reaction performance of 10 mA $cm^{-2}$ at an overpotential of 78 mV. NiCo–Co nanoprisms were used as templates and then used $NaBH_4$ for heat treatment to form NiCo-layered double hydroxide with boron doping (Fig. 7b). The hierarchical heterogeneous structure was created by coupling NiCo-layered double hydroxide nanosheets with $NiCo_2S_4$ nanorods on carbon cloth (Liu et al. 2021d). The hierarchical coupling structure improved the stability of the structure and increased electrical conductivity, the nanorods provided more active sites, the structure improved electrocatalytic performance in alkaline electrolytes, and the structure only needed an overpotential of 219 mV to reach a high current density of 50 mA $cm^{-2}$ for the hydrogen evolution reaction.

NiCo-layered double hydroxide nanosheets loaded on nickel foams were induced to amorphized by Yang et al. (2020c) using a B-doping strategy. This amorphous material's locally disordered structure is rich in oxygen vacancies, exposing more atoms in the unsaturated coordination plane and enabling the material to maintain excellent catalytic activity in 1.0 mol/L potassium hydroxide for at least 72 h. The substance works well as an electrocatalyst for hydrogen evolution reactions. In order to create catalysts with increased basic hydrogen evolution reaction activity, three-dimensional hydroxides (nickel, cobalt, iron, manganese) were grown on two-dimensional sulfide nanosheets (Zhu et al. 2018). At 128 mV at 10 mA $cm^{-2}$ in 1 mol/L potassium hydroxide, the $MoS_2/Co(OH)_2$ hybrid catalyst achieved an exceptionally low overpotential. The formation of a varied surface, which speeds up the process of breaking up the water and lowers the kinetic energy barrier, accounts for the improvement. Dong et al. (2021) also created three-dimensional heterogeneous electrocatalysts made of CoNi, CoNi LDH, and 1T–2H phase molybdenum disulfide using electrodeposition and in situ reduction. Due to the formation of CoNi(CN) alloy on the surface of the double hydroxide and the phase shift of molybdenum sulfide from the 2H phase to the 1T phase, this unique three-dimensional catalyst may decrease the kinetic energy barrier for water activation and boost the effectiveness of the hydrogen evolution process.

In conclusion, the presence of hydroxide in hydroxide makes it water-friendly. It facilitates the generation of intermediates. It is usually present in a lamellar structure, which gives it strong catalytic properties under alkaline conditions, further enhanced by self-supporting and heterogeneous structures.

## Transition metal-based-metal organic framework

Metal–organic frameworks (MOF) compounds are porous compounds in which metal ions (clusters) are interconnected through molecular interactions between organic ligands (Yang et al. 2020c). This gives metal–organic frameworks very good crystallinity, porosity, electrical conductivity, and controllable active site characteristics, which are important in promoting electron transfer and mass transfer rate (Wang et al. 2019a). The electronic coupling at the connection interface between organic ligands and metals in metal–organic frameworks greatly affects the hydrogen evolution reaction process. Changing the electronic coupling by changing different organic ligands and metal connections is possible. These superior features make metal–organic frameworks excellent electrocatalysts for hydrogen precipitation (Hua et al. 2019; Xia et al. 2015). Liquid phase diffusion, solvothermal, microwave, and layering methods can prepare metal–organic frameworks electrocatalysts.

According to Hua et al. (2019), a meso-Cu–BTC metal–organic backbone was developed, which exhibits an electrochemical hydrogen precipitation reaction in 1-mol sodium hydroxide solution with a low Tafel slope of 33.41 mV $decade^{-1}$ and long-term durability. The pristine metal–organic framework also has a porous structure that aids in mass and electron transfer. This device possesses 25 mV to start potential, a low Tafel slope of

33.41 mV decade$^{-1}$, a large current density, and long-term durability. A bimetallic metal–organic framework (CuRu–MOF) was made to aid hydrogen precipitation because bimetallic nodes expose additional active areas. As a result, they achieved a 25 mA cm$^{-2}$ current density at a 22.7 mV overpotential (Qiu et al. 2019).

The coupling of organic ligands also impacts metal–organic frameworks' active region and activity. The conjugated ligand hexaiminohexaazatrinaphthalene (HAHATN) was used (Huang et al. 2020), which led to the creation of an additional (Metal-Nitrogen) metal center with a narrow band gap that is conducive to electron transfer and mass transport. $Ni_3(HAHATN)_2$ nanosheets displayed a tiny overpotential of 115 mV at 10 mA cm$^{-2}$ with a Tafel slope (45.6 mV decade$^{-1}$). Pore engineering can be used to modify the catalytic performance of catalysts. The pores of the metal–organic framework influence the absorption and release of gases as well as the uptake of active compounds. $[Co_6(oba)_5(OH)_2(H_2O)_2(DMF)]_{4n-2}DMF$ was used in the air at a pyrolysis temperature of 100–700 °C as a way to obtain additional pores (Bagheri et al. 2021). At 300 °C, MOF with micro- and mesopores was obtained, effectively improving the catalytic activity.

A two-dimensional to three-dimensional flower-like metal–organic framework material $\{Co(BIPA)(5\text{-}OH\text{-}bdc)(DMF)\}_n$ was developed and then obtained Co-MOF-8001 by calcination with an onset potential (0.12 V) and an $E_j = 10$ value (0.193 V) with no decay in catalytic performance over 20 h of cycling (Pan et al. 2019b). Primitive metal–organic frameworks often need to be compounded with other materials to achieve better catalytic performance because of their poor electrical conductivity. Amorphous molybdenum sulfide was combined with cobalt-based metal–organic frameworks (cobalt-MOF-74) to alter molybdenum sulfide using a solvothermal process (Do et al. 2021). The best performance of 40% $MoS_x$ with a low onset potential of – 147 mV and a Tafel slope of 68 mV decade$^{-1}$ is achieved when Co-MOF-74 interacts with molybdenum sulfide to form CoMoS species, reducing the hydrogen adsorption energy. Co-MOF-74 also provides a porous framework, which results in a significant increase in the amount of surface activity of the obtained material (Fig. 7c). A cobalt-based porphyrin-like metal–organic framework was grown on carbon nanotubes (Micheroni et al. 2018), which has a covalent linkage between the metal–organic framework and carbon nanotubes, thus enhancing the electrical conductivity and the hydrogen evolution reaction conversion number (TON) and conversion frequency (TOF) of the $Hf_{12}$–CoDBP/CNT heterojunction, and this material has become the most active cobalt-based electrocatalyst.

In conclusion, metal–organic frameworks have a naturally microscopic porous structure that allows the catalyst to fully engage with the substrate. On this basis, the catalytic performance is further enhanced by changing the composition of the catalyst and compounding with other materials.

## Optimization strategies

The number of active sites, which is the primary determinant of catalytic efficacy for electrocatalytic processes, decides how effective the process will be (Nai et al. 2017). Nanomaterials can have a larger specific surface area and therefore have more active sites; as a result, nanostructures are good candidates for electrocatalysts (Cao et al. 2020). Optimization of nanostructures can improve the dispersion of metal atoms on the catalyst surface, increase the contact area between the catalyst and the substrate, and decrease the cost of the electrocatalyst (Hu et al. 2018).

The electronic bonding between the atomic orbitals on the electrocatalyst and the ions/molecules deposited on the surface is thought to be the cause of chemisorption on catalysts, according to the Newns–Anderson hypothesis (Jin et al. 2022). Consequently, the orbitals are split into two different states, the bonding state and the antibonding state. The relationship between the electronic configuration and electrocatalytic performance has been a hot topic of study, and the electronic structure is crucial (Ouyang et al. 2020). The main elements that control the electron transfer in electrocatalytic reactions are the concentration of charge carriers, the density of states, the energy band structure of the Fermi energy level, and the charge distribution of metal ions. Valence and spin states are frequently included in the electronic structure.

### Nanostructure optimization

#### Core–shell nanostructures

Materials consisting of internal core and external shell components are called core–shell nanostructures. However, it is important to note that core–shell structures are not restricted to the typical spherical particles often associated with this term (Chaudhuri and Paria 2012). A shell structure can be applied to the exterior of a range of other nanostructures, such as one-dimensional nanowires, two-dimensional nanosheets, and even three-dimensional framework structures. The shells provide the active substance within with dependable protection, permitting full exposure of the catalytic sites and enabling the catalyst to attain long-term stability (Chaudhuri and Paria 2012; Royer et al. 2022). The catalyst's electronic and chemical structure may be changed thanks to the strong connection between the core and shell, which also increases the reaction's intrinsic activity and binding energy of the intermediate. The various material compositions of the core and shell components enable the

core and shell to work together synergistically to address the fundamental phases of the hydrogen precipitation process (Liu et al. 2015). The interaction between the core and the shell will also cause a lattice mismatch in the shell layer compared to the bulk material, allowing for compression or stretching of the aggregate structure and resulting in a strain effect, further described in the following section.

Influenced by core–shell nanostructures, the synthesis of core–shell structures can be attributed to two main categories, top-down and bottom-up (Hunt and Roman-Leshkov 2018). Top-down refers to the use of various external controls (micromachining techniques, mechanical stress) to achieve a reduction in the size of the material. Bottom-up refers to using the chemical properties of molecules or atoms to self-assemble to form the corresponding structure. These include chemical, vapor deposition, and colloidal aggregation methods (Wei et al. 2011). Reaction conditions (temperature, reaction duration, precursor concentration) can be used to control the core–shell structure's size, morphology, and structural features. Bottom-up preparation of core–shell structures exists mainly by one-pot methods (precursors such as metals as well as organic ligands are added together to a specific solvent and synthesized by certain means without separation of intermediates) (Chen et al. 2015), in situ synthesis, self-assembly (precursor molecules or nanoparticles spontaneously form an ordered spatial structure through interactions), and self-templating methods (Gao et al. 2014; Zou et al. 2018).

Due to the substantial impact of the shape and molecular structure of the active site at the core–shell junction in adjusting the activity and selectivity of hydrogen evolution reaction, synergistic catalysis between cores and shells is crucial in hydrogen precipitation. On tungsten sulfide core–shell heterostructure ($FWS_2$) particles, core–shell heterostructures were created with complete tungsten sulfide shells and half-tungsten sulfide shells (Zhang et al. 2020). The heterostructures were found to have an unusually increased electron density at the interface, revealing the number of lone pairs of electrons in the active sulfur site. (Zhou et al. 2021b) developed a ternary metal phosphide using an iron-cobalt Prussian blue analog as the central material and a nickel–cobalt Prussian blue analog as the exterior material. This ternary metal phosphide demonstrated an impressive voltage performance of 1.69 V and an overpotential of just 215 mV when tested at a current density of 10 mA $cm^{-2}$. A core–shell tripartite metal carbide (max phase) structure was created with a Co/Ni-MAX phase at its center (Li et al. 2023b). The $Ta_2CoC@Ta_2CTx$ core–shell structure exhibits exceptional hydrogen evolution catalytic activity, surpassing the catalytic activity of most individual MAX phase and MXenes catalysts. The catalyst's outer shell is composed of MXenes, and it displays an overpotential of 239 mV when operating at a current density of 10 mA $cm^{-2}$.

As the central component of the initial cubic configuration of ferrous phosphide\cobalt phosphide\penta-nickel phosphide-reduced graphene oxide, the MOF–FeCo Prussian blue analog with a porous structure was chosen. This catalyst has a surplus of active sites and good electrical conductivity, requiring a cell voltage of just 1.56 V to produce a current density of 10 mA $cm^{-2}$. Fe–$Co_2P$@Fe–NC demonstrated the best catalytic performance, which was attributed to the synergistic effect between the core–shells, and the carbon shells' textual stability gave the catalyst's durability. M-$Co_2P$@MNC core–shell structures were constructed using secondary metal (iron, nickel, molybdenum, aluminum, manganese) doping (Lv et al. 2021).

Fusing one-dimensional nickel sulfide nanorods with two-dimensional molybdenum sulfide flakes produces cobalt-doped NiS@$MoS_2$ core–shell nanorods. These nanorods display an overpotential of 139.9 mV when operating at a current density of 50 $mA^{-2}$ cm. This combination of nickel sulfide nanorods and molybdenum sulfide flakes improves the contact between the catalyst and the electrolyte, leading to an accelerated charge rate similar to other catalysts. This catalyst has long-term endurance and requires a low cell potential of just 1.44 V at a current density of 10 $mA^{-2}$ cm (Gao et al. 2021). In a separate study, stacked nanosheets of layered double hydroxides were used to encase one-dimensional nanorods of CoNiP, resulting in a highly efficient catalyst. The catalyst exhibited excellent performance, requiring only a low cell potential of 1.44 V (Zhou et al. 2018a).

In conclusion, the presence of the core–shell structure allows a synergistic interaction between the core and shell materials to enhance the catalytic properties of the catalyst. Changing the morphological characteristics of the core–shell structure can further improve the catalytic ability.

### Mesoporous structure

Porous materials have inherent advantages, such as a large specific surface area and exposing more active sites. The void structure also allows the reactants to better access the catalyst, reducing the potential energy to generate reaction intermediates (Kuang et al. 2021). At the same time, generating void structures can introduce more structural defects in the catalyst, such as edges, vacancies, lattice mismatches, and others (Fu et al. 2020; Wang et al. 2021b). Porous structures can be created through various methods, such as using porous materials as templates and growing materials in the voids to obtain porous structures or by epitaxial growth on the substrate to build voids, such as growing nanowires/nanorods on the substrate with a gap between the wires and rods. Exotic three-dimensional structures can also introduce porosity by attaching catalysts to nickel foam surfaces (Dong et al. 2020; Yao et al. 2021).

Creating a permeable two-dimensional layered material is essential because the margins of two-dimensional layered materials have more active sites and catalyst activity. Mesoporous nickel disulfide thin-film electrodes can be produced using the soft template method. It has been discovered that the quantity and size of small pores greatly affect the catalytic performance. The catalyst's ability to have an overpotential in the range of 160–260 mV for 10 mA $cm^{-2}$ in alkaline media is made possible by the difference in microporous structure (Wang et al. 2021b). Mesoporous cobalt sulfide/pyrite nanoarrays ($FeS_2$–$MoS_2$@$CoS_2$–MOF) were developed using a two-dimensional metal–organic framework (Chhetri et al. 2022). The presence of mesoporous structures allowed the catalysts to produce more heterojunction interfaces, accelerating the electron transfer rate and allowing the catalyst to operate in the $FeS_2$–$MoS_2$@$CoS_2$–MOF at 10 mA $cm^{-2}$ hydrogen evolution reaction and 1 mol/L potassium hydroxide solution at 10 mA $cm^{-2}$ with a minimum overpotential of 92 mV at 20 mA $cm^{-2}$ and 211 mV at 20 mA $cm^{-2}$. In order to create mesoporous $MoS_2$/$CoMo_2S_4$ heterostructures under a nitrogen environment, a flexible template was first used (Guo et al. 2020). These heterostructures improved the catalysts' ability to catalyze both the oxygen and hydrogen precipitation reactions.

The material can also be referred to as bimetallic doped. When tested in a 1 mol/L potassium hydroxide solution, at a current density of -10 mA $cm^{-2}$ and loading of 0.35 mg $cm^{-2}$, the NiCoP catalyst demonstrated a Tafel slope of 41 mV ·$decade^{-1}$ and an overpotential of 83 mV. Hexagonal NiCoP porous nanosheets, which have a greater active area, ensure the exclusion of air bubbles, and shorten, were produced using a two-step hydrothermal process (Jia et al. 2022), metal-organic frameworks were used as a model to fabricate a hollow porous polyhedron (Wei et al. 2021). The catalyst's synergistic hollow and porous structure enhances its performance in the hydrogen precipitation reaction and mechanical stability, resulting in small Tafel slopes of 72, 101, and 176 mV ·$decade^{-1}$ and low overpotentials of 82, 102, and 261 mV in 0.5 mol/L sulfuric acid at a current density of 10 mA $cm^{-2}$, as well as in a phosphate buffer solution of 1 mol/L. Bimetallic porous hybrid materials made of nickel and $Mo_6Ni_6C$ were produced by pan using the soft-mold technique. These materials have more than 20 h of chemical endurance and two active species, nickel and $Mo_6Ni_6C$. They also have a large specific surface area and active sites (Pan et al. 2021).

In summary, the mesoporous structure has a specific surface area, and the two-dimensional material possesses more robust catalytic properties at the boundary. The mesoporous structure is introduced into the two-dimensional material to achieve a stronger catalytic effect.

## Electronic structure optimization

The electronic configuration, bonds, coordination, and strain of the atoms on the catalyst surface make up the majority of the electronic structure of catalysts. Techniques for heteroatom doping, vacancies, heterostructures, and strain can all be used to modify these structures. The catalyst's electrocatalytic performance can enhance further (Wei et al. 2021; Xiong et al. 2022).

### Doping

After heteroatoms of different electronegativity are doped into the host material, the heteroatoms may replace the host atoms in the lattice, generating local Coulomb forces and changing the arrangement of atoms in the crystal (Zhang et al. 2018b). Moreover, it can adjust the electronic configuration and vibration mode of the main atom, which affects the charge distribution on the surface of the substrate. The addition of dopants also affects the conductivity and carrier density of the catalyst, which further enhances the charge transfer to the catalyst surface and accelerates the conversion of adsorbed molecules on the catalyst surface (Lau et al. 2019; Shi et al. 2017; Xiao et al. 2018).

It has been developed that cations, anions, and cation–anion combinations different from the matrix have been used as dopants (Fig. 8). Cation doping can optimize the energy level of catalysts, while anion doping is mainly used to change the physical and chemical properties of transition metals (Liu et al. 2020, 2016). Combined cation–anion doping combines the advantages of the above doping methods (Pan et al. 2022).

Two main common ways to introduce heteroatoms into transition metal catalysts are in situ doping and post-doping. Incorporating a dopant into the precursor of the reactant, which accompanies the transition metal catalyst preparation process, and incorporating heteroatoms into the catalyst is called in situ doping. However, there are cases where the dopant and the catalyst precursor are not mutually soluble. This can be achieved by doping the transition metal carbide in an environment containing the dopant, called post-doping (Kisand et al. 2018; Miao et al. 2017).

When diatomic or polyatomic co-doping occurs, the in situ doping requirement is frequently unmet. The tuned transition metal carbide's electronic structure can subsequently be modified using the post-doping technique. The chemical vapor transfer produced NbSSe was hydrothermally post-doped with cobalt to create a two-dimensional electrocatalyst. Due to the multiple active sites acquired by co-doping the conducting phase and ternary mechanism of this catalyst, NbSSe displayed a low overpotential of 173 mV, a Tafel slope of 64 mV $decade^{-1}$, and good

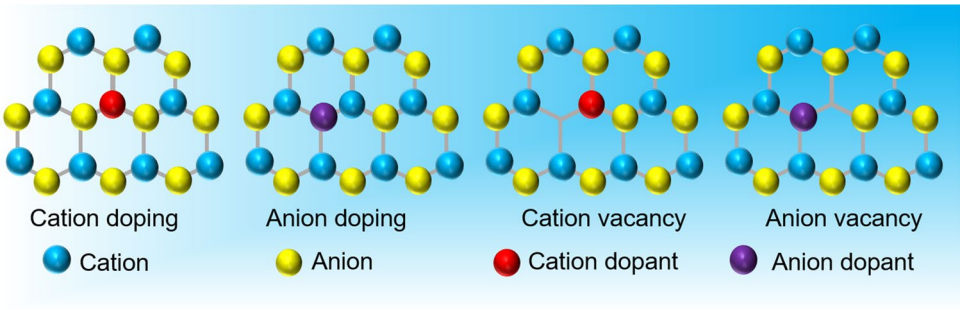


**Fig. 8** Mechanism of doping and vacancy generation. Depending on the charged nature of the doped ions, there are two types of doping: cation doping and anion doping. After doping with external ions, the crystal itself is disturbed to form a lattice distortion, which results in the absence of anions and the formation of vacancies. Both vacancies and doping bring more catalytic sites to the catalyst and enhance the catalytic process. At the same time, it also reduces the potential energy during hydrogen precipitation and optimizes the reaction process. Modified from Liu et al. (2016)

durability at a current density of 10 mA $cm^{-2}$ under 10% cobalt doping conditions (Ren et al. 2023).

Dopants with an ionic radius and electronic structure similar to the catalyst are more likely to be embedded with the transition metal carbide crystal lattice. More in situ doping technology is used to introduce dopants. Iron-doped FeCoSe@NCNSs is an example of a trimetallic catalyst composed of zinc, iron, and cobalt phthalocyanine-conjugated polymer network. This catalyst exhibits good electrocatalytic activity and has a small overpotential of 99 mV at 1 mol/L potassium hydroxide and a current density of 10 mA $cm^{-2}$. Additionally, it is a bifunctional catalyst that can achieve stable total water decomposition at a current density of 10 mA $cm^{-2}$ and a voltage of 1.66 V (Pan et al. 2022).

The physical and chemical characteristics of the catalyst itself are frequently linked to the catalytic activity of transition metal carbide, and the presence of dopants can alter these characteristics to alter the surface reaction kinetics. The vacancies of the catalyst, which can only be formed around the dopant to preserve the electroneutrality, are significantly influenced by the dopant's abundance, molecular arrangement, and valence. The improvement of hydrogen absorption can be achieved by increasing vacancies, as has been empirically proven (Tian et al. 2022; Wang et al. 2021d; Zhao et al. 2022).

Because the hydrogen-dissociation process takes place in an aqueous solution, the wettability of the catalyst's surface influences how it interacts with the reactants. In order to encourage the reciprocal interaction between the catalyst and the electrolyte and thereby support the catalytic process, an extremely hydrophilic surface is advantageous (Gao et al. 2020; Wang et al. 2017b). To increase the contact of reactants and enhance hydrogen evolution reaction activity, for instance, nitrogen and sulfur co-doped molybdenum carbide (ns-doped cobalt carbide) nanosheets with hydrophilic surfaces were produced (Zhang et al. 2021a). With an initial contact angle of 25.11, dynamic water contact angle observations revealed that the ns-doped molybdenum carbide nanosheets were highly hydrophilic. Within 10 s, the raindrops fully dispersed and moistened the surface. In comparison, the early contact angle of the ns-doped cobalt carbide nanosheets was 25.11.

In comparison, the initial contact angle of pure cobalt carbide was 40.21, and it nearly stayed there for 10 s, at 18.01. By nitrogen doping, polar molybdenum nitrogen and molybdenum-sulfur molecules were added, which increased the doped cobalt carbide surface's hydrophilicity. Cation doping, in addition to anion doping, is crucial in the alteration of the transition metal carbide surface wettability. The wettability of the nickel hydroxide nanosheets on the catalyst's surface was changed through the iron ions/nickel ion cation exchange procedure. Nickel hydroxide nanosheets in their purest form had a steady contact angle of 251, whereas $Ni_{0.83}Fe_{0.17}(OH)_2$ nanosheets had a contact angle of 131, suggesting a more hydrophilic surface (Wu et al. 2022b; Zhou et al. 2018b). The hydroxyl groups' migration and the oxygen release from the oxygen evolution reaction were sped up by the catalysts' enhanced surface wettability, which also encouraged the quick penetration of the electrodes. The powerful water-catalyst adsorption in some circumstances, which can prevent the escape of gas during water splitting, can lead to a catalytic performance increase of the hydrophobic surface for catalysts (Díaz-Coello et al. 2021; Li et al. 2019). Doping can change the electronic structure of the catalyst and regulate how reaction intermediates and electrons interact, which will increase activity by causing hybridization in the energy level of the substrate material (Chen et al. 2021c; Duraivel et al. 2022).

Tin-doped cobalt sulfide nanowire arrays have been reported to function as an electrocatalyst for the hydrogen evolution reaction (Liu et al. 2021a). The carbon fabric catalyst doped with an optimal concentration of tin-cobalt sulfide not only exhibited an improved overpotential of 161 mV at 10 mA $cm^{-2}$ and a Tafel slope of 94 mV $decade^{-1}$ but also

demonstrated excellent long-term durability during a 32-h test. The differential charge density plots of cobalt sulfide and Tin–cobalt sulfide showed that sulfur had a reduced electron density and a higher oxidation state, which led to the decision to use the cobalt sulfide-stabilized (001) portion as the active surface. Bader charge estimates, which indicate that the tin dopant can provide fewer electrons to sulfur than cobalt, further support this result. Density functional theory estimates are based on these two features because the intrinsic catalytic activity of hydrogen evolution reaction primarily relies on the intrinsic and $\Delta GH^*$ (Bolar et al. 2021; Díaz-Coello et al. 2021). Near the Fermi energy level, the total density of states of Tin-doped cobalt sulfide and cobalt sulfide is not zero, showing metallic characteristics in both materials. Better intrinsic conductivity and a greater carrier concentration are implied by tin-bigger cobalt sulfide's total density of states near the Fermi energy level compared to cobalt sulfide (Liu et al. 2021a), which improves the electrocatalyst's ability to transfer charges in the hydrogen evolution reaction process.

In summary, doping brings multiple enhancements to the material; conductivity, number of active sites, hydrophilicity, ability to bind to the substrate, and potential reaction energy. It also allows the material to produce vacancies and phase transitions, giving it a stronger catalytic ability.

### Vacancies

Vacancies allow the catalyst surface charge distribution to change without ruining the initial lattice, enhancing the catalytic activity (Lee et al. 2019). By allowing charge to accumulate in one direction and thereby increasing the number of active sites, the presence of vacancies modifies the local atomic structure and coordination number, which further modifies the electronic structure of the catalyst close to the vacancies and the equilibrium binding energy of $H^*$ (Chen et al. 2020a; Lei et al. 2019; Sun et al. 2021b).

Vacancy engineering consists of both cation and anion vacancies. Cation-deficient catalysts can be obtained by removing small amounts of metal cations from the catalyst, while anion vacancies are obtained by removing non-metal anions, which are commonly oxygen, sulfur, phosphorus, selenium, and others (Chuangchote and Roongraung 2023; Pan and Wang 2021; Yan et al. 2017). Vacancies can be generated by selective electrochemical removal, plasma etching, acid–base etching, organic molecular-assisted devices, chemical reduction, and heat treatment. The generation of vacancies affects the charge separation, carrier mobility, and energy band changes of the catalyst, so vacancy engineering affects the conductivity, intrinsic activity, chemical stability, and adsorption of reaction intermediates (Fang et al. 2020; Zhang et al. 2019b; Zhuang et al. 2020).

Oxygen vacancies can greatly enhance electrical conductivity and promote electron transfer, enhancing the electrocatalytic reaction. The nanostructured Co–Mo–B/$CoMoO_{4-x}$ electrocatalysts were attached to the foam cobalt using a hydrothermal method combined with forging $NaBH_4$ reduction treatment, and the attached $CoMoO_{4-x}$ is rich in oxygen vacancies. The relevant density function theory calculations can be obtained that the generation of oxygen vacancies in the $CoMoO_4$ lattice narrows the energy gap (Ren et al. 2021). This catalyst has enhanced catalytic activity thanks to the creation of synergistic active sites, which also improves its electrical conductivity. It swings just by 8 mV throughout a 100-h (100 mA $cm^{-2}$) constant current test and only needs an overpotential of 55 mV to deliver 10 mA $cm^{-2}$.

The electrocatalytic activity of baseline inactive 2H-molybdenum sulfide sites can be activated by adding sulfur vacancies and strain (Ma et al. 2020b). A chemical reduction technique was employed by Gao et al. (2018) to introduce sulfur vacancies in multilayer molybdenum sulfide nanosheets, as well as in bulk and industrial molybdenum sulfide, resulting in improved electrocatalytic properties (Han et al. 2019b). Sulfur and molybdenum voids and the number of electrons close to the molybdenum sulfide Fermi energy level are allowed. The sulfur and molybdenum gaps increase the number of electrons and energy gap near the molybdenum sulfide Fermi energy level to enhance the performance of the hydrogen evolution process. As a result, there is a 126 mV overpotential at a 100 mA $cm^{-2}$ current density and a 38 mV·$decade^{-1}$ Tafel slope.

In summary, vacancy engineering affects the catalyst conductivity, intrinsic activity, chemical stability, and adsorption of reaction intermediates, which are all decisive factors affecting the catalyst, and vacancy is an effective way to improve the catalytic effect of the catalyst.

### Heterogeneous structure

Heterojunction catalysts exhibit superior catalytic performance to single-phase catalysts, making them efficient multiphase catalysts (Yu et al. 2019). In heterojunction catalysts, electrons can rearrange near the heterogeneous structure to enhance the activity of active sites. These active sites can also synergize with each other to realize the enhancement of catalytic performance (Li et al. 2021). The structural diversity of heterojunctions allows the design of nanostructured porous structures or core–shell structures to further enhance the catalyst performance. The synthesis methods of heterostructured catalysts are diverse, and the common methods include the hydrothermal method, crystal growth, electrodeposition, and self-assembly (Li et al. 2023a; Sun et al. 2021a).

The presence of heterojunctions first increases the active catalytic site, which enhances the H* adsorption/desorption

during the catalytic process and promotes the precipitation of hydrogen gas. The hydrothermal method synthesized the disulfide rhenium/ nickel sulfide heterostructure in situ on nickel foam (Liu et al. 2023). The heterostructure showed excellent hydrophilicity and electron redistribution at the interface of disulfide rhenium and nickel sulfide, accumulating electrons on disulfide rhenium. This enhanced the formation of sulfur-hydrogen bonds, optimized the absorption energy of H*, and facilitated hydrogen desorption during the hydrogen evolution reaction and hydrogen gas precipitation. The catalyst demonstrated an overpotential of 78 mV at a current density of 10 mA $cm^{-2}$, outperforming platinum/carbon significantly at high current densities. In contrast, cobalt-doped cobalt disulfide/nickel disulfide heterostructures were synthesized on carbon substrates using a three-step hydrothermal method, where lattice mismatch promotes defect generation and accelerates the electron transfer rate, allowing the metallicity with cobalt sulfide(II) to change from semiconductor properties to a band gap with 0 eV, reducing the free energy of hydrogen adsorption during hydrogen evolution reaction and enhancing the hydrogen evolution reaction process (Zheng et al. 2021). Nickel heterostructured catalyst can achieve tunable binding of hydroxyl and hydrogen to promote $H^*$ conversion, exhibiting a rather high mass activity (20.6 A $mg^{-1}$) at 100 mV overpotential (Zhou et al. 2021a).

Adjusting the heterojunction structure can improve the stability and durability of the catalyst. Using chalcogenide oxide ($La_{0.5}Sr_{0.5}CoO_{3-\delta}$) and molybdenum diselenide to construct the heterostructure allows for stable catalyst operation within 1000 h with extreme electrochemical durability and negligible performance fluctuations (Oh et al. 2019). The overall water electrolysis at a current density of 100 mA $cm^{-2}$ energy efficiency was calculated to be 63.9%.

The electrocatalytic reaction generally occurs at the interface part of the heterojunction. The interfacial engineering in the heterojunction strongly influences the electron transfer, further changing the adsorption/desorption energy of $H^*$ in the hydrogen evolution reaction (Wang et al. 2020a, c; Yang et al. 2020a). 1T-molybdenum sulfide is an acidic catalyst that does not achieve good catalysis under alkaline conditions. However, when it forms a heterostructure with alkaline hydroxide, it has an enhanced alkaline hydrogen evolution reaction capability. Modification of 1T-molybdenum sulfide by interface engineering with nickel hydroxide (Chen et al. 2020b), This catalyst is set up at the junction border of molybdenum sulfide and nickel hydroxide, and it has a low Tafel slope of 30 mV $decade^{-1}$ in 1 mol/L potassium hydroxide. It only needs 57 and 112 mV overpotential to generate hydrogen evolution reaction current densities of 10 and 100 mA $cm^{-2}$, respectively. The catalyst surface and electron density can both be successfully changed by nitrogen doping. The nickel sulfide/molybdenum disulfide heterostructure was modified by Yang et al. (2019), using nitrogen doping. It has improved hydrogen evolution reaction characteristics under alkaline circumstances with a low excess current density of 71 mV (10 mA $cm^{-2}$), a tiny Tafel slope of 79 mV $decade^{-1}$, and good stability (Yang et al. 2019).

In summary, heterojunctions effectively increase the number of active sites and stabilize the catalyst. Increasing active sites is often at junctions, so building more heterojunctions and junctions is an excellent way to enhance catalytic performance.

### Strain

The interatomic lengths on the catalyst surface are modified by strain engineering. The strain on the surface is accomplished in transition electrocatalysts, which are typically elastic and contain tensile and compressive strains (Yang et al. 2021). This alters the catalyst's electronic structure, which is closely linked to the reaction intermediates' adsorption and activation energy bases. The existing reported strain engineering is mainly present in the core–shell structure with lattice mismatch, loaded catalysts, defects, dimensional changes, and doped alloys. Under the core–shell structure, the materials of the core and shell are not the same, resulting in different lattice parameters between cores and shells, and there exists a lattice shape variation between core–shell interfaces and the strain between cores and shells is mainly affected by the core–shell lattice mismatch, the size of the shell, and the shape of the core (Tian et al. 2019; Zhao et al. 2020). The CuPd@NiPd core–shell structure was constructed (Liu et al. 2022). Subjected to lattice strain, the lattice in the core–shell region was compressed, allowing the d-band center of the palladium site to produce a downward shift, giving it good catalytic properties.

With a current density of 10 mA $cm^{-2}$ for hydrogen evolution reaction in 1 mol/L potassium hydroxide at 85 mV overpotential, a layered core–shell $NiWO_4$@$NiCoO_xS_y$/NCF was built on NiCo foam (Yang et al. 2023b), which benefited from the strain effect and allowed the catalyst to have strong synergy as well as a high exposure area, thus exhibiting good catalytic properties. The catalyst continued to have a good catalytic effect after 72 h of operation.

The loaded catalysts' strain mechanism is essentially the same as that of the core–shell structure because both are strained due to the difference in materials. The lattice gap between the carrier and the loadings produces lattice mismatch and electronic structure at the interface. Metal oxide oxygen gaps may deform the lattice. In order to cause strain generation and improve catalytic performance, titanium oxide on a platinum electrode was first loaded with a large oxygen vacancy content (Cheng et al. 2021). When used as positive and negative electrodes for all-water electrolysis

in alkaline media, (Song et al. 2020a) used molybdenum disulfide-coated tri-nickel disulfide, whose original lattice became distorted due to stretching. With a hydrogen evolution reaction of 81 mV at 10 mA $cm^{-2}$, this structure offered the material a greater specific surface area and more active sites during exposure, needing a cell voltage of just 1.54 V at 100 mA $cm^{-2}$.

Defect-induced strain is distinct from lattice-induced strain mostly due to the defects' effect on the interatomic bond lengths close by, which greatly affects the catalyst's efficiency. One study used metal–organic frameworks as a template, reducing agent, and carbon supply during cold and hot impact calcination to create a tubular electrocatalyst out of carbon flakes and nickel nanoparticles (Zhang et al. 2021b). The calcination time and temperature can be used to control the density of defects, which induces strain effects, which would accelerate the kinetics of the hydrogen evolution reaction process. Using selenium instead of sulfur in $Cu_2WS_4$ promotes chemical strain generation in the lattice, thus increasing the active sites for hydrogen adsorption and desorption, allowing the catalyst to perform substantially better and maintain good stability (Tiwari et al. 2018). When different atoms are doped into a catalyst with metallic elements, the interatomic distances are affected due to the size difference between the base atom and the doped atom, which results in lattice strain, most typically in bimetallic alloys.

The surface of the nano-ion, due to the effect brought by the size, will make a mismatch between its interatomic distance and that of the native material, having a higher surface energy, which will further cause a passing strain. Cobalt(II) oxide is a good electrocatalyst, and cobalt oxide nanorods using strain engineering could be prepared, thanks to the strain on the surface of the nanorods, allowing a large number of oxygen vacancies to be created on the surface of the oxides, as well as allowing the energy band of oxygens 2p of cobalt oxide to shift upward and the hydrogen adsorption energy to tend to the optimal value, weakening the hydrogen adsorption (Ling et al. 2017).

In summary, various sources of strain can enhance a catalyst's active site and reaction kinetics, leading to improved catalytic ability. Transition metal-based catalysts with different electronic and nanostructures can also improve the hydrogen evolution reaction properties, as shown in Table 2.

## Perspective

Despite various theories proposed for the hydrogen evolution reaction of electrolyzed water under alkaline conditions, the mechanism through which pH affects its activity remains unclear. It was suggested that the reaction rate is determined by the additional energy barrier introduced by hydrolysis on the surface of platinum (Subbaraman et al. 2011). In contrast, other authors pointed out that the reaction kinetics are determined by the binding energy between the catalyst and hydrogen intermediate H* (Sheng et al. 2015). Other influencing factors are reported in the literature, such as the potential of zero free charges and anion transfer efficiency through the electrochemical bilayer region. These theories focus on answering two key questions about the alkaline hydrogen evolution reaction mechanism: (1) What is the real reason for the slow kinetics? (2) To what extent does the hydrolysis process affect the overall reaction kinetics compared with other factors (such as the potential of zero free charges) (Kim et al. 2019)?

Because the reaction mechanism is unclear, developing related catalysts depends on repeated tests and accumulated experience. In particular, the adsorption of all intermediates should be considered in the design of catalysts when the influence weights of the intermediates involved in the reaction (i.e., $H^*$, $OH^*$, and $H_2O^*$) are uncertain (Abdelghafar et al. 2022). It is hoped that catalysts with the lowest activation barrier and suitable interaction force with intermediate products can be designed by adjusting the electronic and physical structure of materials (Oh et al. 2016). Calculation methods such as density functional theory are usually used to clarify the quantitative relationship between the inherent characteristics of different materials and reaction properties (Liu et al. 2023).

Although these findings align with the experimental data of hydrogen evolution reaction under acidic conditions, they may not accurately predict the reaction in an alkaline environment. This is because multiple rate control steps likely determine reactivity in alkaline electrolytes. Additionally, other factors, such as the electrochemical environment of the reaction interface and the hybrid physical structure of the catalyst, may have a greater influence on the reaction process than the pH environment (Jin et al. 2018). Hence, it is essential for researchers to further explore how to design highly active electrocatalysts by regulating the electronic structure or constructing active sites.

Based on the analysis, the future research and development trend of hydrogen evolution catalysts based on transition metals exhibits the following characteristics: (1) excellent hydrogen evolution catalysts require more active sites and lower charge transfer impedance. Self-supporting materials can avoid adhesives, effectively reducing the charge transfer impedance of electrodes and generating more catalytic active sites for the reaction. (2) Stability is crucial for hydrogen evolution catalysts to meet the requirements of industrial production. Element doping and composite engineering are effective methods for enhancing material stability. (3) Considering the impact on the environment and the electrocatalyst itself, the future development of electrolytic

**Table 2** Hydrogen evolution reaction properties of transition metal-based catalysts with various electronic and nanostructures

| Optimization method | Strategy | Catalyst | Electrolyte | $\eta_{10}$ (mV) | Tafel slope (mV·decade$^{-1}$) | References |
|---|---|---|---|---|---|---|
| Nanostructure | Core–shell nanostructures | $Co_9S_8/HWS_2/CNFs$ | 1 mol/L potassium hydroxide | 87 | 72 | Zhang et al. (2020) |
| | | $Ta_2CoC@Ta_2CT_x$ | | 239 | 56 | Li et al. (2023b) |
| | | CoNiP@LDH-50 | | 89 | 82 | Zhou et al. (2018a) |
| | Mesoporous structure | $FeS_2–MoS_2@CoS_2–MOF$ | | 90.2 | 70.2 | Chhetri et al. (2022) |
| | | NiCoP | | 83 | 41 | Jia et al. (2022) |
| Electronic Structure | Doping | h-CoFeNi LDHs | 1 mol/L potassium hydroxide | 71 | 83 | Sun et al. (2020) |
| | | Ni–FeP/TiN/CC | | 75 | 73 | Peng et al. (2018) |
| | | Ni–CoP/HPFs | | 92 | 71 | Pan et al. (2019a) |
| | | $Co–NiS_2$ NSs | | 80 | 43 | Yin et al. (2019) |
| | | $Ni_{0.89}Co_{0.11}Se_2$ MNSN/NF | | 85 | 52 | Liu et al. (2017) |
| | | NiFeRu–LDH | | 29 | 31 | Chen et al. (2018a) |
| | | Ni, Zn CoO NRs (nanorods) | | 53 | 47 | Ling et al. (2019) |
| | | C, N–$NiPS_3$ | | 53.2 | 38.2 | Wang et al. (2020d) |
| | Vacancies | $MoS_2$ | 0.1 mol/L potassium hydroxide | 160 | 80 | Wang et al. (2020d) |
| | | $MoO_{3-x}$ | | 140 | 56 | Luo et al. (2016) |
| | | NiP@NF | 1 mol/L potassium hydroxide | 27.7 | 30.88 | Duan et al. (2020) |
| | | NiO NRs | | 110 | 100 | Zhang et al. (2018d) |
| | | P–$Co_3O_4$ | | 120 | 52 | Xiao et al. (2017) |
| | Heterostructures | 2DPC–RuMo (Nanosheets) | 1 mol/L potassium hydroxide | 18 | 25 | Tu et al. (2020) |
| | | $MoO_2$–FeP@C | | 103 | 48 | Yang et al. (2020a) |
| | | $NiPS_3/Ni_2P$ | | 85 | 82 | Liang et al. (2019) |
| | Strain | $NiS_{0.5}Se_{0.5}$ | 1 mol/L potassium hydroxide | 70 | 78 | Wang et al. (2020e) |
| | | Ru/np–$MoS_2$ | | 30 | 31 | Jiang et al. (2021) |

Nanostructure control plays a crucial role in enhancing the physical properties of materials by increasing specific surface area and the number of active sites. Meanwhile, electronic structure regulation can improve the intrinsic activity of the catalyst, lower the activation energy of reaction intermediates, and optimize the electronic energy band structure. Doping and vacancy can affect the catalyst's performance by altering the number of anions, cations, and anions. Both nanostructures and electronic structures also impact the conductivity of materials, thereby ensuring high electrocatalyst performance. Density function theory calculation can be used to evaluate the catalyst's performance and provide guidance for further improving its catalytic efficiency

water decomposition medium tends to move toward a neutral medium with mild conditions (Anantharaj et al. 2021).

## Conclusion

Water electrolysis is a commonly employed technique for generating hydrogen, but there is a pressing need to develop highly active hydrogen evolution catalysts that can lower the reaction barrier. Electrochemical hydrogen evolution materials based on transition metals are promising due to their affordability, good conductivity, and high stability. This review provides a brief overview of the electrocatalytic hydrogen evolution mechanism and summarizes various approaches to enhance the hydrogen evolution activity of transition metal-based compounds. Additionally, we classify and discuss the electrocatalytic activity and optimization methods of transition metal-based materials.

Transition metal-based electrocatalysts have been extensively researched and utilized as catalysts in the hydrogen evolution reaction during alkaline water electrolysis. These catalysts consist of various transition metals, such as iron, cobalt, nickel, manganese, and copper. Their utilization has the potential to greatly enhance the efficiency and cost-effectiveness of hydrogen production through this process. These metals' flexible and intricate electronic structures provide ample opportunities to fine-tune and enhance their catalytic activity and stability for the hydrogen evolution reaction in alkaline water electrolysis.

Developing additional hydrogen evolution catalysts compatible with alkaline water is a prevailing trend. Further exploration of transition metal-based electrocatalysts

is essential, particularly in preventing the decline of catalytic efficiency or deactivation of catalytic materials during long-term operation. By integrating the approaches mentioned above for enhancing the hydrogen evolution activity of materials, new electrocatalysts with low costs and high efficiency and stability can be designed, paving the way for sustainable large-scale hydrogen production and clean utilization in the future.

**Acknowledgements** Dr. Ahmed I. Osman and Prof. David W. Rooney wish to acknowledge the support of The Bryden Centre project (Project ID VA5048), which was awarded by The European Union's INTERREG VA Programme, managed by the Special EU Programmes Body (SEUPB), with match funding provided by the Department for the Economy in Northern Ireland and the Department of Business, Enterprise and Innovation in the Republic of Ireland.

**Funding** This project was supported by SEUPB Bryden Centre project (Project ID VA5048).

## Declarations

**Conflict of interest** The authors declare no conflict of interest.



## References

Abdel Maksoud MIA, Fahim RA, Shalan AE, Abd Elkodous M, Olojede SO, Osman AI, Farrell C, AaH A-M, Awed AS, Ashour AH, Rooney DW (2020) Advanced materials and technologies for supercapacitors used in energy conversion and storage: a review. Environ Chem Lett 19:375–439. https://doi.org/10.1007/s10311-020-01075-w

Abdel Maksoud MIA, Bedir AG, Bekhit M, Abouelela MM, Fahim RA, Awed AS, Attia SY, Kassem SM, Elkodous MA, El-Sayyad GS, Mohamed SG, Osman AI, AaH A-M, Rooney DW (2021) $MoS_2$-based nanocomposites: synthesis, structure, and applications in water remediation and energy storage: a review. Environ Chem Lett 19:3645–3681. https://doi.org/10.1007/s10311-021-01268-x

Abdelghafar F, Xu X, Jiang SP, Shao Z (2022) Designing single-atom catalysts toward improved alkaline hydrogen evolution reaction. Mater Rep Energy. https://doi.org/10.1016/j.matre.2022.100144

Anantharaj S, Noda S, Jothi VR, Yi S, Driess M, Menezes PW (2021) Strategies and perspectives to catch the missing pieces in energy-efficient hydrogen evolution reaction in alkaline media. Angew Chem Int Ed 60:18981–19006. https://doi.org/10.1002/anie.202015738

Ang H, Tan HT, Luo ZM, Zhang Y, Guo YY, Guo G, Zhang H, Yan Q (2015) Hydrophilic nitrogen and sulfur co-doped molybdenum carbide nanosheets for electrochemical hydrogen evolution. Small 11:6278–6284. https://doi.org/10.1002/smll.201502106

Bagheri M, Masoomi MY, Dominguez E, Garcia H (2021) High hydrogen release catalytic activity by quasi-MOFs prepared via post-synthetic pore engineering. Sustain Energy Fuels 5:4587–4596. https://doi.org/10.1039/d1se00661d

Bolar S, Shit S, Murmu NC, Samanta P, Kuila T (2021) Activation strategy of MoS(2) as HER electrocatalyst through doping-induced lattice strain, band gap engineering, and active crystal plane design. ACS Appl Mater Interfaces 13:765–780. https://doi.org/10.1021/acsami.0c20500

Cao LM, Lu D, Zhong DC, Lu TB (2020) Prussian blue analogues and their derived nanomaterials for electrocatalytic water splitting. Coord Chem Rev 407:213156. https://doi.org/10.1016/j.ccr.2019.213156

Carenco S, Portehault D, Boissiere C, Mezailles N, Sanchez C (2013) Nanoscaled metal borides and phosphides: recent developments and perspectives. Chem Rev 113:7981–8065. https://doi.org/10.1021/cr400020d

Chen PZ, Xu K, Fang ZW, Tong Y, Wu JC, Lu XL, Peng X, Ding H, Wu CZ, Xie Y (2015) Metallic $Co_4N$ porous nanowire arrays activated by surface oxidation as electrocatalysts for the oxygen evolution reaction. Angew Chem Int Ed 54:14710–14714. https://doi.org/10.1002/anie.201506480

Chen Z, Ma Z, Song J, Wang L, Shao G (2016) Novel one-step synthesis of wool-ball-like Ni-carbon nanotubes composite cathodes with favorable electrocatalytic activity for hydrogen evolution reaction in alkaline solution. J Power Sources 324:86–96. https://doi.org/10.1016/j.jpowsour.2016.04.101

Chen P, Zhou T, Zhang M, Tong Y, Zhong C, Zhang N, Zhang L, Wu C, Xie Y (2017) 3D nitrogen-anion-decorated nickel sulfides for highly efficient overall water splitting. Adv Mater. https://doi.org/10.1002/adma.201701584

Chen GB, Wang T, Zhang J, Liu P, Sun HJ, Zhuang XD, Chen MW, Feng XL (2018a) Accelerated hydrogen evolution kinetics on NiFe-layered double hydroxide electrocatalysts by tailoring water dissociation active sites. Adv Mater 30:1706279. https://doi.org/10.1002/adma.201706279

Chen J, Jia J, Wei Z, Li G, Yu J, Yang L, Xiong T, Zhou W, Tong Q (2018b) Ni and N co-doped $MoC_x$ as efficient electrocatalysts for hydrogen evolution reaction at all-pH values. Int J Hydrog Energy 43:14301–14309. https://doi.org/10.1016/j.ijhydene.2018.05.162

Chen H, Liang X, Liu Y, Ai X, Asefa T, Zou X (2020a) Active site engineering in porous electrocatalysts. Adv Mater 32:e2002435. https://doi.org/10.1002/adma.202002435

Chen WS, Gu JJ, Du YP, Song F, Bu FX, Li JH, Yuan Y, Luo RC, Liu QL, Zhang D (2020b) Achieving rich and active alkaline hydrogen evolution heterostructures via interface engineering on 2D 1T-$MoS_2$ quantum sheets. Adv Funct Mater 30:2000551. https://doi.org/10.1002/adfm.202000551

Chen LW, Guo X, Shao RY, Yan QQ, Zhang LL, Li QX, Liang HW (2021a) Structurally ordered intermetallic Ir3V electrocatalysts for alkaline hydrogen evolution reaction. Nano Energy. https://doi.org/10.1016/j.nanoen.2020.105636

Chen PR, Ye JS, Wang H, Ouyang LZ, Zhu M (2021b) Recent progress of transition metal carbides/nitrides for electrocatalytic water splitting. J Alloys Compd. https://doi.org/10.1016/j.jallcom.2021.160833

Chen XB, Sheng L, Li SX, Cui Y, Lin TR, Que XY, Du ZH, Zhang ZY, Peng J, Ma HL, Li JQ, Qiu JY, Zhai ML (2021c) Facile syntheses and in-situ study on electrocatalytic properties of superaerophobic $Co_xP$-nanoarray in hydrogen evolution reaction. Chem Eng J 426:131029. https://doi.org/10.1016/j.cej.2021.131029

Cheng X, Lu Y, Zheng LR, Pupucevski M, Li HY, Chen G, Sun SR, Wu G (2021) Engineering local coordination environment of atomically dispersed platinum catalyst via lattice distortion of support for efficient hydrogen evolution reaction. Mater Today Energy 20:100653. https://doi.org/10.1016/j.mtener.2021.100653

Chhetri K, Muthurasu A, Dahal B, Kim T, Mukhiya T, Chae SH, Ko TH, Choi YC, Kim HY (2022) Engineering the abundant heterointerfaces of integrated bimetallic sulfide-coupled 2D MOF-derived mesoporous $CoS_2$ nanoarray hybrids for electrocatalytic water splitting. Mater Today Nano 17:100146. https://doi.org/10.1016/j.mtnano.2021.100146

Chuangchote S, Roongraung K (2023) Perovskite materials for hydrogen production. Mater Hydrog Prod Convers Storage. https://doi.org/10.1002/9781119829584.ch18

Csernica PM, McKone JR, Mulzer CR, Dichtel WR, Abruna HD, DiSalvo FJ (2017) Electrochemical hydrogen evolution at ordered $Mo_7Ni_7$. ACS Catal 7:3375–3383. https://doi.org/10.1021/acscatal.7b00344

Dai RJ, Zhang H, Zhou WJ, Zhou Y, Ni ZT, Chen J, Zhao SW, Zhao YF, Yu FY, Chen AR, Wang RF, Sun T (2022) Interface engineering of bimetallic nitrides nanowires as a highly efficient bifunctional electrocatalyst for water splitting. J Alloys Comps 919:165862. https://doi.org/10.1016/j.jallcom.2022.165862

Datta RS, Haque F, Mohiuddin M, Carey BJ, Syed N, Zavabeti A, Zhang B, Khan H, Berean KJ, Ou JZ, Mahmood N, Daeneke T, Kalantar-zadeh K (2017) Highly active two dimensional α-$MoO_{3-x}$ for the electrocatalytic hydrogen evolution reaction. J Mater Chem A 5:24223–24231. https://doi.org/10.1039/C7TA07705J

David M, Ocampo-Martínez C, Sánchez-Peña R (2019) Advances in alkaline water electrolyzers: a review. J Energy Storage 23:392–403. https://doi.org/10.1016/j.est.2019.03.001

Díaz-Coello S, Afonso MM, Palenzuela JA, Pastor E, García G (2021) Composite materials from transition metal carbides and ionic liquids as electrocatalyst for hydrogen evolution in alkaline media. J Electroanal Chem 898:115620. https://doi.org/10.1016/j.jelechem.2021.115620

Dittmeyer R, Grunwaldt JD, Pashkova A (2015) A review of catalyst performance and novel reaction engineering concepts in direct synthesis of hydrogen peroxide. Catal Today 248:149–159. https://doi.org/10.1016/j.cattod.2014.03.055

Do HH, Van Le Q, Tekalgne MA, Tran AV, Lee TH, Hong SH, Han SM, Ahn SH, Kim YJ, Jang HW (2021) Metal–organic framework-derived $MoS_x$ composites as efficient electrocatalysts for hydrogen evolution reaction. J Alloys Compd 852:156952. https://doi.org/10.1016/j.jallcom.2020.156952

Dong X, Liu X, Chen H, Xu X, Jiang H, Gu C, Li Q, Qiao S, Zhang X, Hu Y (2020) Hard template-assisted N, P-doped multifunctional mesoporous carbon for supercapacitors and hydrogen evolution reaction. J Mater Sci 56:2385–2398. https://doi.org/10.1007/s10853-020-05303-0

Dong JN, Zhang XN, Huang JY, Hu J, Chen Z, Lai YK (2021) In-situ formation of unsaturated defect sites on converted CoNi alloy/Co-Ni LDH to activate $MoS_2$ nanosheets for pH-universal hydrogen evolution reaction. Chem Eng J 412:128556. https://doi.org/10.1016/j.cej.2021.128556

Duan JJ, Chen S, Ortiz-Ledon CA, Jaroniec M, Qiao SZ (2020) Phosphorus vacancies that boost electrocatalytic hydrogen evolution by two orders of magnitude. Angew Chem Int Ed 59:8181–8186. https://doi.org/10.1002/anie.201914967

Duraivel M, Nagappan S, Park KH, Ha CS, Prabakar K (2022) Transition metal oxy/hydroxides functionalized flexible halloysite nanotubes for hydrogen evolution reaction. J Colloid Interface Sci 618:518–528. https://doi.org/10.1016/j.jcis.2022.03.095

Dutta S, Indra A, Feng Y, Han H, Song T (2019) Promoting electrocatalytic overall water splitting with nanohybrid of transition metal nitride-oxynitride. Appl Catal B Environ 241:521–527. https://doi.org/10.1016/j.apcatb.2018.09.061

Faid AY, Barnett AO, Seland F, Sunde S (2020) Ni/NiO nanosheets for alkaline hydrogen evolution reaction: in situ electrochemical-Raman study. Electrochim Acta 361:137040. https://doi.org/10.1016/j.electacta.2020.137040

Fan MH, Chen H, Wu YY, Feng LL, Liu YP, Li GD, Zou XX (2015) Growth of molybdenum carbide micro-islands on carbon cloth toward binder-free cathodes for efficient hydrogen evolution reaction. J Mater Chem A 3:16320–16326. https://doi.org/10.1039/C5TA03500G

Fang HX, Guo H, Niu CG, Liang C, Huang DW, Tang N, Liu HY, Yang YY, Li L (2020) Hollow tubular graphitic carbon nitride catalyst with adjustable nitrogen vacancy: enhanced optical absorption and carrier separation for improving photocatalytic activity. Chem Eng J 402:126185. https://doi.org/10.1016/j.cej.2020.126185

Fu HQ, Zhang L, Wang CW, Zheng LR, Liu PF, Yang HG (2018) 1D/1D hierarchical nickel sulfide/phosphide nanostructures for electrocatalytic water oxidation. ACS Energy Lett 3:2021–2029. https://doi.org/10.1021/acsenergylett.8b00982

Fu HH, Chen L, Gao HJ, Yu XK, Hou J, Wang G, Yu F, Li HQ, Fan CC, Shi YL, Guo XH (2020) Walnut shell-derived hierarchical porous carbon with high performances for electrocatalytic hydrogen evolution and symmetry supercapacitors. Int J Hydrog Energy 45:443–451. https://doi.org/10.1016/j.ijhydene.2019.10.159

Gao Q, Liu N, Wang S, Tang Y (2014) Metal non-oxide nanostructures developed from organic-inorganic hybrids and their catalytic application. Nanoscale 6:14106–14120. https://doi.org/10.1039/c4nr05035e

Gao DQ, Xia BR, Wang YY, Xiao W, Xi PX, Xue DS, Ding J (2018) Dual-native vacancy activated basal plane and conductivity of $MoSe_2$ with high-efficiency hydrogen evolution reaction. Small 14:1704150. https://doi.org/10.1002/smll.201704150

Gao B, Du XY, Li YH, Song ZX (2020) Wettability transition of $Ni_3B_4$-doped $MoS_2$ for hydrogen evolution reaction by magnetron sputtering. Appl Surf Sci 510:145368. https://doi.org/10.1016/j.apsusc.2020.145368

Gao HW, Zang JB, Wang YH, Zhou SY, Tian PF, Song SW, Tian XQ, Li W (2021) One-step preparation of cobalt-doped NiS@$MoS_2$ core-shell nanorods as bifunctional electrocatalyst for overall water splitting. Electrochim Acta 377:138051. https://doi.org/10.1016/j.electacta.2021.138051

Geng S, Liu Y, Yu YS, Yang W, Li H (2019) Engineering defects and adjusting electronic structure on S doped $MoO_2$ nanosheets toward highly active hydrogen evolution reaction. Nano Res 13:121–126. https://doi.org/10.1007/s12274-019-2582-6

Gennero de Chialvo MR, Chialvo AC (1999) The Tafel-Heyrovsky route in the kinetic mechanism of the hydrogen evolution reaction. Electrochem Commun 1:379–382. https://doi.org/10.1016/S1388-2481(99)00078-8

Ghosh Chaudhuri R, Paria S (2012) Core/shell nanoparticles: classes, properties, synthesis mechanisms, characterization, and applications. Chem Rev 112:2373–2433. https://doi.org/10.1021/cr100449n

Guo D, Song X, Tan L, Ma H, Pang H, Wang X, Zhang L (2018a) Metal-organic framework template-directed fabrication of well-aligned pentagon-like hollow transition-metal sulfides as the anode and cathode for high-performance asymmetric supercapacitors. ACS Appl Mater Interfaces 10:42621–42629. https://doi.org/10.1021/acsami.8b14839

Guo DX, Song XM, Li FB, Tan LC, Ma HY, Zhang LL, Zhao YQ (2018b) Oriented synthesis of $Co_3O_4$ core-shell microspheres for high-performance asymmetric supercapacitor. Colloids Surf A

Physicochem Eng Asp 546:1–8. https://doi.org/10.1016/j.colsurfa.2018.02.072

Guo Y, Park T, Yi JW, Henzie J, Kim J, Wang Z, Jiang B, Bando Y, Sugahara Y, Tang J, Yamauchi Y (2019) Nanoarchitectonics for transition-metal-sulfide-based electrocatalysts for water splitting. Adv Mater 31:e1807134. https://doi.org/10.1002/adma.201807134

Guo Y, Tang J, Henzie J, Jiang B, Xia W, Chen T, Bando Y, Kang YM, Hossain MSA, Sugahara Y, Yamauchi Y (2020) Mesoporous iron-doped MoS(2)/CoMo(2)S(4) heterostructures through organic-metal cooperative interactions on spherical micelles for electrochemical water splitting. ACS Nano 14:4141–4152. https://doi.org/10.1021/acsnano.9b08904

Hall DS, Lockwood DJ, Bock C, MacDougall BR (2015) Nickel hydroxides and related materials: a review of their structures, synthesis and properties. Proc R Soc A Math Phys Eng Sci 471:20140792. https://doi.org/10.1098/rspa.2014.0792

Han L, Liu X, Chen J, Lin R, Liu H, Lu F, Bak S, Liang Z, Zhao S, Stavitski E, Luo J, Adzic RR, Xin HL (2019a) Atomically dispersed molybdenum catalysts for efficient ambient nitrogen fixation. Angew Chem Int Ed Engl 58:2321–2325. https://doi.org/10.1002/anie.201811728

Han Y-X, Hou L-J, Zhang Q, Wu B-W, Kong C, Geng Z-Y (2019b) Mechanism of $H_2$ generation on the unsaturated Mo and S of Mo-Edge in 2H-$MoS_2$ from density functional theory. Comput Theor Chem 1168:112623. https://doi.org/10.1016/j.comptc.2019.112623

Han GH, Kim H, Kim J, Kim J, Kim SY, Ahn SH (2020) Micro-nanoporous $MoO_2$@CoMo heterostructure catalyst for hydrogen evolution reaction. Appl Catal B Environ 270:118895. https://doi.org/10.1016/j.apcatb.2020.118895

Hao L, He H, Qin J, Ma C, Luo L, Yang L, Huang H (2022) MXene nanosheets induce efficient iron selenide active sites to boost the electrocatalytic hydrogen evolution reaction. Inorg Chem 61:21087–21094. https://doi.org/10.1021/acs.inorgchem.2c03666

He R, Hua J, Zhang A, Wang C, Peng J, Chen W, Zeng J (2017) Molybdenum disulfide-black phosphorus hybrid nanosheets as a superior catalyst for electrochemical hydrogen evolution. Nano Lett 17:4311–4316. https://doi.org/10.1021/acs.nanolett.7b01334

He WJ, Han LL, Hao QY, Zheng XR, Li Y, Zhang J, Liu CC, Liu H, Xin HLL (2019) Fluorine-anion-modulated electron structure of nickel sulfide nanosheet arrays for alkaline hydrogen evolution. ACS Energy Lett 4:2905–2912. https://doi.org/10.1021/acsenergylett.9b02316

Hou J, Wu Y, Zhang B, Cao S, Li Z, Sun L (2019) Nanoarray architectures: rational design of nanoarray architectures for electrocatalytic water splitting (Adv Funct Mater 20/2019). Adv Funct Mater 29:1970132. https://doi.org/10.1002/adfm.201970132

Hu C, Zhang L, Zhao ZJ, Li A, Chang X, Gong J (2018) Synergism of geometric construction and electronic regulation: 3D Se-(NiCo)S($x$)/(OH)($x$) nanosheets for highly efficient overall water splitting. Adv Mater 30:e1705538. https://doi.org/10.1002/adma.201705538

Hu Y, Xiong T, Balogun MSJT, Huang Y, Adekoya D, Zhang S, Tong Y (2020) Enhanced metallicity boosts hydrogen evolution capability of dual-bimetallic Ni–Fe nitride nanoparticles. Mater Today Phys 15:100267. https://doi.org/10.1016/j.mtphys.2020.100267

Hu WJ, Shi Q, Chen ZJ, Yin H, Zhong HF, Wang P (2021) $Co_2N$/$Co_2Mo_3O_8$ heterostructure as a highly active electrocatalyst for an alkaline hydrogen evolution reaction. ACS Appl Mater Interfaces 13:8337–8343. https://doi.org/10.1021/acsami.0c20271

Hua Y, Li XX, Chen CY, Pang H (2019) Cobalt based metal-organic frameworks and their derivatives for electrochemical energy conversion and storage. Chem Eng J 370:37–59. https://doi.org/10.1016/j.cej.2019.03.163

Huang ZF, Song J, Li K, Tahir M, Wang YT, Pan L, Wang L, Zhang X, Zou JJ (2016) Hollow cobalt-based bimetallic sulfide polyhedra for efficient all-pH-value electrochemical and photocatalytic hydrogen evolution. J Am Chem Soc 138:1359–1365. https://doi.org/10.1021/jacs.5b11986

Huang B, Zhou NG, Chen XZ, Ong WJ, Li N (2018) Insights into the electrocatalytic hydrogen evolution reaction mechanism on two-dimensional transition-metal carbonitrides (MXene). Chem Eur J 24:18479–18486. https://doi.org/10.1002/chem.201804686

Huang H, Zhao Y, Bai Y, Li F, Zhang Y, Chen Y (2020) Conductive metal-organic frameworks with extra metallic sites as an efficient electrocatalyst for the hydrogen evolution reaction. Adv Sci (weinh) 7:2000012. https://doi.org/10.1002/advs.202000012

Hunt ST, Roman-Leshkov Y (2018) Principles and methods for the rational design of core-shell nanoparticle catalysts with ultralow noble metal loadings. Acc Chem Res 51:1054–1062. https://doi.org/10.1021/acs.accounts.7b00510

Jia YB, Zhu L, Pan HW, Liao YX, Zhang Y, Zhang X, Jiang ZG, Chen MT, Wang KK (2022) Excellent electrocatalytic hydrogen evolution performance of hexagonal NiCoP porous nanosheets in alkaline solution. Appl Surf Sci 580:152314. https://doi.org/10.1016/j.apsusc.2021.152314

Jian J, Yuan L, Qi H, Sun X, Zhang L, Li H, Yuan H, Feng S (2018) Sn-$Ni_3S_2$ ultrathin nanosheets as efficient bifunctional water-splitting catalysts with a large current density and low overpotential. ACS Appl Mater Interfaces 10:40568–40576. https://doi.org/10.1021/acsami.8b14603

Jiang K, Luo M, Liu Z, Peng M, Chen D, Lu YR, Chan TS, de Groot FMF, Tan Y (2021) Rational strain engineering of single-atom ruthenium on nanoporous $MoS_2$ for highly efficient hydrogen evolution. Nat Commun 12:1687. https://doi.org/10.1038/s41467-021-21956-0

Jin H, Guo C, Liu X, Liu J, Vasileff A, Jiao Y, Zheng Y, Qiao S-Z (2018) Emerging two-dimensional nanomaterials for electrocatalysis. Chem Rev 118:6337–6408. https://doi.org/10.1021/acs.chemrev.7b00689

Jin HY, Gu QF, Chen B, Tang C, Zheng Y, Zhang H, Jaroniec M, Qiao SZ (2020) Molten salt-directed catalytic synthesis of 2D layered transition-metal nitrides for efficient hydrogen evolution. Chem 6:2382–2394. https://doi.org/10.1016/j.chempr.2020.06.037

Jin J, Yin J, Liu H, Huang B, Hu Y, Zhang H, Sun M, Peng Y, Xi P, Yan CH (2021a) Atomic sulfur filling oxygen vacancies optimizes H absorption and boosts the hydrogen evolution reaction in alkaline media. Angew Chem Int Ed Engl 60:14117–14123. https://doi.org/10.1002/anie.202104055

Jin Z, Wang L, Chen T, Liang J, Zhang Q, Peng W, Li Y, Zhang F, Fan X (2021b) Transition metal/metal oxide interface (Ni–Mo–O/$Ni_4Mo$) stabilized on N-doped carbon paper for enhanced hydrogen evolution reaction in alkaline conditions. Ind Eng Chem Res 60:5145–5150. https://doi.org/10.1021/acs.iecr.1c00039

Jin L, Wang Q, Wang K, Lu Y, Huang B, Xu H, Qian X, Yang L, He G, Chen H (2022) Engineering $NiMoO_4$/NiFe LDH/rGO multi-component nanosheets toward enhanced electrocatalytic oxygen evolution reaction. Dalton Trans 51:6448–6453. https://doi.org/10.1039/d2dt00115b

Kim J, Kim H, Lee W-J, Ruqia B, Baik H, Oh H-S, Paek S-M, Lim H-K, Choi CH, Choi S-I (2019) Theoretical and experimental understanding of hydrogen evolution reaction kinetics in alkaline electrolytes with Pt-based core–shell nanocrystals. J Am Chem Soc 141:18256–18263. https://doi.org/10.1021/jacs.9b09229

Kisand K, Sarapuu A, Peikolainen AL, Seemen H, Kook M, Kaarik M, Leis J, Sammelselg V, Tammeveski K (2018) Oxygen reduction on Fe- and Co-containing nitrogen-doped nanocarbons.

ChemElectroChem 5:2002–2009. https://doi.org/10.1002/celc.201800353

Kou T, Smart T, Yao B, Chen I, Thota D, Ping Y, Li Y (2018) Theoretical and experimental insight into the effect of nitrogen doping on hydrogen evolution activity of Ni3S2 in alkaline medium. Adv Energy Mater. https://doi.org/10.1002/aenm.201703538

Krstajić N, Popović M, Grgur B, Vojnović M, Šepa D (2001) On the kinetics of the hydrogen evolution reaction on nickel in alkaline solution: part I. The mechanism. J Electroanal Chem 512:16–26. https://doi.org/10.1016/S0022-0728(01)00590-3

Kuang M, Wang QH, Han P, Zheng GF (2017) Cu, Co-embedded N-enriched mesoporous carbon for efficient oxygen reduction and hydrogen evolution reactions. Adv Energy Mater. https://doi.org/10.1002/aenm.201700193

Kuang P, Wang Y, Zhu B, Xia F, Tung CW, Wu J, Chen HM, Yu J (2021) Pt single atoms supported on N-doped mesoporous hollow carbon spheres with enhanced electrocatalytic $H_2$-evolution activity. Adv Mater 33:e2008599. https://doi.org/10.1002/adma.202008599

Lasia A (2019) Mechanism and kinetics of the hydrogen evolution reaction. Int J Hydrog Energy 44:19484–19518. https://doi.org/10.1016/j.ijhydene.2019.05.183

Lau THM, Wu S, Kato R, Wu TS, Kulhavy J, Mo JY, Zheng JW, Foord JS, Soo YL, Suenaga K, Darby MT, Tsang SCE (2019) Engineering monolayer 1T-$MoS_2$ into a bifunctional electrocatalyst via sonochemical doping of isolated transition metal atoms. ACS Catal 9:7527–7534. https://doi.org/10.1021/acscatal.9b01503

Lee HJ, Back S, Lee JH, Choi SH, Jung Y, Choi JW (2019) Mixed transition metal oxide with vacancy-induced lattice distortion for enhanced catalytic activity of oxygen evolution reaction. ACS Catal 9:7099–7108. https://doi.org/10.1021/acscatal.9b01298

Lei L, Huang DL, Zeng GM, Cheng M, Jiang DN, Zhou CY, Chen S, Wang WJ (2019) A fantastic two-dimensional $MoS_2$ material based on the inert basal planes activation: electronic structure, synthesis strategies, catalytic active sites, catalytic and electronics properties. Coord Chem Rev 399:213020. https://doi.org/10.1016/j.ccr.2019.213020

Li P, Zeng HC (2017) Advanced oxygen evolution catalysis by bimetallic Ni–Fe phosphide nanoparticles encapsulated in nitrogen, phosphorus, and sulphur tri-doped porous carbon. Chem Commun (camb) 53:6025–6028. https://doi.org/10.1039/c7cc03005c

Li T, Wang JJ, Wang FL, Zhang LS, Jiang YY, Arandiyan H, Li H (2019) The effect of surface wettability and coalescence dynamics in catalytic performance and catalyst preparation: a review. ChemCatChem 11:1576–1586. https://doi.org/10.1002/cctc.201801925

Li ZX, Hu ML, Wang P, Liu JH, Yao JS, Li CY (2021) Heterojunction catalyst in electrocatalytic water splitting. Coord Chem Rev 439:213953. https://doi.org/10.1016/j.ccr.2021.213953

Li Y, Wang L, Zhang F, Zhang W, Shao G, Zhang P (2023a) Detecting and quantifying wavelength-dependent electrons transfer in heterostructure catalyst via in situ irradiation XPS. Adv Sci (weinh) 10:e2205020. https://doi.org/10.1002/advs.202205020

Li Y, Zhu S, Wu E, Ding H, Lu J, Mu X, Chen L, Zhang Y, Palisaitis J, Chen K, Li M, Yan P, Persson POA, Hultman L, Eklund P, Du S, Kuang Y, Chai Z, Huang Q (2023b) Nanolaminated ternary transition metal carbide (MAX phase)-derived core–shell structure electrocatalysts for hydrogen evolution and oxygen evolution reactions in alkaline electrolytes. J Phys Chem Lett 14:481–488. https://doi.org/10.1021/acs.jpclett.2c03230

Liang Q, Zhong L, Du C, Luo Y, Zhao J, Zheng Y, Xu J, Ma J, Liu C, Li S, Yan Q (2019) Interfacing epitaxial dinickel phosphide to 2D nickel thiophosphate nanosheets for boosting electrocatalytic water splitting. ACS Nano 13:7975–7984. https://doi.org/10.1021/acsnano.9b02510

Liang CW, Zou PC, Nairan A, Zhang YQ, Liu JX, Liu KW, Hu SY, Kang FY, Fan HJ, Yang C (2020) Exceptional performance of hierarchical Ni–Fe oxyhydroxide@NiFe alloy nanowire array electrocatalysts for large current density water splitting. Energy Environ Sci 13:86–95. https://doi.org/10.1039/c9ee02388g

Lin HL, Liu N, Shi ZP, Guo YL, Tang Y, Gao QS (2016) Cobalt-doping in molybdenum-carbide nanowires toward efficient electrocatalytic hydrogen evolution. Adv Funct Mater 26:5590–5598. https://doi.org/10.1002/adfm.201600915

Lin LL, Zhou W, Gao R, Yao SY, Zhang X, Xu WQ, Zheng SJ, Jiang Z, Yu QL, Li YW, Shi C, Wen XD, Ma D (2017) Low-temperature hydrogen production from water and methanol using Pt/alpha-MoC catalysts. Nature 544:80. https://doi.org/10.1038/nature21672

Lin ZP, Xiao BB, Wang ZP, Tao WY, Shen SJ, Huang LA, Zhang JT, Meng FQ, Zhang QH, Gu L, Zhong WW (2021) Planar-coordination $PdSe_2$ nanosheets as highly active electrocatalyst for hydrogen evolution reaction. Adv Funct Mater 31:2102321. https://doi.org/10.1002/adfm.202102321

Ling T, Yan DY, Wang H, Jiao Y, Hu Z, Zheng Y, Zheng L, Mao J, Liu H, Du XW, Jaroniec M, Qiao SZ (2017) Activating cobalt(II) oxide nanorods for efficient electrocatalysis by strain engineering. Nat Commun 8:1509. https://doi.org/10.1038/s41467-017-01872-y

Ling T, Zhang T, Ge B, Han L, Zheng L, Lin F, Xu Z, Hu WB, Du XW, Davey K, Qiao SZ (2019) Well-dispersed nickel- and zinc-tailored electronic structure of a transition metal oxide for highly active alkaline hydrogen evolution reaction. Adv Mater 31:e1807771. https://doi.org/10.1002/adma.201807771

Liu YP, Yu GT, Li GD, Sun YH, Asefa T, Chen W, Zou XX (2015) Coupling $Mo_2C$ with nitrogen-rich nanocarbon leads to efficient hydrogen-evolution electrocatalytic sites. Angew Chem Int Ed 54:10752. https://doi.org/10.1002/anie.201504376

Liu Y, Hua X, Xiao C, Zhou T, Huang P, Guo Z, Pan B, Xie Y (2016) Heterogeneous spin states in ultrathin nanosheets induce subtle lattice distortion to trigger efficient hydrogen evolution. J Am Chem Soc 138:5087–5092. https://doi.org/10.1021/jacs.6b00858

Liu B, Zhao YF, Peng HQ, Zhang ZY, Sit CK, Yuen MF, Zhang TR, Lee CS, Zhang WJ (2017) Nickel–cobalt diselenide 3D mesoporous nanosheet networks supported on Ni foam: an all-pH highly efficient integrated electrocatalyst for hydrogen evolution. Adv Mater 29:1606521. https://doi.org/10.1002/adma.201606521

Liu B, He B, Peng HQ, Zhao Y, Cheng J, Xia J, Shen J, Ng TW, Meng X, Lee CS, Zhang W (2018a) Unconventional nickel nitride enriched with nitrogen vacancies as a high-efficiency electrocatalyst for hydrogen evolution. Adv Sci (weinh) 5:1800406. https://doi.org/10.1002/advs.201800406

Liu H, Ma X, Rao Y, Liu Y, Liu J, Wang L, Wu M (2018b) Heteromorphic $NiCo_2S_4$/$Ni_3S_2$/Ni foam as a self-standing electrode for hydrogen evolution reaction in alkaline solution. ACS Appl Mater Interfaces 10:10890–10897. https://doi.org/10.1021/acsami.8b00296

Liu XX, Zhang L, Lan XW, Hu XL (2018c) Paragenesis of $Mo_2C$ nanocrystals in mesoporous carbon nanofibers for electrocatalytic hydrogen evolution. Electrochim Acta 274:23–30. https://doi.org/10.1016/j.electacta.2018.04.080

Liu H, Li XN, Ge LB, Peng CL, Zhu LY, Zou W, Chen JF, Wu QM, Zhang YX, Huang HL, Wang JL, Cheng ZX, Fu ZP, Lu YL (2020) Accelerating hydrogen evolution in Ru-doped FeCoP nanoarrays with lattice distortion toward highly efficient overall water splitting. Catal Sci Technol 10:8314–8324. https://doi.org/10.1039/d0cy01727b

Liu F, He W, Li Y, Wang F, Zhang J, Xu X, Xue Y, Tang C, Liu H, Zhang J (2021a) Activating sulfur sites of $CoS_2$ electrocatalysts

through tin doping for hydrogen evolution reaction. Appl Surf Sci 546:149101. https://doi.org/10.1016/j.apsusc.2021.149101

Liu MY, He Q, Huang SW, Zou WH, Cong J, Xiao XQ, Li P, Cai JY, Hou LX (2021b) NiCo-layered double hydroxide-derived B-doped CoP/$Ni_2P$ hollow nanoprisms as high-efficiency electrocatalysts for hydrogen evolution reaction. ACS Appl Mater Interfaces 13:9932–9941. https://doi.org/10.1021/acsami.0c20294

Liu W, Wang X, Wang F, Du K, Zhang Z, Guo Y, Yin H, Wang D (2021c) A durable and pH-universal self-standing MoC-$Mo_2C$ heterojunction electrode for efficient hydrogen evolution reaction. Nat Commun 12:6776. https://doi.org/10.1038/s41467-021-27118-6

Liu YX, Bai Y, Yang WW, Ma JH, Sun KN (2021d) Self-supported electrode of NiCo–LDH/$NiCo_2S_4$/CC with enhanced performance for oxygen evolution reaction and hydrogen evolution reaction. Electrochim Acta 367:137534. https://doi.org/10.1016/j.electacta.2020.137534

Liu D, Zeng Q, Hu C, Liu H, Chen D, Han Y, Xu L, Yang J (2022) Core–shell CuPd@NiPd nanoparticles: coupling lateral strain with electronic interaction toward high-efficiency electrocatalysis. ACS Catal 12:9092–9100. https://doi.org/10.1021/acscatal.2c02274

Liu YW, Zhang H, Song WM, Zhang Y, Hou ZP, Zhou GF, Zhang Z, Liu JM (2023) In-situ growth of $ReS_2$/NiS heterostructure on Ni foam as an ultra-stable electrocatalyst for alkaline hydrogen generation. Chem Eng J 451:138905. https://doi.org/10.1016/j.cej.2022.138905

Lu C, Tranca D, Zhang J, Rodri Guez Hernandez FN, Su Y, Zhuang X, Zhang F, Seifert G, Feng X (2017a) Molybdenum carbide-embedded nitrogen-doped porous carbon nanosheets as electrocatalysts for water splitting in alkaline media. ACS Nano 11:3933–3942. https://doi.org/10.1021/acsnano.7b00365

Lu T, Dong SM, Zhang CJ, Zhang LX, Cui GL (2017b) Fabrication of transition metal selenides and their applications in energy storage. Coord Chem Rev 332:75–99. https://doi.org/10.1016/j.ccr.2016.11.005

Luo Z, Miao R, Huan TD, Mosa IM, Poyraz AS, Zhong W, Cloud JE, Kriz DA, Thanneeru S, He J, Zhang Y, Ramprasad R, Suib SL (2016) Mesoporous $MoO_{3-x}$ material as an efficient electrocatalyst for hydrogen evolution reactions. Adv Energy Mater 6:1600528. https://doi.org/10.1002/aenm.201600528

Luo QM, Zhao YW, Sun L, Wang C, Xin HQ, Song JX, Li DY, Ma F (2022) Interface oxygen vacancy enhanced alkaline hydrogen evolution activity of cobalt-iron phosphide/$CeO_2$ hollow nanorods. Chem Eng J 437:135376. https://doi.org/10.1016/j.cej.2022.135376

Lv L, Yang Z, Chen K, Wang C, Xiong Y (2019) 2D layered double hydroxides for oxygen evolution reaction: from fundamental design to application. Adv Energy Mater 9:1803358. https://doi.org/10.1002/aenm.201803358

Lv XW, Xu WS, Tian WW, Wang HY, Yuan ZY (2021) Activity promotion of core and shell in multifunctional core–shell $Co_2$ P@NC electrocatalyst by secondary metal doping for water electrolysis and Zn–air batteries. Small 17:e2101856. https://doi.org/10.1002/smll.202101856

Ma Z, Zhao Q, Li J, Tang B, Zhang Z, Wang X (2018) Three-dimensional well-mixed/highly-densed NiS–CoS nanorod arrays: an efficient and stable bifunctional electrocatalyst for hydrogen and oxygen evolution reactions. Electrochim Acta 260:82–91. https://doi.org/10.1016/j.electacta.2017.11.055

Ma YL, Zhu XQ, Wang BY, Liu SY, Meng TT, Chen H, Peng B, Deng ZW (2020a) Sacrificial template synthesis of hierarchical nickel hydroxidenitrate hollow colloidal particles for electrochemical energy storage. Chem Eng Sci. https://doi.org/10.1016/j.ces.2020.115548

Ma YS, Wang Y, Jiang TY, Zhang FX, Li XM, Zhu YY (2020b) Hydrothermal synthesis of novel 1-aminoperylene diimide/$TiO_2$/$MoS_2$ composite with enhanced photocatalytic activity. Sci Rep 10:22005. https://doi.org/10.1038/s41598-020-78894-y

Men Y, Li P, Zhou JH, Chen SL, Luo W (2020) Trends in alkaline hydrogen evolution activity on cobalt phosphide electrocatalysts doped with transition metals. Cell Rep Phys Sci 1:100136. https://doi.org/10.1016/j.xcrp.2020.100136

Miao M, Pan J, He T, Yan Y, Xia BY, Wang X (2017) Molybdenum carbide-based electrocatalysts for hydrogen evolution reaction. Chem Eur J 23:10947. https://doi.org/10.1002/chem.201701064

Micheroni D, Lan G, Lin W (2018) Efficient electrocatalytic proton reduction with carbon nanotube-supported metal-organic frameworks. J Am Chem Soc 140:15591–15595. https://doi.org/10.1021/jacs.8b09521

Mir RA, Upadhyay S, Pandey OP (2023) A review on recent advances and progress in $Mo_2C$@C: a suitable and stable electrocatalyst for HER. Int J Hydrog Energy. https://doi.org/10.1016/j.ijhydene.2022.12.179

Muthurasu A, Maruthapandian V, Kim HY (2019) Metal-organic framework derived $Co_3O_4$/$MoS_2$ heterostructure for efficient bifunctional electrocatalysts for oxygen evolution reaction and hydrogen evolution reaction. Appl Catal B Environ 248:202–210. https://doi.org/10.1016/j.apcatb.2019.02.014

Nai J, Lu Y, Yu L, Wang X, Lou XWD (2017) Formation of Ni–Fe mixed diselenide nanocages as a superior oxygen evolution electrocatalyst. Adv Mater 29:1703870. https://doi.org/10.1002/adma.201703870

Oh A, Sa YJ, Hwang H, Baik H, Kim J, Kim B, Joo SH, Lee K (2016) Rational design of Pt–Ni–Co ternary alloy nanoframe crystals as highly efficient catalysts toward the alkaline hydrogen evolution reaction. Nanoscale 8:16379–16386. https://doi.org/10.1039/c6nr04572c

Oh NK, Kim C, Lee J, Kwon O, Choi Y, Jung GY, Lim HY, Kwak SK, Kim G, Park H (2019) In-situ local phase-transitioned $MoSe_2$ in $La_{0.5}Sr_{0.5}CoO$(3-delta) heterostructure and stable overall water electrolysis over 1000 hours. Nat Commun 10:1723. https://doi.org/10.1038/s41467-019-09339-y

Osman AI, Mehta N, Elgarahy AM, Hefny M, Al-Hinai A, AaH A-M, Rooney DW (2022) Hydrogen production, storage, utilisation and environmental impacts: a review. Environ Chem Lett 20:153–188. https://doi.org/10.1007/s10311-021-01322-8

Osman AI, Chen L, Yang M, Msigwa G, Farghali M, Fawzy S, Rooney DW, Yap P-S (2023) Cost, environmental impact, and resilience of renewable energy under a changing climate: a review. Environ Chem Lett 21:741–764. https://doi.org/10.1007/s10311-022-01532-8

Ouyang T, Wang XT, Mai XQ, Chen AN, Tang ZY, Liu ZQ (2020) Coupling magnetic single-crystal $Co_2Mo_3O_8$ with ultrathin nitrogen-rich carbon layer for oxygen evolution reaction. Angew Chem Int Ed 59:11948–11957. https://doi.org/10.1002/anie.202004533

Oyama ST, Gott T, Zhao HY, Lee YK (2009) Transition metal phosphide hydroprocessing catalysts: a review. Catal Today 143:94–107. https://doi.org/10.1016/j.cattod.2008.09.019

Pan QW, Wang L (2021) Recent perspectives on the structure and oxygen evolution activity for non-noble metal-based catalysts. J Power Sources 485:229335. https://doi.org/10.1016/j.jpowsour.2020.229335

Pan Y, Liu YR, Zhao JC, Yang K, Liang JL, Liu DD, Hu WH, Liu DP, Liu YQ, Liu CG (2015) Monodispersed nickel phosphide nanocrystals with different phases: synthesis, characterization and electrocatalytic properties for hydrogen evolution. J Mater Chem A 3:1656–1665. https://doi.org/10.1039/c4ta04867a

Pan Y, Sun K, Lin Y, Cao X, Cheng Y, Liu S, Zeng L, Cheong W-C, Zhao D, Wu K, Liu Z, Liu Y, Wang D, Peng Q, Chen C, Li Y (2019a) Electronic structure and d-band center control engineering over M-doped CoP (M = Ni, Mn, Fe) hollow polyhedron frames for boosting hydrogen production. Nano Energy 56:411–419. https://doi.org/10.1016/j.nanoen.2018.11.034

Pan Z, Pan N, Chen L, He J, Zhang M (2019b) Flower-like MOF-derived Co–N-doped carbon composite with remarkable activity and durability for electrochemical hydrogen evolution reaction. Int J Hydrog Energy 44:30075–30083. https://doi.org/10.1016/j.ijhydene.2019.09.117

Pan QQ, Xu CY, Li X, Zhang JF, Hu XL, Geng Y, Su ZM (2021) Porous Ni–Mo bimetallic hybrid electrocatalyst by intermolecular forces in precursors for enhanced hydrogen generation. Chem Eng J 405:126962. https://doi.org/10.1016/j.cej.2020.126962

Pan Y, Wang MM, Li M, Sun GX, Chen YJ, Liu YQ, Zhu W, Wang B (2022) In-situ construction of N-doped carbon nanosnakes encapsulated FeCoSe nanoparticles as efficient bifunctional electrocatalyst for overall water splitting. J Energy Chem 68:699–708. https://doi.org/10.1016/j.jechem.2021.12.008

Park SH, Jo TH, Lee MH, Kawashima K, Mullins CB, Lim H-K, Youn DH (2021) Highly active and stable nickel–molybdenum nitride ($Ni_2Mo_3N$) electrocatalyst for hydrogen evolution. J Mater Chem A 9:4945–4951. https://doi.org/10.1039/d0ta10090k

Pataniya PM, Late D, Sumesh CK (2021) Photosensitive $WS_2$/ZnO nano-heterostructure-based electrocatalysts for hydrogen evolution reaction. Acs Appl Energy Mater 4:755–762. https://doi.org/10.1021/acsaem.0c02608

Peng X, Qasim AM, Jin WH, Wang L, Hu LS, Miao YP, Li W, Li Y, Liu ZT, Huo KF, Wong KY, Chu PK (2018) Ni-doped amorphous iron phosphide nanoparticles on TiN nanowire arrays: an advanced alkaline hydrogen evolution electrocatalyst. Nano Energy 53:66–73. https://doi.org/10.1016/j.nanoen.2018.08.028

Peng X, Yan YJ, Jin X, Huang C, Jin WH, Gao B, Chu PK (2020) Recent advance and prospectives of electrocatalysts based on transition metal selenides for efficient water splitting. Nano Energy 78:105234. https://doi.org/10.1016/j.nanoen.2020.105234

Pu ZH, Liu TT, Amiinu IS, Cheng RL, Wang PY, Zhang CT, Ji PX, Hu WH, Liu J, Mu SC (2020) Transition-metal phosphides: activity origin, energy-related electrocatalysis applications, and synthetic strategies. Adv Funct Mater 30:2004009. https://doi.org/10.1002/adfm.202004009

Qiu TJ, Liang ZB, Guo WH, Gao S, Qu C, Tabassum H, Zhang H, Zhu BJ, Zou RQ, Shao-Horn Y (2019) Highly exposed ruthenium-based electrocatalysts from bimetallic metal-organic frameworks for overall water splitting. Nano Energy 58:1–10. https://doi.org/10.1016/j.nanoen.2018.12.085

Ren Y, Wang J, Hu W, Wen H, Qiu Y, Tang P, Chen M, Wang P (2021) Hierarchical nanostructured Co–Mo–B/$CoMoO_{4-x}$ amorphous composite for the alkaline hydrogen evolution reaction. ACS Appl Mater Interfaces 13:42605–42612. https://doi.org/10.1021/acsami.1c08350

Ren YX, Miao XY, Zhang JX, Lu QD, Chen Y, Fan HB, Teng F, Zhai HF, He XX, Long Y, Zhang CM, Hu P (2023) Post cobalt doping and defect engineering of NbSSe for efficient hydrogen evolution reaction. J Mater Chem A 11:2690–2697. https://doi.org/10.1039/d2ta06913j

Roger I, Shipman MA, Symes MD (2017) Earth-abundant catalysts for electrochemical and photoelectrochemical water splitting. Nat Rev Chem. https://doi.org/10.1038/s41570-016-0003

Roldan Cuenya B, Behafarid F (2015) Nanocatalysis: size- and shape-dependent chemisorption and catalytic reactivity. Surf Sci Rep 70:135–187. https://doi.org/10.1016/j.surfrep.2015.01.001

Rosalbino F, Macciò D, Saccone A, Scavino G (2014) Study of Co–W crystalline alloys as hydrogen electrodes in alkaline water electrolysis. Int J Hydrog Energy 39:12448–12456. https://doi.org/10.1016/j.ijhydene.2014.06.082

Rossmeisl J, Logadottir A, Nørskov JK (2005) Electrolysis of water on (oxidized) metal surfaces. Chem Phys 319:178–184. https://doi.org/10.1016/j.chemphys.2005.05.038

Royer L, Bonnefont A, Asset T, Rotonnelli B, Velasco-Vélez J-JS, Holdcroft S, Hettler S, Arenal R, Pichon B, Savinova E (2022) Cooperative redox transitions drive electrocatalysis of the oxygen evolution reaction on cobalt-iron core–shell nanoparticles. ACS Catal 13:280–286. https://doi.org/10.1021/acscatal.2c04512

Safizadeh F, Ghali E, Houlachi G (2015) Electrocatalysis developments for hydrogen evolution reaction in alkaline solutions: a review. Int J Hydrog Energy 40:256–274. https://doi.org/10.1016/j.ijhydene.2014.10.109

Santhosh Kumar R, Ramakrishnan S, Prabhakaran S, Kim AR, Kumar DR, Kim DH, Yoo DJ (2022) Structural, electronic, and electrocatalytic evaluation of spinel transition metal sulfide supported reduced graphene oxide. J Mater Chem A 10:1999–2011. https://doi.org/10.1039/d1ta08224h

Seh ZW, Kibsgaard J, Dickens CF, Chorkendorff IB, Norskov JK, Jaramillo TF (2017) Combining theory and experiment in electrocatalysis: Insights into materials design. Science. https://doi.org/10.1126/science.aad4998

Shen L, Yu L, Wu HB, Yu XY, Zhang X, Lou XW (2015) Formation of nickel cobalt sulfide ball-in-ball hollow spheres with enhanced electrochemical pseudocapacitive properties. Nat Commun 6:6694. https://doi.org/10.1038/ncomms7694

Sheng W, Zhuang Z, Gao M, Zheng J, Chen JG, Yan Y (2015) Correlating hydrogen oxidation and evolution activity on platinum at different pH with measured hydrogen binding energy. Nat Commun 6:5848. https://doi.org/10.1038/ncomms6848

Shi Y, Zhou Y, Yang DR, Xu WX, Wang C, Wang FB, Xu JJ, Xia XH, Chen HY (2017) Energy level engineering of $MoS_2$ by transition-metal doping for accelerating hydrogen evolution reaction. J Am Chem Soc 139:15479–15485. https://doi.org/10.1021/jacs.7b08881

Shi H, Zhou YT, Yao RQ, Wan WB, Ge X, Zhang W, Wen Z, Lang XY, Zheng WT, Jiang Q (2020) Spontaneously separated intermetallic $Co_3Mo$ from nanoporous copper as versatile electrocatalysts for highly efficient water splitting. Nat Commun 11:2940. https://doi.org/10.1038/s41467-020-16769-6

Song S, Wang Y, Li W, Tian P, Zhou S, Gao H, Tian X, Zang J (2020a) Amorphous $MoS_2$ coated $Ni_3S_2$ nanosheets as bifunctional electrocatalysts for high-efficiency overall water splitting. Electrochim Acta. https://doi.org/10.1016/j.electacta.2019.135454

Song S, Yu L, Xiao X, Qin Z, Zhang W, Wang D, Bao J, Zhou H, Zhang Q, Chen S, Ren Z (2020b) Outstanding oxygen evolution reaction performance of nickel iron selenide/stainless steel mat for water electrolysis. Mater Today Phys 13:100216. https://doi.org/10.1016/j.mtphys.2020.100216

Structural aspects of layered double hydroxides. In: Layered double hydroxides, pp 1-87. https://doi.org/10.1007/430_005

Su J, Yang Y, Xia G, Chen J, Jiang P, Chen Q (2017) Ruthenium-cobalt nanoalloys encapsulated in nitrogen-doped graphene as active electrocatalysts for producing hydrogen in alkaline media. Nat Commun 8:14969. https://doi.org/10.1038/ncomms14969

Subbaraman R, Tripkovic D, Strmcnik D, Chang K-C, Uchimura M, Paulikas AP, Stamenkovic V, Markovic NM (2011) Enhancing hydrogen evolution activity in water splitting by tailoring $Li^+$–$Ni(OH)_2$–Pt interfaces. Science 334:1256–1260. https://doi.org/10.1126/science.1211934

Suen NT, Hung SF, Quan Q, Zhang N, Xu YJ, Chen HM (2017) Electrocatalysis for the oxygen evolution reaction: recent

development and future perspectives. Chem Soc Rev 46:337–365. https://doi.org/10.1039/c6cs00328a

Sultan S, Tiwari JN, Singh AN, Zhumagali S, Ha M, Myung CW, Thangavel P, Kim KS (2019) Single atoms and clusters based nanomaterials for hydrogen evolution, oxygen evolution reactions, and full water splitting. Adv Energy Mater. https://doi.org/10.1002/aenm.201900624

Sun YG, Alimohammadi F, Zhang DT, Guo GS (2017) Enabling colloidal synthesis of edge-oriented $MoS_2$ with expanded interlayer spacing for enhanced HER catalysis. Nano Lett 17:1963–1969. https://doi.org/10.1021/acs.nanolett.6b05346

Sun H, Chen L, Lian YB, Yang WJ, Lin L, Chen YF, Xu JB, Wang D, Yang XQ, Rummerli MH, Guo J, Zhong J, Deng Z, Jiao Y, Peng Y, Qiao SZ (2020) Topotactically transformed polygonal mesopores on ternary layered double hydroxides exposing undercoordinated metal centers for accelerated water dissociation. Adv Mater 32:2006784. https://doi.org/10.1002/adma.202006784

Sun J, Xue H, Guo NK, Song TS, Hao YR, Sun JW, Zhang JW, Wang Q (2021a) Synergetic metal defect and surface chemical reconstruction into $NiCo_2S_4$/ZnS heterojunction to achieve outstanding oxygen evolution performance. Angew Chem Int Ed 60:19435–19441. https://doi.org/10.1002/anie.202107731

Sun T, Mitchell S, Li J, Lyu P, Wu X, Perez-Ramirez J, Lu J (2021b) Design of local atomic environments in single-atom electrocatalysts for renewable energy conversions. Adv Mater 33:e2003075. https://doi.org/10.1002/adma.202003075

Tahira A, Ibupoto ZH, Willander M, Nur O (2019) Advanced $Co_3O_4$–CuO nano-composite based electrocatalyst for efficient hydrogen evolution reaction in alkaline media. Int J Hydrog Energy 44:26148–26157. https://doi.org/10.1016/j.ijhydene.2019.08.120

Tareen AK, Priyanga GS, Khan K, Pervaiz E, Thomas T, Yang MH (2019) Nickel-based transition metal nitride electrocatalysts for the oxygen evolution reaction. Chemsuschem 12:3941–3954. https://doi.org/10.1002/cssc.201900553

Theerthagiri J, Karuppasamy K, Park J, Rahamathulla N, Kumari MLA, Souza MKR, Cardoso ESF, Murthy AP, Maia G, Kim H-S, Choi MY (2022) Electrochemical conversion of biomass-derived aldehydes into fine chemicals and hydrogen: a review. Environ Chem Lett. https://doi.org/10.1007/s10311-022-01543-5

Tian X, Zhao X, Su YQ, Wang L, Wang H, Dang D, Chi B, Liu H, Hensen EJM, Lou XWD, Xia BY (2019) Engineering bunched Pt–Ni alloy nanocages for efficient oxygen reduction in practical fuel cells. Science 366:850–856. https://doi.org/10.1126/science.aaw7493

Tian JY, Yang CD, Hao RH, Li FN, Liu ZR, Chen W, Lv YC, Lin C (2022) Fabrication of phosphorus-mediated $MoS_2$ nanosheets on carbon cloth for enhanced hydrogen evolution reaction. Int J Hydrog Energy 47:17871–17878. https://doi.org/10.1016/j.ijhydene.2022.03.288

Tiwari AP, Azam A, Novak TG, Prakash O, Jeon S (2018) Chemical strain formation through anion substitution in $Cu_2WS_4$ for efficient electrocatalysis of water dissociation. J Mater Chem A 6:7786–7793. https://doi.org/10.1039/c8ta01061g

Tu KJ, Tranca D, Rodriguez-Hernandez F, Jiang KY, Huang SH, Zheng Q, Chen MX, Lu CB, Su YZ, Chen ZY, Mao HY, Yang CQ, Jiang JY, Liang HW, Zhuang XD (2020) A novel heterostructure based on RuMo nanoalloys and N-doped carbon as an efficient electrocatalyst for the hydrogen evolution reaction. Adv Mater 32:2005433. https://doi.org/10.1002/adma.202005433

Ursua A, Gandia LM, Sanchis P (2012) Hydrogen production from water electrolysis: current status and future trends. Proc IEEE 100:410–426. https://doi.org/10.1109/JPROC.2011.2156750

Vrubel H, Hu X (2012) Molybdenum boride and carbide catalyze hydrogen evolution in both acidic and basic solutions. Angew Chem Int Ed Engl 51:12703–12706. https://doi.org/10.1002/anie.201207111

Wang T, Guo Y, Zhou Z, Chang X, Zheng J, Li X (2016a) Ni–Mo nanocatalysts on N-doped graphite nanotubes for highly efficient electrochemical hydrogen evolution in acid. ACS Nano 10:10397–10403. https://doi.org/10.1021/acsnano.6b06259

Wang Y, Liu D, Liu Z, Xie C, Huo J, Wang S (2016b) Porous cobalt-iron nitride nanowires as excellent bifunctional electrocatalysts for overall water splitting. Chem Commun (camb) 52:12614–12617. https://doi.org/10.1039/c6cc06608a

Wang L, Zhu YH, Zeng ZH, Lin C, Giroux M, Jiang L, Han Y, Greeley J, Wang C, Jin J (2017a) Platinum–nickel hydroxide nanocomposites for electrocatalytic reduction of water. Nano Energy 31:456–461. https://doi.org/10.1016/j.nanoen.2016.11.048

Wang Y, Kong B, Zhao DY, Wang HT, Selomulya C (2017b) Strategies for developing transition metal phosphides as heterogeneous electrocatalysts for water splitting. Nano Today 15:26–55. https://doi.org/10.1016/j.nantod.2017.06.006

Wang B, Shang J, Guo C, Zhang J, Zhu F, Han A, Liu J (2019a) A general method to ultrathin bimetal-MOF nanosheets arrays via in situ transformation of layered double hydroxides arrays. Small 15:e1804761. https://doi.org/10.1002/smll.201804761

Wang L, Duan X, Liu X, Gu J, Si R, Qiu Y, Qiu Y, Shi D, Chen F, Sun X, Lin J, Sun J (2019b) Atomically dispersed Mo supported on metallic Co9S8 nanoflakes as an advanced noble-metal-free bifunctional water splitting catalyst working in universal pH conditions. Adv Energy Mater. https://doi.org/10.1002/aenm.201903137

Wang C, Lu HL, Mao ZY, Yan CL, Shen GZ, Wang XF (2020a) Bimetal Schottky heterojunction boosting energy-saving hydrogen production from alkaline water via urea electrocatalysis. Adv Funct Mater 30:2000556. https://doi.org/10.1002/adfm.202000556

Wang G, Chen W, Chen G, Huang J, Song C, Chen D, Du Y, Li C, Ostrikov KK (2020b) Trimetallic Mo–Ni–Co selenides nanorod electrocatalysts for highly-efficient and ultra-stable hydrogen evolution. Nano Energy 71:104637. https://doi.org/10.1016/j.nanoen.2020.104637

Wang HX, Fu WW, Yang XH, Huang ZY, Li J, Zhang HJ, Wang Y (2020c) Recent advancements in heterostructured interface engineering for hydrogen evolution reaction electrocatalysis. J Mater Chem A 8:6926–6956. https://doi.org/10.1039/c9ta11646j

Wang J, Li XZ, Wei B, Sun R, Yu W, Hoh HY, Xu HM, Li J, Ge XB, Chen ZX, Su CL, Wang ZC (2020d) Activating basal planes of $NiPS_3$ for hydrogen evolution by nonmetal heteroatom doping. Adv Funct Mater 30:1908708. https://doi.org/10.1002/adfm.201908708

Wang Y, Li X, Zhang M, Zhou Y, Rao D, Zhong C, Zhang J, Han X, Hu W, Zhang Y, Zaghib K, Wang Y, Deng Y (2020e) Lattice-strain engineering of homogeneous $NiS_{0.5}$ $Se_{0.5}$ core–shell nanostructure as a highly efficient and robust electrocatalyst for overall water splitting. Adv Mater 32:e2000231. https://doi.org/10.1002/adma.202000231

Wang C, Sui G, Guo D, Li J, Zhang L, Li S, Xin J, Chai DF, Guo W (2021a) Structure-designed synthesis of hollow/porous cobalt sulfide/phosphide based materials for optimizing supercapacitor storage properties and hydrogen evolution reaction. J Colloid Interface Sci 599:577–585. https://doi.org/10.1016/j.jcis.2021.04.118

Wang H, Jiao S, Liu S, Wang S, Zhou T, Xu Y, Li X, Wang Z, Wang L (2021b) Mesoporous bimetallic Au@Rh core-shell nanowires as efficient electrocatalysts for pH-universal hydrogen evolution. ACS Appl Mater Interfaces 13:30479–30485. https://doi.org/10.1021/acsami.1c01796

Wang H, Li J, Li K, Lin Y, Chen J, Gao L, Nicolosi V, Xiao X, Lee JM (2021c) Transition metal nitrides for electrochemical energy applications. Chem Soc Rev 50:1354–1390. https://doi.org/10.1039/d0cs00415d

Wang J, Fang WH, Hu Y, Zhang YH, Dang JQ, Wu Y, Chen BZ, Zhao H, Li ZX (2021d) Single atom Ru doping 2H-$MoS_2$ as highly efficient hydrogen evolution reaction electrocatalyst in a wide pH range. Appl Catal B Environ. https://doi.org/10.1016/j.apcatb.2021.120490

Wang T, Tao L, Zhu X, Chen C, Chen W, Du S, Zhou Y, Zhou B, Wang D, Xie C, Long P, Li W, Wang Y, Chen R, Zou Y, Fu X-Z, Li Y, Duan X, Wang S (2022) Combined anodic and cathodic hydrogen production from aldehyde oxidation and hydrogen evolution reaction. Nat Catal 5:66–73. https://doi.org/10.1038/s41929-021-00721-y

Wei S, Wang Q, Zhu J, Sun L, Lin H, Guo Z (2011) Multifunctional composite core–shell nanoparticles. Nanoscale 3:4474–4502. https://doi.org/10.1039/C1NR11000D

Wei H, Xi Q, Chen X, Guo D, Ding F, Yang Z, Wang S, Li J, Huang S (2018a) Molybdenum carbide nanoparticles coated into the graphene wrapping N-doped porous carbon microspheres for highly efficient electrocatalytic hydrogen evolution both in acidic and alkaline media. Adv Sci (weinh) 5:1700733. https://doi.org/10.1002/advs.201700733

Wei J, Zhou M, Long A, Xue Y, Liao H, Wei C, Xu ZJ (2018b) Heterostructured electrocatalysts for hydrogen evolution reaction under alkaline conditions. Nanomicro Lett 10:75. https://doi.org/10.1007/s40820-018-0229-x

Wei YR, Zhang XX, Wang ZH, Yin JM, Huang JZ, Zhao G, Xu XJ (2021) Metal-organic framework derived NiCoP hollow polyhedrons electrocatalyst for pH-universal hydrogen evolution reaction. Chin Chem Lett 32:119–124. https://doi.org/10.1016/j.cclet.2020.10.046

Wilson JA, Di Salvo FJ, Mahajan S (2001) Charge-density waves and superlattices in the metallic layered transition metal dichalcogenides (Reprinted from Adv Phys 32: 882 1974). Adv Phys. 50: 1171–1248. https://doi.org/10.1080/00018730110102718

Wu HB, Xia BY, Yu L, Yu XY, Lou XW (2015) Porous molybdenum carbide nano-octahedrons synthesized via confined carburization in metal-organic frameworks for efficient hydrogen production. Nat Commun 6:6512. https://doi.org/10.1038/ncomms7512

Wu X, Han X, Ma X, Zhang W, Deng Y, Zhong C, Hu W (2017) Morphology-controllable synthesis of Zn–Co–mixed sulfide nanostructures on carbon fiber paper toward efficient rechargeable zinc–air batteries and water electrolysis. ACS Appl Mater Interfaces 9:12574–12583. https://doi.org/10.1021/acsami.6b16602

Wu L, Zhang F, Song S, Ning M, Zhu Q, Zhou J, Gao G, Chen Z, Zhou Q, Xing X, Tong T, Yao Y, Bao J, Yu L, Chen S, Ren Z (2022a) Efficient alkaline water/seawater hydrogen evolution by a nanorod-nanoparticle-structured Ni–MoN catalyst with fast water-dissociation kinetics. Adv Mater 34:e2201774. https://doi.org/10.1002/adma.202201774

Wu X, Cai Y, Yong C, Wang J, Liu X, Wang W, An X, Kong Q, Yao W, Wang Q, Li X, Zhao Y (2022b) Rapid screening of $NixFe_{1-x}$/$Fe_2O_3$/$Ni(OH)_2$ complexes with excellent oxygen evolution reaction activity and durability by a two-step electrodeposition method. Appl Surf Sci 592:153251. https://doi.org/10.1016/j.apsusc.2022.153251

Xia W, Mahmood A, Zou R, Xu Q (2015) Metal–organic frameworks and their derived nanostructures for electrochemical energy storage and conversion. Energy Environ Sci 8:1837–1866. https://doi.org/10.1039/c5ee00762c

Xiao Z, Wang Y, Huang Y-C, Wei Z, Dong C-L, Ma J, Shen S, Li Y, Wang S (2017) Filling the oxygen vacancies in $Co_3O_4$ with phosphorus: an ultra-efficient electrocatalyst for overall water splitting. Energy Environ Sci 10:2563–2569. https://doi.org/10.1039/c7ee01917c

Xiao X, Tao L, Li M, Lv X, Huang D, Jiang X, Pan H, Wang M, Shen Y (2018) Electronic modulation of transition metal phosphide via doping as efficient and pH-universal electrocatalysts for hydrogen evolution reaction. Chem Sci 9:1970–1975. https://doi.org/10.1039/c7sc04849a

Xiao WY, Li X, Fu CC, Zhao XW, Cheng YH, Zhang JY (2021) Morphology and distribution of in-situ grown MoP nanoparticles on carbon nanotubes to enhance hydrogen evolution reaction. J Alloys Compd 877:160214. https://doi.org/10.1016/j.jallcom.2021.160214

Xing JN, Li Y, Guo SW, Jin T, Li HX, Wang YJ, Jiao LF (2019) Molybdenum carbide in-situ embedded into carbon nanosheets as efficient bifunctional electrocatalysts for overall water splitting. Electrochim Acta 298:305–312. https://doi.org/10.1016/j.electacta.2018.12.091

Xiong J, Cai WW, Shi WJ, Zhang XL, Li J, Yang ZH, Feng LG, Cheng HS (2017) Salt-templated synthesis of defect-rich MoN nanosheets for boosted hydrogen evolution reaction. J Mater Chem A 5:24193–24198. https://doi.org/10.1039/c7ta07566a

Xiong J, Li J, Shi J, Zhang X, Suen N-T, Liu Z, Huang Y, Xu G, Cai W, Lei X, Feng L, Yang Z, Huang L, Cheng H (2018) In situ engineering of double-phase interface in Mo/$Mo_2C$ heteronanosheets for boosted hydrogen evolution reaction. ACS Energy Lett 3:341–348. https://doi.org/10.1021/acsenergylett.7b01180

Xiong LW, Qiu YF, Peng X, Liu ZT, Chu PK (2022) Electronic structural engineering of transition metal-based electrocatalysts for the hydrogen evolution reaction. Nano Energy. https://doi.org/10.1016/j.nanoen.2022.107882

Xu B, Chen ZM, Zhang HJ, Sun YQ, Li CC (2017) Novel $Ni(S_{0.49}Se_{0.51})_2$ porous flakes array on carbon fiber cloth for efficient hydrogen evolution reaction. Int J Hydrog Energy 42:30119–30125. https://doi.org/10.1016/j.ijhydene.2017.10.081

Xu L, Wang Z, Chen X, Qu ZK, Li F, Yang WS (2018) Ultrathin layered double hydroxide nanosheets with Ni(III) active species obtained by exfoliation for highly efficient ethanol electrooxidation. Electrochim Acta 260:898–904. https://doi.org/10.1016/j.electacta.2017.12.065

Yan D, Li Y, Huo J, Chen R, Dai L, Wang S (2017) Defect chemistry of nonprecious-metal electrocatalysts for oxygen reactions. Adv Mater 29:1606459. https://doi.org/10.1002/adma.201606459

Yan L, Zhang B, Wu SY, Yu JL (2020) A general approach to the synthesis of transition metal phosphide nanoarrays on MXene nanosheets for pH-universal hydrogen evolution and alkaline overall water splitting. J Mater Chem A 8:14234–14242. https://doi.org/10.1039/d0ta05189f

Yang M, Jiang Y, Liu S, Zhang M, Guo Q, Shen W, He R, Su W, Li M (2019) Regulating the electron density of dual transition metal sulfide heterostructures for highly efficient hydrogen evolution in alkaline electrolytes. Nanoscale 11:14016–14023. https://doi.org/10.1039/c9nr03401c

Yang G, Jiao Y, Yan H, Xie Y, Wu A, Dong X, Guo D, Tian C, Fu H (2020a) Interfacial engineering of $MoO_2$ -FeP heterojunction for highly efficient hydrogen evolution coupled with biomass electrooxidation. Adv Mater 32:e2000455. https://doi.org/10.1002/adma.202000455

Yang HH, Huang Y, Teoh WY, Jiang LJ, Chen WJ, Zhang L, Yan JH (2020b) Molybdenum selenide nanosheets surrounding nickel selenides sub-microislands on nickel foam as high-performance bifunctional electrocatalysts for water splitting. Electrochim Acta 349:136336. https://doi.org/10.1016/j.electacta.2020.136336

Yang HY, Chen ZL, Guo PF, Fei B, Wu RB (2020c) B-doping-induced amorphization of LDH for large-current-density hydrogen evolution reaction. Appl Catal B Environ 261:118240. https://doi.org/10.1016/j.apcatb.2019.118240

Yang X, Wang Y, Tong X, Yang N (2021) Strain engineering in electrocatalysts: fundamentals, progress, and perspectives. Adv Energy Mater 12:2102261. https://doi.org/10.1002/aenm.202102261

Yang M, Chen L, Wang J, Msigwa G, Osman AI, Fawzy S, Rooney DW, Yap P-S (2023a) Circular economy strategies for combating climate change and other environmental issues. Environ Chem Lett 21:55–80. https://doi.org/10.1007/s10311-022-01499-6

Yang YX, Zhang L, Guo FY, Wang DX, Guo XW, Zhou XZ, Sun DF, Yang ZW, Lei ZQ (2023b) A robust octahedral $NiCoO_xS_y$ core–shell structure decorated with $NiWO_4$ nanoparticles for enhanced electrocatalytic hydrogen evolution reaction. Electrochim Acta 439:141618. https://doi.org/10.1016/j.electacta.2022.141618

Yao N, Li P, Zhou ZR, Zhao YM, Cheng GZ, Chen SL, Luo W (2019) Synergistically tuning water and hydrogen binding abilities over $Co_4N$ by Cr doping for exceptional alkaline hydrogen evolution electrocatalysis. Adv Energy Mater 9:1902449. https://doi.org/10.1002/aenm.201902449

Yao MQ, Wang BJ, Sun BL, Luo LF, Chen YJ, Wang JW, Wang N, Komarneni S, Niu XB, Hu WC (2021) Rational design of self-supported Cu@WC core–shell mesoporous nanowires for pH-universal hydrogen evolution reaction. Appl Catal B Environ 280:119451. https://doi.org/10.1016/j.apcatb.2020.119451

Ye L, Du YQ, Zhao YG, Zhao LJ (2020) W-doped $Ni_3S_2$ nanoparticles modified with NiFeLa hydroxide for hydrogen evolution. ACS Appl Nano Mater 3:8372–8381. https://doi.org/10.1021/acsanm.0c01790

Yin J, Jin J, Zhang H, Lu M, Peng Y, Huang BL, Xi PX, Yan CH (2019) Atomic arrangement in metal-doped $NiS_2$ boosts the hydrogen evolution reaction in alkaline media. Angew Chem Int Ed 58:18676–18682. https://doi.org/10.1002/anie.201911470

Yu XY, David Lou XW (2018) Mixed metal sulfides for electrochemical energy storage and conversion. Adv Energy Mater. https://doi.org/10.1002/aenm.201701592

Yu MZ, Zhou S, Wang ZY, Zhao JJ, Qiu JS (2018) Boosting electrocatalytic oxygen evolution by synergistically coupling layered double hydroxide with MXene. Nano Energy 44:181–190. https://doi.org/10.1016/j.nanoen.2017.12.003

Yu J, He QJ, Yang GM, Zhou W, Shao ZP, Ni M (2019) Recent advances and prospective in ruthenium-based materials for electrochemical water splitting. ACS Catal 9:9973–10011. https://doi.org/10.1021/acscatal.9b02457

Yuan S, Peng J, Cai B, Huang Z, Garcia-Esparza AT, Sokaras D, Zhang Y, Giordano L, Akkiraju K, Zhu YG, Hubner R, Zou X, Roman-Leshkov Y, Shao-Horn Y (2022) Tunable metal hydroxide-organic frameworks for catalysing oxygen evolution. Nat Mater 21:673–680. https://doi.org/10.1038/s41563-022-01199-0

Zeng K, Zhang DK (2011) Recent progress in alkaline water electrolysis for hydrogen production and applications (vol 36, pg 307, 2010). Progress Energy Combust Sci 37: 631–631. https://doi.org/10.1016/j.pecs.2011.02.002

Zeng M, Li YG (2015) Recent advances in heterogeneous electrocatalysts for the hydrogen evolution reaction. J Mater Chem A 3:14942–14962. https://doi.org/10.1039/c5ta02974k

Zhang HW, Lv RT (2018) Defect engineering of two-dimensional materials for efficient electrocatalysis. J Materiomics 4:95–107. https://doi.org/10.1016/j.jmat.2018.02.006

Zhang J, Wang T, Liu P, Liao Z, Liu S, Zhuang X, Chen M, Zschech E, Feng X (2017) Efficient hydrogen production on $MoNi_4$ electrocatalysts with fast water dissociation kinetics. Nat Commun 8:15437. https://doi.org/10.1038/ncomms15437

Zhang G, Feng YS, Lu WT, He D, Wang CY, Li YK, Wang XY, Cao FF (2018a) Enhanced catalysis of electrochemical overall water splitting in alkaline media by Fe doping in Ni3S2 nanosheet arrays. Acs Catal 8:5431. https://doi.org/10.1021/acscatal.8b00413

Zhang JY, Liu YC, Sun CQ, Xi PX, Peng SL, Gao DQ, Xue DS (2018b) Accelerated hydrogen evolution reaction in $CoS_2$ by transition-metal doping. ACS Energy Lett 3:779–786. https://doi.org/10.1021/acsenergylett.8b00066

Zhang L, Yang Y, Ziaee MA, Lu K, Wang R (2018c) Nanohybrid of carbon quantum dots/molybdenum phosphide nanoparticle for efficient electrochemical hydrogen evolution in alkaline medium. ACS Appl Mater Interfaces 10:9460–9467. https://doi.org/10.1021/acsami.8b00211

Zhang T, Wu MY, Yan DY, Mao J, Liu H, Hu WB, Du XW, Ling T, Qiao SZ (2018d) Engineering oxygen vacancy on NiO nanorod arrays for alkaline hydrogen evolution. Nano Energy 43:103–109. https://doi.org/10.1016/j.nanoen.2017.11.015

Zhang J, Zhang Q, Feng X (2019a) Support and interface effects in water-splitting electrocatalysts. Adv Mater 31:1808167. https://doi.org/10.1002/adma.201808167

Zhang YC, Afzal N, Pan L, Zhang XW, Zou JJ (2019b) Structure-activity relationship of defective metal-based photocatalysts for water splitting: experimental and theoretical perspectives. Adv Sci 6:1900053. https://doi.org/10.1002/advs.201900053

Zhang S, Li Y, Zhu H, Lu S, Ma P, Dong W, Duan F, Chen M, Du M (2020) Understanding the role of nanoscale heterointerfaces in core/shell structures for water splitting: covalent bonding interaction boosts the activity of binary transition-metal sulfides. ACS Appl Mater Interfaces 12:6250–6261. https://doi.org/10.1021/acsami.9b19382

Zhang A, Liang Y, Zhang H, Geng Z, Zeng J (2021a) Doping regulation in transition metal compounds for electrocatalysis. Chem Soc Rev 50:9817–9844. https://doi.org/10.1039/d1cs00330e

Zhang XF, Li XC, Pan ZWH, Lai YJ, Lu Y, Wang Y, Song SQ (2021b) Boosting hydrogen evolution electrocatalysis through defect engineering: A strategy of heat and cool shock. Chem Eng J 426:131524. https://doi.org/10.1016/j.cej.2021.131524

Zhao Y, Mao G, Du Y, Cheng G, Luo W (2018) Colloidal synthesis of NiWSe nanosheets for efficient electrocatalytic hydrogen evolution reaction in alkaline media. Chem Asian J 13:2040–2045. https://doi.org/10.1002/asia.201800692

Zhao J, Chen B, Wang F (2020) Shedding light on the role of misfit strain in controlling core-shell nanocrystals. Adv Mater 32:e2004142. https://doi.org/10.1002/adma.202004142

Zhao ZW, Liu CM, Tsai HS, Zhou JM, Zhang YQ, Wang TQ, Ma GL, Qi CH, Huo MX (2022) The strain and transition metal doping effects on monolayer $Cr_2O_3$ for hydrogen evolution reaction: the first principle calculations. Int J Hydrog Energy 47:37429–37437. https://doi.org/10.1016/j.ijhydene.2021.07.117

Zheng H, Mou Z, Zhou K (2020) Incorporation of core–shell-structured zwitterionic carbon dots in thin-film nanocomposite membranes for simultaneously improved perm-selectivity and anti-fouling properties. ACS Appl Mater Interfaces 12:53215–53229. https://doi.org/10.1021/acsami.0c13386

Zheng YH, Rong J, Xu JC, Zhu Y, Zhang T, Yang DY, Qiu FX (2021) Accessible active sites activated by cobalt-doping into $MoS_2$/$NiS_2$ nanosheet array electrocatalyst for enhanced hydrogen evolution reaction. Appl Surf Sci 563:150385. https://doi.org/10.1016/j.apsusc.2021.150385

Zhong X, Zhang L, Tang J, Chai J, Xu J, Cao L, Yang M, Yang M, Kong W, Wang S, Cheng H, Lu Z, Cheng C, Xu B, Pan H (2017) Efficient coupling of a hierarchical $V_2O_5$@$Ni_3S_2$hybrid nanoarray for pseudocapacitors and hydrogen production. J Mater Chem A 5:17954–17962. https://doi.org/10.1039/c7ta04755j

Zhou H, He FJ (2021) Copper modified titania nanocomposites with a high photocatalytic inactivation of *Escherichia coli*. J Nanosci Nanotechnol 21:5486–5492. https://doi.org/10.1166/jnn.2021.19463

Zhou L, Jiang S, Liu Y, Shao M, Wei M, Duan X (2018a) Ultrathin CoNiP@Layered double hydroxides core–shell nanosheets arrays

for largely enhanced overall water splitting. ACS Appl Energy Mater 1:623–631. https://doi.org/10.1021/acsaem.7b00151

Zhou Q, Chen YP, Zhao GQ, Lin Y, Yu ZW, Xu X, Wang XL, Liu HK, Sun WP, Dou SX (2018b) Active-site-enriched iron-doped nickel/cobalt hydroxide nanosheets for enhanced oxygen evolution reaction. Acs Catal 8:5382. https://doi.org/10.1021/acscatal.8b01332

Zhou KL, Wang Z, Han CB, Ke X, Wang C, Jin Y, Zhang Q, Liu J, Wang H, Yan H (2021a) Platinum single-atom catalyst coupled with transition metal/metal oxide heterostructure for accelerating alkaline hydrogen evolution reaction. Nat Commun 12:3783. https://doi.org/10.1038/s41467-021-24079-8

Zhou X, Zi Y, Xu L, Li T, Yang J, Tang J (2021b) Core–shell-structured Prussian blue analogues ternary metal phosphides as efficient bifunctional electrocatalysts for OER and HER. Inorg Chem 60:11661–11671. https://doi.org/10.1021/acs.inorgchem.1c01694

Zhu ZL, Chueh CC, Li N, Mao CY, Jen AKY (2018) Realizing efficient lead-free formamidinium tin triiodide perovskite solar cells via a sequential deposition route. Adv Mater 30:1703800. https://doi.org/10.1002/adma.201703800

Zhu L, Liu L, Huang G, Zhao Q (2020) Hydrogen evolution over N-doped $CoS_2$ nanosheets enhanced by superaerophobicity and electronic modulation. Appl Surf Sci. https://doi.org/10.1016/j.apsusc.2019.144490

Zhuang GX, Chen YW, Zhuang ZY, Yu Y, Yu JG (2020) Oxygen vacancies in metal oxides: recent progress towards advanced catalyst design. Sci China-Mater 63:2089–2118. https://doi.org/10.1007/s40843-020-1305-6

Zou XX, Wu YY, Liu YP, Liu DP, Li W, Gu L, Liu H, Wang PW, Sun L, Zhang Y (2018) In situ generation of bifunctional, efficient Fe-based catalysts from mackinawite iron sulfide for water splitting. Chem 4:1139–1152. https://doi.org/10.1016/j.chempr.2018.02.023